



DETAILED DESIGN OF THE
RIGIDIZABLE INFLATABLE GET-AWAY-SPECIAL EXPERIMENT

THESIS

Jeremy S. Goodwin, Captain, USAF

AFIT/GA/ENY/06-M05

DEPARTMENT OF THE AIR FORCE
AIR UNIVERSITY

AIR FORCE INSTITUTE OF TECHNOLOGY

Wright-Patterson Air Force Base, Ohio

APPROVED FOR PUBLIC RELEASE; DISTRIBUTION UNLIMITED.

The views expressed in this thesis are those of the author and do not reflect the official policy or position of the United States Air Force, Department of Defense, or the United States Government.

AFIT/GA/ENY/06-M05

DETAILED DESIGN OF THE
RIGIDIZABLE INFLATABLE GET-AWAY-SPECIAL EXPERIMENT

THESIS

Presented to the Faculty
Department of Aeronautics and Astronautics
Graduate School of Engineering and Management
Air Force Institute of Technology
Air University
Air Education and Training Command
In Partial Fulfillment of the Requirements for the
Degree of Master of Science in Astronautical Engineering

Jeremy S. Goodwin, B.S.A.E.
Captain, USAF

23 March 2006

APPROVED FOR PUBLIC RELEASE; DISTRIBUTION UNLIMITED.

AFIT/GA/ENY/06-M05

DETAILED DESIGN OF THE
RIGIDIZABLE INFLATABLE GET-AWAY-SPECIAL EXPERIMENT

Jeremy S. Goodwin, B.S.A.E.
Captain, USAF

Approved:

/signed/

13 Mar 2006

Richard G. Cobb, PhD (Chairman)

date

/signed/

13 Mar 2006

Bradley S. Liebst, PhD (Member)

date

/signed/

13 Mar 2006

Richard A. Raines, PhD (Member)

date

Abstract

This research effort builds upon the previous design of the Rigidizable Inflatable Get-Away-Special Experiment (RIGEX). RIGEX is a Space Shuttle experiment that will study the effects of the zero-gravity space environment on the deployment and modal analysis of three inflatable and rigidizable tubes using a sub- T_g rigidization technique. By comparing space-based modal testing with similar ground-based tests, the experiment intends to verify and validate ground-testing techniques as a viable substitute for zero-gravity tests, thus minimizing cost and complexity for future Air Force and commercial spacecraft rigidization implementations.

With the transition from the Space Shuttle's Get-Away-Special (GAS) canister to its Canister for All Payload Ejections (CAPE) in 2004, there have been several requirements and associated modifications affecting the design. The result of these modifications, along with further refinements made to previous efforts, are presented here as the detailed design of the experiment. Along with the design modifications, a containment analysis was performed on an aluminum shroud for the experiment, indicating that a thickness of 0.027 inches (0.68 millimeters) is required to prevent a broken tube from escaping and damaging the interior of the CAPE. Finally, numerous methods of improving modal analysis results were studied, ultimately resulting in a significant noise reduction in the measured frequency response functions of the deployed tubes.

Acknowledgements

First and foremost, I thank God for this opportunity to come back to school, and for staying by my side as I accomplished my studies. To my beautiful bride, thank you for your amazing love and encouragement, especially throughout all those evenings when school kept us from spending more quality time together.

I also thank my friends and family for your support in this endeavor, especially those that live in Ohio. You successfully diverted my attention away from school, helping my wife and I take better advantage of our time in the Buckeye State. You are true friends, and you will be greatly missed when we leave.

Next, the incredible folks at the DoD Space Test Program were instrumental in helping to get RIGEX approved and ready for launch. Specifically, I am indebted to Mr. Scott Ritterhouse for his electrical engineering assistance, and for converting me into a bit of a spark chaser after all. Thanks for your professionalism, dedication, and willingness to share your expertise.

Thanks also go to Jay Anderson, Wilber Lacy, and Andy Pitts for your invaluable assistance in the lab. Also, to the past RIGEX researchers, and to Captain Dave Moody in particular, thank you for taking the time to answer my questions and help me better understand the outstanding work each of you did. A special thanks also goes out to Mr. Andrew Marcum, an intern from Rose-Hulman Institute of Technology, for the two summers you devoted to the RIGEX experiment. Your contributions were not only extremely significant, but also very much appreciated.

Finally, to my advisor and friend, Dr. Rich Cobb, thank you for listening to me think out loud as we struggled through the obstacles of bringing this experiment closer to launch. With your leadership and guidance, I know RIGEX will be successful.

I wish you all the best of luck and God speed.

Jeremy S. Goodwin

Table of Contents

	Page
Abstract	iv
Acknowledgements	v
List of Figures	x
List of Tables	xiii
List of Symbols	xv
List of Abbreviations	xvii
 I. Introduction	 1-1
1.1 Background Information	1-2
1.2 Experiment Objectives	1-5
1.3 Thesis Overview	1-6
 II. RIGEX Evolution	 2-1
2.1 John D. DiSebastian, Thesis, 2001	2-1
2.1.1 Systems Engineering Approach	2-1
2.1.2 Component Selection	2-2
2.1.3 Component Layout	2-3
2.1.4 Preliminary Analyses	2-4
2.1.5 Operations Concept	2-4
2.1.6 Section Summary	2-5
2.2 Thomas G. Single, Thesis, 2002	2-5
2.2.1 Tube Characterization	2-6
2.2.2 Vibration Testing	2-8
2.2.3 Section Summary	2-11
2.3 Thomas L. Philley, Thesis, 2003	2-12
2.3.1 RIGEX Prototype	2-12
2.3.2 Deployment Tests	2-12
2.3.3 Vibration Analysis	2-13
2.3.4 DoD Space Experiments Review Board	2-15
2.3.5 Section Summary	2-16
2.4 Raymond G. Holstein III, Thesis, 2004	2-17
2.4.1 Finite Element Analysis	2-17
2.4.2 Experimental Testing	2-21

	Page
2.4.3 Section Summary	2-22
2.5 Steven N. Lindemuth, Thesis, 2004	2-23
2.5.1 Heating System Testing	2-23
2.5.2 Inflation System Testing	2-25
2.5.3 SERB Efforts	2-28
2.5.4 Section Summary	2-28
2.6 David C. Moody, Thesis, 2004	2-29
2.6.1 Computer Modification	2-29
2.6.2 Flight Software Development	2-30
2.6.3 Post-Mission Data Analysis	2-31
2.6.4 Section Summary	2-31
2.7 Chad R. Moeller, Thesis, 2005	2-33
2.7.1 Inflation System Modification	2-34
2.7.2 Determination of Tube Cooling Profile	2-35
2.7.3 Section Summary	2-37
2.8 Chapter Summary	2-37
III. Design Modifications	3-1
3.1 Mechanical Subsystem	3-1
3.1.1 Shroud	3-3
3.1.2 CAPE Mounting Plate	3-6
3.1.3 Top Plate	3-8
3.1.4 Vertical Ribs	3-9
3.1.5 Snubber Design	3-10
3.1.6 Stabilizing Feet/Lifting Handles	3-11
3.1.7 Mass Properties	3-12
3.2 Electrical Subsystem	3-14
3.2.1 Shuttle Feedback Circuits	3-14
3.2.2 Fusing Architecture	3-17
3.2.3 Power Distribution Scheme	3-24
3.2.4 Wiring Harness Layout	3-26
3.3 Inflation Subsystem Model	3-30
3.3.1 Requirement Description	3-30
3.3.2 Design	3-31
3.4 Command and Data Handling Subsystem	3-32
3.5 Chapter Summary	3-33

	Page
IV. Analysis and Results	4-1
4.1 Shroud Containment Analysis	4-1
4.2 Tube Modal Analysis	4-3
4.2.1 Frequency Response Function	4-4
4.2.2 Test Setup	4-8
4.2.3 Accelerometer	4-10
4.2.4 Excitation Signal	4-12
4.2.5 Filter	4-14
4.2.6 Conclusions	4-14
4.3 Chapter Summary	4-15
V. Recommendations and Conclusion	5-1
5.1 Recommendations	5-1
5.1.1 Mechanical Subsystem Tasks	5-1
5.1.2 Electrical Subsystem	5-2
5.2 Conclusion	5-4
Appendix A. Memorandum of Agreement	A-1
Appendix B. Program Requirements Document	B-1
Appendix C. Containment Analysis	C-1
C.1 Background Information	C-1
C.2 Analysis Calculations	C-2
C.3 Summary of Results	C-5
Appendix D. Drawing Package	D-1
D.1 CAPE Mounting Plate	D-2
D.2 Experiment Top Plate	D-4
D.3 Large Rib with Computer	D-6
D.4 Large Rib without Computer	D-9
D.5 Small Rib with Pin Puller Hole	D-11
D.6 Small Rib without Pin Puller Hole	D-13
D.7 Oven Mounting Plate	D-15
D.8 Shroud	D-21
D.9 Inflation Mounting Plate	D-22
D.10 Snubber	D-23
D.11 Top Lifting Handle	D-24
D.12 Bottom Lifting Plate	D-25

	Page
Appendix E. Electrical Architecture	E-1
E.1 Computer Harness Wiring Pinouts	E-1
E.2 Experiment Harness Layout	E-5
E.3 Mission Profile	E-8
E.4 Filter Design	E-8
Appendix F. Experiment Software Code	F-1
Bibliography	BIB-1
Vita	VIT-1

List of Figures

Figure		Page
1.1	Inflatable Antenna Experiment	1-2
1.2	Images of GAS and CAPE Canisters	1-4
2.1	DiSebastian's Preliminary Design Assembly	2-4
2.2	Single's Tube Orientation Scheme	2-7
2.3	Tube Surface Irregularity Example	2-8
2.4	Hewlett Packard VXI Data Acquisition System	2-9
2.5	Single's Experiment Setup	2-9
2.6	PSV 300 Laser Vibrometer	2-11
2.7	Philley's Quarter Structure	2-13
2.8	Philley's Deployment Tests	2-14
2.9	Philley's Vibration Test Configurations	2-14
2.10	Example Tube Frequency Response Function	2-16
2.11	Holstein's Finite Element Models.	2-18
2.12	Holstein's Tube Finite Element Analysis Results	2-19
2.13	Structural Finite Element Analysis Results	2-20
2.14	Holstein's Full Structure Stress Analysis Results	2-21
2.15	Holstein's Ping Test Setup	2-22
2.16	Result of Poor Tube Heating	2-24
2.17	Lindemuth's Tube Heating Profile Test	2-24
2.18	Lindemuth's Time Phased Tube Inflation	2-26
2.19	Repositioned Inflation System	2-27
2.20	Lindemuth's Calculated Inflation System Loss Rate	2-28
2.21	Moody's 3-Tube Test Results	2-32
2.22	Battery Storage Volume	2-33

Figure		Page
2.23	Moeller's Pressure System Breakdown	2-35
2.24	Moeller's Inflation Test Results	2-36
2.25	Inflatable Tube Cooling Profile	2-36
2.26	Summary of Student Design Efforts	2-37
3.1	Comparison of Preliminary Design with Detailed Design	3-2
3.2	RIGEX Structure	3-3
3.3	Shroud Concepts.	3-4
3.4	Shroud Design	3-5
3.5	Helicoil Screw-Lock® Inserts	3-6
3.6	CAPE Interface Schematic	3-7
3.7	CAPE Mounting Plate	3-7
3.8	Top Plate Comparison	3-9
3.9	Rib Layout	3-11
3.10	Holstein's Snubber Design	3-12
3.11	Snubber Design and Implementation	3-13
3.12	Lifting Handles	3-13
3.13	Shuttle Feedback Circuit Design	3-16
3.14	A/D Board Digital Operation	3-17
3.15	New Oven Circuit Design Characteristics	3-24
3.16	Power Distribution Plate	3-26
3.17	Computer Connector Plate	3-26
3.18	Computer Interface Harnessing	3-28
3.19	Computer Bay Harness Layout	3-29
3.20	Inflation System Design	3-31
4.1	FRF Test Layout	4-9
4.2	Matlab® Hamming Window	4-10
4.3	Tube FRF as Determined by Moody	4-11

Figure		Page
4.4	Accelerometer Comparison	4-12
4.5	Results of KXPA-4 Accelerometer Test	4-13
4.6	Power Spectral Density of 3V, 0-1000MHz Chirp Signal	4-14
4.7	Results of Excitation Signal Modifications	4-15
E.1	Experiment Harness Layout (1 of 2)	E-6
E.2	Experiment Harness Layout (2 of 2)	E-7
E.3	Schematic of Moody's Filter Board	E-9

List of Tables

Table		Page
1.1	Cost of Launching Heavy Launch Vehicles	1-1
1.2	CAPE vs. GAS Payload Envelope Comparison	1-4
2.1	NASA Systems Engineering Process	2-2
2.2	DiSebastian's Component Selection Decisions	2-3
2.3	DiSebastian's Sensor Requirements	2-3
2.4	DiSebastian's Preliminary Analyses Results	2-4
2.5	DiSebastian's Main Event Calendar	2-5
2.6	Tube Physical Properties	2-7
2.7	Summary of Tube Modal Properties Using Shaker Excitation .	2-10
2.8	Comparison of Tube Modal Properties Under Varying Excitation Sources	2-10
2.9	Summary of Single's Vacuum Test Results for Short Tubes . .	2-11
2.10	Philley's Vibration Results	2-15
2.11	Holstein's Tube Finite Element Analysis Results	2-19
2.12	Holstein's Structural Finite Element Analysis Results	2-20
2.13	Holstein's Experimental Results	2-23
3.1	Driving Requirements for Design Modifications	3-1
3.2	Structure Mass Properties	3-14
3.3	NASA Current Ratings by Payload Location for 200°C	3-19
3.4	Computer Current Consumption Determination	3-21
3.5	Previous Oven Circuit Characteristics	3-23
4.1	Containment Analysis Assumptions and Values	4-2
4.2	Containment Analysis Results	4-3

Table		Page
E.1	DAC Power Supply (PWR1) Board Pinout	E-2
E.2	IC Power Supply (PWR2) Board Pinout	E-2
E.3	Analog/Digital Converter (ADC) Board Pinout	E-2
E.4	Thermocouple (TC) Board Pinout	E-3
E.5	Filter (F) Board Pinout	E-3
E.6	Camera Board (CB) Board Pinout	E-3
E.7	Data Acquisition Computer Counter (DACC) Board Pinout . .	E-4
E.8	Imaging Computer Counter (ICC) Board Pinout	E-4
E.9	Relay Board Pinout, J4 Side (J4), Relays 1-12	E-5
E.10	Relay Board Pinout, J3 Side (J3), Relays 13-24	E-5
E.11	labelapp:MissionProfileMission Profile / Timeline	E-8

List of Symbols

Symbol		Page
ζ	Damping ratio	2-15
ω	Natural frequency	2-15
P	Pressure	2-34
V	Volume	2-34
n	Number of moles of an ideal gas	2-34
R	Ideal gas constant	2-34
T	Temperature	2-34
I	Current	3-19
V	Voltage	3-19
R_{eq}	Equivalent resistance	3-19
P	Power	3-20
A_{LF}	Low Frequency Acceleration	4-1
f_n	Fundamental Frequency	4-1
a	Shuttle Acceleration	4-1
S_d	Travel Distance	4-1
m	Mass	4-2
V	Velocity	4-2
$perim$	Perimeter	4-2
YS_w	Yield Strength	4-2
$H(s)$	Transfer function	4-4
$X(s)$	Output signal, in frequency domain	4-4
$F(s)$	Input signal, in frequency domain	4-4
k	k^{th} harmonic of sampling frequency	4-5
T	Period of data block	4-5
r	r^{th} sample of data block	4-5

Symbol		Page
N	Block size of data	4-5
x_r	Value of x at r^{th} sample	4-5
\imath	Complex number, $\sqrt{-1}$	4-5
Δ	Sampling period	4-5
R_r	Autocorrelation function	4-6
x_s	Value of x at sample s	4-6
x_{s+r}	Value of x at sample s+r (time shift implied in r)	4-6
R_r^{xy}	Cross-correlation function	4-6
S^{xx}	Power spectral density of S	4-7

List of Abbreviations

Abbreviation		Page
RIGEX	Rigidizable Inflatable Get-Away-Special Experiment . . .	1-1
AFIT	Air Force Institute of Technology	1-1
LEO	Low-Earth Orbit	1-1
GTO	Geosynchronous Transfer Orbit	1-1
IAE	Inflatable Antenna Experiment	1-2
JPL	Jet Propulsion Laboratory	1-2
psi	Pounds Per Square Inch	1-3
T_g	Glass Transition Temperature	1-3
DARPA	Defense Advanced Research Projects Agency	1-3
NASA	National Aeronautics and Space Administration	1-3
DoD	Department of Defense	1-3
STP	Space Test Program	1-3
GAS	Get-Away-Special	1-4
CAPE	Canister for All Payload Ejections	1-4
MOA	Memorandum of Agreement	1-5
SE	Systems Engineering	2-1
SMAD	Space Mission Analysis and Design	2-1
IEEE	Institute of Electrical and Electronics Engineers	2-1
PZT	Lead-Zirconate-Titanate	2-8
ERA	Eigenstructure Realization Algorithm	2-9
PSV	Polytec Scanning Vibrometer	2-9
psig	Pounds Per Square Inch (Gauge)	2-12
FRF	Frequency Response Function	2-15
SERB	Space Experiments Review Board	2-15
PDR	Preliminary Design Review	2-17







Abbreviation		Page
FEA	Finite Element Analysis	2-17
FEM	Finite Element Model	2-17
EMP	Experiment Mounting Plate	3-6
LED	Light Emitting Diode	3-8
AWG	American Wire Gauge	3-18
VDC	DC Voltage	3-23
PDP	Power Distribution Plate	3-24
CDH	Command and Data Handling	3-32
SNR	Signal-to-Noise Ratio	4-5
PSD	Power Spectral Density	4-6
CPSD	Cross Power Spectral Density	4-7
ASIC	Application-Specific Integrated Circuit	4-11
DFN	Dual Flat No-Lead	4-11
TVAC	Thermal Vacuum	5-2
EMI	Electromagnetic Interference	5-2
IVT	Initial Verification Test	5-3

DETAILED DESIGN OF THE RIGIDIZABLE INFLATABLE GET-AWAY-SPECIAL EXPERIMENT

I. Introduction

Launching a satellite into space is extremely expensive, especially as the size of the satellite and the altitude of the orbit increase. As seen in Table 1.1, launching a heavy satellite (classified as roughly 11,000 kg – or 25,000 lbs – and greater) can cost more than \$50,000 per kg (\$23,000+ per pound)! The Rigidizable Inflatable Get-Away-Special Experiment (RIGEX) is a space experiment developed by the Air Force Institute (AFIT), designed to test a method of reducing a satellite’s structural weight and volume without sacrificing the large size and strength needed for supporting large objects in space.

Table 1.1: Cost of Launching Various Heavy Launch Vehicles [14]. Included in the table are costs to Low-Earth (LEO) and Geosynchronous Transfer Orbit (GTO) (FY2000 \$USD).

						
Vehicle Name	Ariane 5G	Long March 3B	Proton	Space Shuttle	Zenit 2	Zenit 3SL
Country/Region of Origin	Europe	China	Russia	USA	Ukraine	Multinational
Ref. LEO Altitude(km)	342	124	124	127	124	124
GTO Capacity(kg)	6,800	5,200	4,630	5,900	0	5,250
Est. Launch Price (\$USD, Million)	165	60	85	300	42.5	85
Est. LEO cost per kg (\$USD)	9,167	4,412	4,302	10,416	3,093	5,354
Est. GTO cost per kg (\$USD)	24,265	11,538	18,359	50,847	N/A	15,190

1.1 Background Information

RIGEX extends technology that has already been used in space. Inflatable structures have been flown multiple times in the past (dating back through the 1960's), while inflatable *rigidizable* structures are still relatively untested. The Inflatable Antenna Experiment, (IAE shown in Figure 1.1), developed by the Jet Propulsion Laboratory (JPL) and flown in 1996, is one example of a satellite that has used inflatable technology. Onboard the satellite was a 50-ft inflatable antenna, three 92-ft inflatable struts (built by L'Garde Inc., the same company that built the structures used in the RIGEX experiment), and all of the subsystems required to make the satellite work. Using this inflatable technology, the experiment condensed into the size of a grand piano and weighed only 60kg [20]. It flew successfully on Space Shuttle mission STS-77, helping to pave the way for new research in inflatable (and ultimately *rigidizable*) technology.

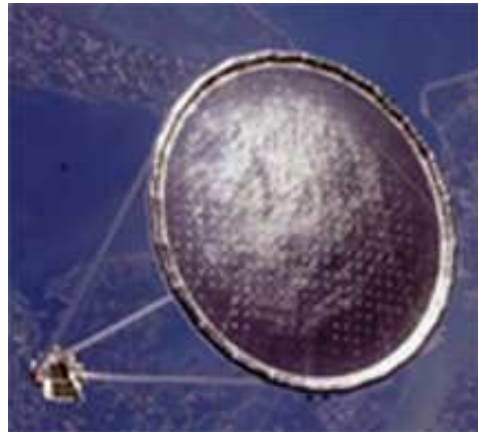


Figure 1.1: The Inflatable Antenna Experiment [20]. Shown here fully inflated, the experiment used three 92-ft inflatable struts to support its 50-ft inflatable antenna.

The key advantage to rigidizing inflatable structures is found in combining the strength of rigid structures with the low mass and volume characteristics boasted by their inflatable counterparts. Specifically, rigidized structures eliminate the need for the large, often bulky inflation system typically required to maintain a constant pressure throughout the length of their mission. With the vacuum of space, only

a very small amount of pressure can be used to inflate many structures (3-10 psi; IAE inflated with just 3psi [20]), which can be done with a relatively small system for initial pressurization. Once they are inflated and rigidized, they can be vented in a controlled manner (thus minimizing the risk of leaks acting as mini-thrusters if gas is inadvertently vented later on). Furthermore, since mass and volume are often tight commodities in the spacecraft-building business, the margins gained by using a smaller inflation system can be directed towards other more critical subsystems.

RIGEX uses inflatable tubes made from Kevlar and a proprietary polyurethane-based resin, provided by L'Garde Inc. With this combination of composite materials, the material exhibits what is known as a *Sub- T_g* property. The notation T_g refers to the *glass transition temperature* of the material, at which point it undergoes a slight phase change, transitioning from being firm and rigid to being soft and flexible. For example, the tubes used for RIGEX have a T_g of $125^{\circ}C$. Below this temperature, they are rigid, and the Kevlar fiber matrix will crack if it is bent. However, if heat is applied to the tubes such that the material temperature surpasses $125^{\circ}C$, they become soft and pliable. At this point, the tubes can be reset to any orientation. Then, once the material temperature cools below $125^{\circ}C$, it starts to become rigid again.

At the request of the Defense Advanced Research Projects Agency (DARPA), the RIGEX preliminary design began with a Master's thesis written by Captain John D. DiSebastian in 2000/2001. Since then, there have been six additional theses covering a variety of RIGEX topics in greater detail. Throughout its development, overall form, fit and function requirements of the National Aeronautics and Space Administration's (NASA) Space Shuttle have helped drive design decisions. Further, with the work of Lieutenant Thomas Philley and Captain Steven Lindemuth, RIGEX began working with the Department of Defense (DoD) Space Test Program's (STP) Shuttle Payloads Office in Houston, TX.

In 2004, STP revealed that the Get-Away-Special (GAS) canister (the method the Shuttle uses to carry smaller payloads into space that RIGEX was originally designed for) was no longer going to be flown on future missions. Instead, a new device called the Canister for All Payload Ejections (CAPE, developed by STP) would be used, shown in Figure 1.2.

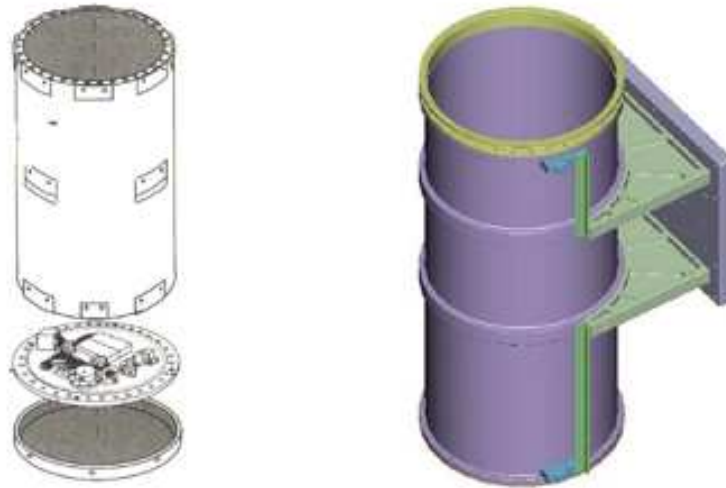


Figure 1.2: Images of GAS (left) and CAPE (right) Canisters. NOTE: Figure Not To Scale.

By switching over to the CAPE, there were design changes that needed to be made, but the advantages were well worth it. In particular, CAPE accommodates almost twice as much weight and volume than GAS does, so all prior concerns of saving (and *shaving*) weight were eliminated (see Table 1.2 for a comparison of GAS capabilities with those of the CAPE).

Table 1.2: CAPE vs. GAS Payload Envelope Comparison [23, p.25].

Maximum Allowable Specification	GAS	CAPE	Percent Difference
Weight (lb)	200	350	175%
Dimensions (in)	19.75(dia) x 28.25(height)	21(dia) x 53(height)	212%
Total Volume (in ³)	8,655	18,357	

In addition to the increased capabilities of the CAPE, STP also offered the use of Shuttle power, which eliminated approximately 80 pounds of batteries from the RIGEX design. While this made RIGEX safer (when using batteries in space, special caution must be taken to ensure no leakage can occur), modifications to the electrical power system were required to properly interface with the Shuttle’s avionics.

In 2005, a Memorandum of Agreement (MOA) between AFIT and STP was signed, creating a close-working partnership critical to the success of the mission. This thesis picks up from past students with the signing of the MOA and covers the modifications made in order to transfer RIGEX from GAS to CAPE, as well as a few additional modifications made in order to ensure mission success.

1.2 *Experiment Objectives*

There are two types of objectives identified below. *Primary* objectives are those considered essential for mission success, while *secondary* objectives identify tasks required to improve the quality of the experiment. From the very beginning, the RIGEX mission and objectives have been clear. In his thesis, DiSebastian defined the following [11]:

- **Mission Statement:** Verify and validate ground testing of inflation and rigidization methods for inflatable space structures against the zero-gravity space environment
- **Primary Objective:** Design a Get-Away-Special (REVISED: CANISTER FOR ALL PAYLOAD EJECTIONS) experiment to collect data on space rigidized structures for validation of ground testing methods
- **Secondary Objectives:**
 - Return inflated/rigidized structures to laboratory for additional testing
 - Enable application of rigidized structures to operational space systems
 - Implement systems engineering principles into the experiment’s design

With the exception of the revision to the primary objective, all of the original objectives are still in effect today. These objectives, along with the Shuttle’s requirements, guide all decisions made by the RIGEX team. In addition to the objectives

identified above, however, the lack of an onboard telemetry system also implies the following objectives required for a successful mission:

- **Additional Primary Objectives**

- Recover the RIGEX payload
- Post-process the experiment’s flight data at AFIT

Perhaps the most significant of all objectives is *recovering the RIGEX payload*. This one objective alone drives nearly every decision involved on the RIGEX program as it narrows the field of applicable launch vehicles down to just the Space Shuttle, currently the United States’ only method of recoverable access to space. Furthermore, the manned nature of a Shuttle spaceflight mission extends *significant* responsibility, particularly in the area of safety, to each of its payloads. Although RIGEX was quoted to be “the easiest program I’ve ever dealt with [in part due to the elimination of safety concerns from earlier design decisions]” by STP’s lead safety engineer for RIGEX [28], there were still significant design changes needed in order to satisfy safety-driven requirements. As a result, many of the topics discussed in this thesis will cover safety-related updates.

1.3 Thesis Overview

The big picture presented by this thesis is outlined and then briefly discussed below:

- Chapter I: Introduction of the experiment and research goals
- Chapter II: Review of past student research
- Chapter III: Discussion of modifications to the experiment
- Chapter IV: Discussion of analyses and results
- Chapter V: Conclusion and recommendations
- Appendices: Memorandum of Agreement with the Department of Defense Space Test Program; Program Requirements Document; shroud containment analyses; mechanical drawings; electrical architecture

Following this introduction, Chapter II reviews pertinent information presented in each of the past theses written by RIGEX researchers. In particular, each student's methodology and results are discussed to provide a general idea of the experiment's historical progress and status before the requirement-related changes covered in Chapter III took place.

Chapter III then presents the decisions and modifications made to RIGEX (along with their associated rationale) in order to meet Shuttle specifications. While most modifications were to the structural or electrical in nature, changes were also made to the inflation system and command and data handling system.

Chapter IV presents the results of a shroud containment analysis, as well as the results of modifications made to the modal analysis methods performed by the experiment.

Chapter V concludes with a description and recommendations involving steps and tasks that will need to be accomplished before RIGEX is delivered to STP.

II. RIGEX Evolution

The RIGEX payload has come a long way over the past 5 years, and in order to fully appreciate the modifications discussed in Chapter III, it is important to understand this evolution. Therefore, beginning with DiSebastian’s preliminary design, this chapter summarizes the key contributions made by each of the previous RIGEX researchers, along with their pertinent results.

2.1 *John D. DiSebastian, Thesis, 2001*

Captain John DiSebastian was the first student to work on the RIGEX program. As such, he was responsible for initiating the experiment’s design. To do this, he worked together with L’Garde Incorporated to utilize the latest technology in inflatable and rigidizable structures. He also coordinated with the Defense Advance Research Projects Agency (DARPA), the experiment’s sponsor, to ensure the methods he used would accurately represent efficient methods for use in the future.

In this section, DiSebastian’s journey from preliminary discussions to preliminary design is reviewed. In particular, he began with an analysis of several systems engineering (SE) approaches used in satellite development. Then, after deciding upon one to follow, he tackled the plethora of iterations necessary to determine the design layout as well as the types of components best suited for the payload. Next, he conducted a number of preliminary analyses (cost, weight, etc.) to get an idea of what to expect as the payload matured. Finally, he wrapped up his efforts with the first definition of the operations concept for the on-orbit mission.

2.1.1 Systems Engineering Approach. First, as a graduate student of the Systems Engineering program at AFIT, DiSebastian studied and considered the following systems engineering approaches used throughout the engineering industry:

- The Space Mission Analysis and Design (SMAD) model [32]
- The Institute of Electrical and Electronics Engineers (IEEE) model [1]
- Hall’s model [16]

After weighing the advantages and disadvantages of each, he ultimately decided to follow the NASA process, shown in Table 2.1.

Table 2.1: NASA Systems Engineering Process. DiSebastian used this to accomplish the preliminary design. [11, p. 1-6]

Step	Description
1	Recognize Need or Opportunity
2	Identify or Quantify Goals
3	Create Alternative Design Concepts
4	Do Trade Studies
5	Select Concept
6	Increase Resolution of the Design
7	Perform the Mission

The NASA process was chosen because it offered the most applicable framework for this kind of project. Furthermore, since the experiment was baselined to fly on the Shuttle, the NASA model was expected to offer additional compatibility. Following this process, DiSebastian defined the experiment’s mission statement and objectives identified in Chapter I. All of the results presented in the remainder of this section came about by following this SE process.

2.1.2 Component Selection. Selecting components for a preliminary design is iterative, refining with each advancement of the design layout. In his thesis, DiSebastian describes his component selection iterations in detail for each of his defined RIGEX subsystems. These subsystems included the mechanical structure, the inflatable structures, the inflation and rigidization methods, the electrical power subsystem, the thermal subsystem, command and control, data collection and storage, and the payload’s sensors. Table 2.2 summarizes the decisions made throughout this phase of his research. Further information, including the reasoning behind each decision identified in the table, is given in Chapter III of his thesis.

DiSebastian was also able to narrow down the requirements for the particular sensors that would be needed on RIGEX. While the actual sensors were not chosen at the time, Table 2.3 lists the requirements he defined for each particular one.

Table 2.2: DiSebastian’s Component Selection Decisions [11, p. 3-17].

Component	Decision
Mechanical Structure	Layout driven by component selection (see Figure 2.1)
Inflatable Structure	Tube with 2-inch diameter, 22-inch length
Inflation System	Nitrogen gas at 4 pounds per square inch (absolute)
Rigidization System	Sub- T_g tube (T_g = Glass Temperature, or the temperature at which the tube transitions from a rigid to a flexible state; set to $125^\circ C$ for RIGEX)
Electrical Power	Alkaline D-size batteries, scaled to power requirement
Command & Control	Computer using PC-104 architecture
Data Handling	Non-volatile memory chips in computer
Sensors	Pressure, acceleration, voltage, force, static position (using digital camera), temperature (using MINCO heaters)

Table 2.3: DiSebastian’s Sensor Requirements [11, p. 3-17].

Sensor Type	Location	Sensitivity	Size
Pressure	Tubes	0.001 atm	1/4-inch fitting
	Environment	0.001 atm	n/a
Acceleration	Tubes	10 mV/g	\leq 1-inch cube
	Environment	20 mV/g	n/a
Voltage	Power Supply	0.5 V	n/a
Static Position	Flight	1 mm	\leq 2-inch height
	Ground Testing	5 μ m	n/a
Temperature	Tubes	$0.5^\circ C$	0.5-inch square
	Environment	$0.5^\circ C$	1-inch square
	Components	$1^\circ C$	internal

Although components have been upgraded and further defined since DiSebastian’s time, his efforts in this area were crucial to the results of a complete preliminary design.

2.1.3 Component Layout. Using the components described above, DiSebastian laid the critical foundation of the experiment, integrating each component together to form the complete assembly shown in Figure 2.1. Visible in the image are his designs for the mechanical structure, the sub- T_g tubes, a portion of the infla-

tion system, the oven assemblies, and the locations for the battery and the PC-104 computer.

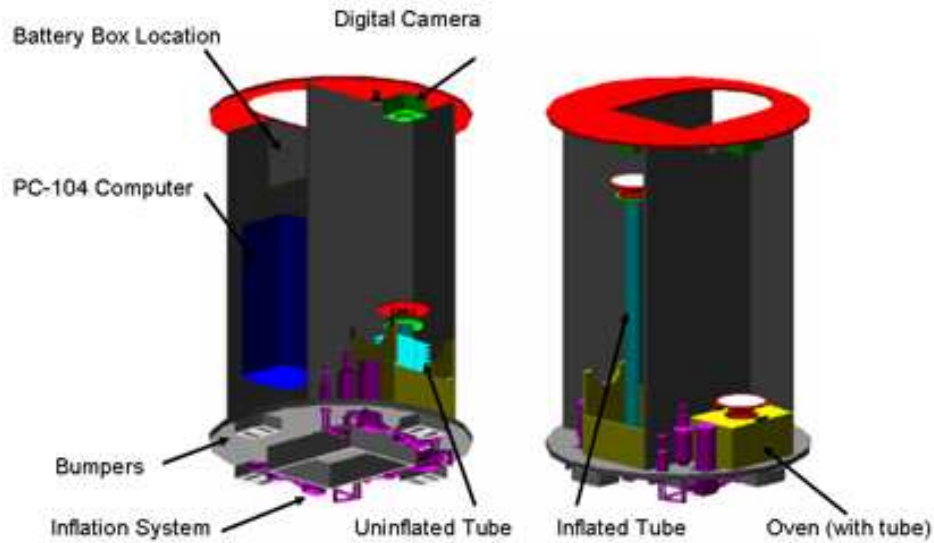


Figure 2.1: DiSebastian's Preliminary Design Assembly [11, p 4.2].

2.1.4 Preliminary Analyses. Next, in addition to the physical aspects of RIGEX's preliminary design, DiSebastian also performed a number of analyses on the payload. Namely, he completed the first cost, weight, and data storage analyses. A summary of his results is shown in Table 2.4.

Table 2.4: DiSebastian's Preliminary Analyses Results [11, pp.4-34,41,42].

Analysis	Result	Value
Data Storage	Memory required	52.88 Mb
Weight	Total Weight	191.62 lb
Cost	Total Cost	\$29,130

2.1.5 Operations Concept. Finally, the last key result of DiSebastian's efforts was a well-defined Main Event Calendar, or operations concept, shown in Table 2.5. The particular items to notice are events 7, 8, and 9, which point out that initially, each one of these operations was to be completed for each tube before the next operation would begin. This has since been changed such that the operations

for an entire tube would be completed before the operations of a next tube would begin. From a mission success standpoint, completing one tube as quickly as possible minimizes the effects of a loss of power, computer upset, or similar interruption to the experiment.

Table 2.5: DiSebastian's Main Event Calendar [11, p. 4-31].

Event	Description
1	Activate environmental heaters at 50,000 feet
2	Shuttle crew activates experiment
3	Computer boot-up & diagnostic
4	Reset primary timer to Zero
5	Activate Environmental sensors
6	Check failsafe file and skip to appropriate point of experiment
7	Begin inflation process (inflate 3 tubes sequentially)
8	Begin venting process (vent 3 tubes sequentially)
9	Begin excitation process (excite 3 tubes sequentially)
10	Deactivate environmental sensors
11	Mark final failsafe point
12	Shutdown computer
13	Shuttle crew deactivates experiment

2.1.6 Section Summary. DiSebastian took advantage of his systems engineering education and experience to set RIGEX off on a strong foot forward. His key contributions to its development included a defined systems engineering approach, decisions for preliminary component selection and layout, important preliminary analyses, and an operations concept. The remaining sections in this chapter will all build upon his initial efforts.

2.2 Thomas G. Single, Thesis, 2002

The second engineer to work on the RIGEX program, Captain Thomas Single, was a student of the astronautical engineering program at AFIT. He was primarily interested in the study of vibrations, and as such, he set the next step in the evolution of RIGEX to be the vibration analysis of the inflatable tubes. Using both long and short tubes supplied from L'Garde, Inc (50 inches and 20 inches, respectively), as well

as the vibration facility and thermal vacuum chamber at AFIT, Single was able to accurately determine the tubes' modal properties (natural frequencies and damping coefficients) at varying ambient temperatures and internal pressure levels.

Single had six of the short inflatable tubes and three of the long ones to use for his tests. Unfortunately, because the technology to make them is still emerging even to this day, there were some irregularities that occurred during their construction. Due to these irregularities, Single defined a way to label and keep track of each tube. Section 2.2.1 describes his tube nomenclature and the irregularities, while Section 2.2.2 describes the tests he conducted.

2.2.1 Tube Characterization. Before performing any tests, Single knew he would need to define a method of identifying and tracking which tube was being used for each test. Furthermore, since the tubes' flanges had four holes in them (for mounting them to the main RIGEX structure), and since the irregularities were at different locations among each individual tube, he also knew that he would need a method of identifying the orientation of the tube during each test.

To do this, he numbered each short tube as "S" 01-06, and each long tube as "L" 01-03. Then, in order to keep the orientation consistent, he also numbered each hole 1-4. Finally, when he mounted each tube on his vibration table, he noted the hole closest to the table's shaker arm. Using all of this information, he defined the tube designator for each test. For example, referring to Figure 2.2, L01-1 would indicate a test using long tube #1, with hole #1 being closest to the shaker arm.

During testing, he discovered that different orientations revealed only a *very small* difference in the first bending modes of the tubes. This was due to the manufacturing process. When L'Garde created the tubes, they needed to join the two ends of Kevlar to form a tube. The seam this created appeared to add a slight amount of stiffness, but only enough to raise the natural frequencies by less than 1/2 Hz. Therefore, it is accurate to say that tube orientation during his tests proved to be insignificant.

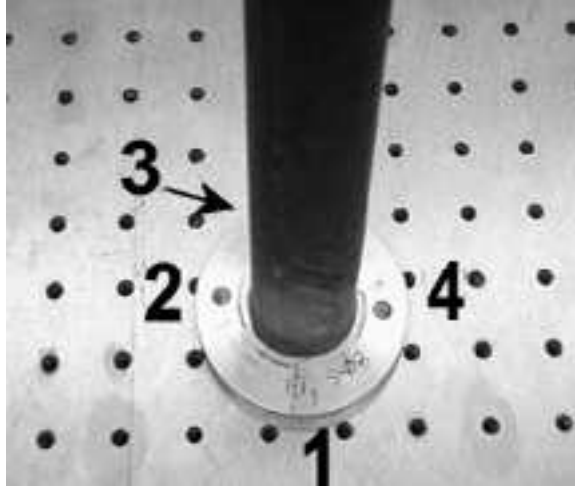


Figure 2.2: Single's Tube Orientation Scheme. Using this scheme, Single was able to keep track of not only which tube he used for each of his tests, but also of which orientation the tube was placed in [29, p.3-3].

Next, the tube irregularities themselves included differences in height, diameter, weight, and surface properties. The height variance among all the tubes was estimated to be less than $1/4$ of an inch, but exact height measurements were not recorded at the time. The remaining physical properties are summarized in Table 2.6

Table 2.6: Tube Physical Properties. Shown here are the differences among each tube [29, pp.3-7,8].

Tube	Property	
	<i>Average Diameter (in)</i>	<i>Mass (g)</i>
S02	1.55	199.13
S03	1.57	194.90
S04	1.42	197.79
S05	1.53	190.34
S06	1.38	197.64
L01	1.43	245.02
L03	1.59	247.25

Each tube had at least some form of irregularity, but most were suitable for testing. In fact, only tubes S01 and L02 were eliminated from testing due to their

excessive leakage characteristics. Figure 2.3 shows an example of a surface irregularity in L03 as compared to L01, which was noted to be among the smoothest of all tubes.

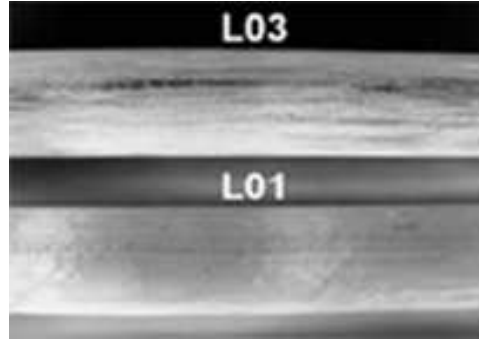


Figure 2.3: Tube Surface Irregularity Example. This image was taken with a digital camera's negative effect to enhance clarity [29, p.3-6]

2.2.2 Vibration Testing. Once the tubes were fully characterized, Single began his vibration tests, dividing them into one of two areas:

- Vibration tests in ambient conditions using shaker under varying internal tube pressures.
- Vibration tests using piezoelectric (Lead-Zirconate-Titanate PZT) patches attached to the base of the tube
- Collect data inside the vacuum chamber at both ambient and vacuum pressure, at $10^{\circ}C$ increments from $25^{\circ}C$ to $95^{\circ}C$, using HP VXI.

The first set of tests were conducted using the vibration facility's shaker and an HP VXI data acquisition system (also referred to as *dSpace*). The HP VXI, coupled with Data Physics Corporation's *SignalCalc* software, is a 16-channel data acquisition system, shown in Figure 2.4. The intent of this test was to determine the modal characteristics of the tubes using the well-understood shaker before moving to the PZTs. This portion of his experimental setup is shown in Figure 2.5.

The test verified that the length of the tubes significantly affected the tubes modal properties, as expected. The longer tubes had lower natural frequencies than the short tubes, as is the case for beams and tubes that have the same material properties and cross-sectional geometry. The results are shown in Table 2.7.



Figure 2.4: HP VXI Data Acquisition System. Included in the image is a screen capture of the SignalCalc software [29, p.3-12].

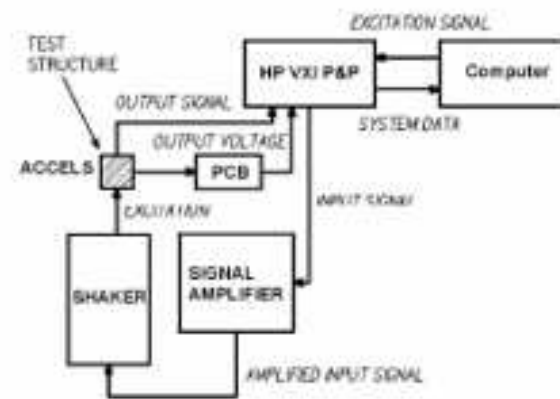


Figure 2.5: Single's Experiment Setup. Shown in the figure is the HP VXI acquisition system he used [29, p.3-11].

Although he performed tests with varying levels of tube internal pressure, only values for 0 psi gauge are presented for brevity (as well as the fact that tube internal pressure will be 0 psi gauge during flight). To determine these values, he utilized an Eigenstructure Realization Algorithm (ERA) routine (developed using Matlab® by Cobb [5]).

For the second set of tests, he used the Polytec Scanning Vibrometer (PSV) and its software to compare the modal results of PZT actuation with those of shaker actuation. The PSV is a laser vibrometer that measures and records velocity of a moving object. The software then uses the recorded data to determine not only the

Table 2.7: Summary of Tube Modal Properties Using Shaker Excitation. The modal properties included in this table were found by mounting each tube on the test stand using a tube internal pressure of 0 psi gauge [29, pp4-8,13].

Tube	Mode #	Frequency (Hz)	Damping (%)
S02	1	32.12	2.16
	2	61.26	1.8
	3	230.22	1.19
S04	1	31.63	2.43
	2	60.87	1.67
	3	229.59	1.27
L01	1	24.4	2.4
	2	55.4	4.95
	3	117.0	0.7
L03	1	24.5	1.95
	2	56.8	1.96
	3	115.7	0.46

object's natural frequencies, but perhaps more significantly, the object's mode shapes. It will even animate the mode shapes to enhance understanding of how the object deflects at certain frequencies. The PSV and its software are shown in Figure 2.6, and the results are shown in Table 2.8.

Table 2.8: Comparison of Tube Modal Properties Under Varying Excitation Sources. The following data was taken from Tube S03 mounted to the test stand [29, p.4-22].

Mode	PZT Driving	Shaker Driving
1	32.76	33.44
2	61.82	62.19
3	229.96	231.88

Next, during the third set of tests, he noted that increased temperature (particularly between $45^{\circ}C$ and $65^{\circ}C$), moderately effected to the tubes modal properties. As expected, increased heat softens the tube, lowering its natural frequency and increasing its damping coefficients. A summary of these results can be seen in Table 2.9.

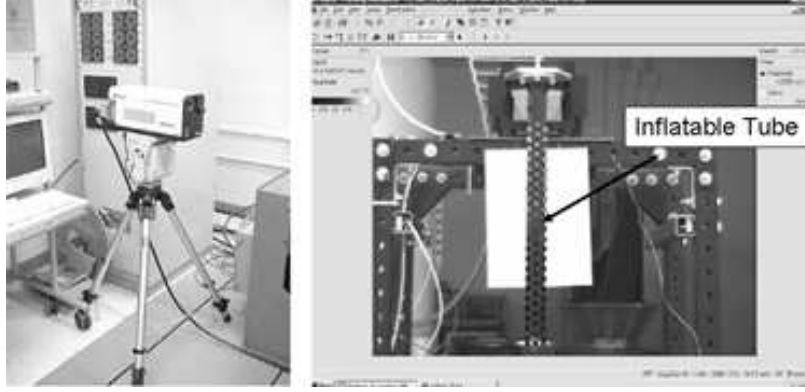


Figure 2.6: PSV 300 Laser Vibrometer. A screen shot of the software is also included in the image. Note the square mesh covering the inflated tube. The PSV uses a laser to measure velocity at each of these nodes *sequentially* [29, p.3-25].

Table 2.9: Summary of Single’s Vacuum Test Results for Short Tubes [29, p.4-23]. Note: tube internal pressure during test was 0 psi gauge.

Temperature ($^{\circ}C$):	25	35	45	55	65	75	85	95
Mode 1 (Hz):	51.18	51.1	50.81	50.08	49.13	47.74	46.59	45.55
Mode 2 (Hz):	64.25	63.78	63.43	62.82	62.61	62.4	62.23	62.15
Mode 3 (Hz):	231.58	231.42	235.05	227.89	229.14	229.26	229.77	222.98

The pressure level inside the tubes was found to have almost no impact on the modal properties. However, testing in the vacuum chamber did identify a reduction of up to 1.5% in damping coefficients at near-vacuum levels. This was expected as the presence of air molecules will typically add a small amount of damping to a structure.

2.2.3 Section Summary. In summary, Single’s efforts led to a much better understanding of the tube’s modal properties. With the completion of his research, RIGEX took its first steps in the area of experimental analysis. Now, follow-on students could focus on overall payload development, including integrating the vibration tests Single did onto the payload itself.

2.3 Thomas L. Philley, Thesis, 2003

Capt “Lee” Philley was the third graduate student to work on the RIGEX project. His goals were to:

- Build and test a working prototype of RIGEX
- Perform vibration analysis of new inflatable tubes
- Begin coordination with the DoD Space Test Program

During his time at AFIT, new Sub- T_g tubes were provided by L’Garde. To enhance pressure retention, L’Garde built new tubes, each with Kapton tape lining the internal and external faces of the Sub- T_g material. Using these new tubes and AFIT’s thermal vacuum chamber, he was able to accomplish these tasks.

2.3.1 RIGEX Prototype. As part of building and testing a working prototype of RIGEX, Philley wanted his results to represent flight conditions as closely as possible. Therefore, he set out to use AFIT’s thermal vacuum chamber for his research. Unfortunately, the opening of the chamber was only 18 inches, or 1.5 inches too small for the 19.5-inch diameter top and bottom surfaces. Therefore, he instead built what is now called the *quarter structure* (see Figure 2.7). The quarter structure included one full bay of the RIGEX experiment, including the inflatable tube assembly, oven, inflation system, and digital camera.

2.3.2 Deployment Tests. Using his quarter structure, Philley conducted two deployment tests using the new tubes, recording oven and tube temperature throughout each. The first was not as successful as the second, however. Unfortunately, there was a manufacturing error with the new tubes [27, p.4-17], and although 20-inch tubes were requested, 24-inch tubes were delivered (in a folded configuration, this difference was unnoticed). The quarter structure setup, however, was only designed to take the 20-inch tubes. In particular, the location of the digital camera interfered with the tube’s inflation. In addition, Philley also saw an unexpectedly high pressure level of 6 psi (gauge) inside the tube (4 psig was expected). He attributed this error to a malfunctioning pressure regulator.

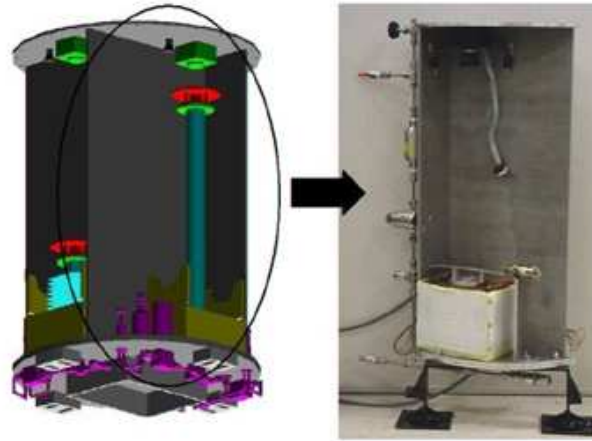


Figure 2.7: Philley's Quarter Structure. The quarter structure was built to fit inside the thermal vacuum chamber at AFIT [27, p.3-2].

After moving the camera out of the way, introducing a flow control valve to prevent rapid over-pressurization, and readjusting the pressure regulator to only allow 4 psig into the tube, Philley used a second inflatable tube for his second deployment test. This time, the test was nearly perfect; however, there was a small glitch in the inflation again, however, as the pressure inside the tube only reached 2.5 psig. Apparently, the combination of the flow control valve, the pressure regulator, and what Philley thought to be an apparent leak in the new tube, had prevented the complete pressurization of the tube. That being said, it still inflated perfectly, as seen in Figure 2.8. Therefore, with this test, Philley was able to successfully verify the heating and inflation systems, as well as the fact that proper inflation is somewhat insensitive to pressurization levels.

2.3.3 Vibration Analysis. Philley used PZT's to excite the new tubes, taking data with both the HP and the PSV. Using the configurations shown in Figure 2.9, he determined the natural frequencies and modal damping coefficients of the tubes.



Figure 2.8: Philley's Deployment Tests [27, pp.4-18,26]. The tubes supplied by L'Garde were 4 inches longer than expected, as seen in the left image. After modifying the structure, the inflation was successful.

Test Configuration	Description
1a	Table-mounted using HP system
1b	Table-mounted using PSV system
2a	Stand-mounted using HP system
2b	Stand-mounted using PSV system
3a	Structure-mounted on stand using HP system
3b	Structure-mounted on stand using PSV system
4	Structure-mounted in vacuum tank using HP system



(a) 1a



(b) 1b



(c) 2b



(d) 3a



(e) 3b



(f) 4

Figure 2.9: Philley's Vibration Test Configurations [27, p.3-21].

The results for the vibration tests are summarized in Table 2.10. The key data points are the *structure-mounted* values, for it will be these values that flight data is compared with.

Table 2.10: Philley’s Vibration Results [27, pp.4-34].

First Bending Mode				
Parameter	Mount Location			
	Table	Stand	Structure	Vacuum Tank
Natural Frequency (Hz)	59.6875	37.5	60.3125	60.625
Damping Ration (%)	0.78	0.83	0.52	1.04
Second Bending Mode				
Parameter	Mount Location			
	Table	Stand	Structure	Vacuum Tank
Natural Frequency (Hz)	660	542.1875	654.0625	651.25
Damping Ration (%)	0.64	0.32	0.53	0.57

The other results in the table are the damping values of the tubes. Philley attributed the small errors between values to inaccuracies in using the half-power method ($\zeta = \frac{\omega_2 - \omega_1}{\omega_2 + \omega_1}$). In this method, a frequency response function (FRF, see Figure 2.10 for an example of one of Philley’s FRF’s) is used to find frequencies associated with a 3 dB drop in power from a natural frequency’s peak, both above and below the natural frequency (ω_2 and ω_1 , respectively). The frequencies are then plugged into the equation for the half-power method, and the damping ratio (ζ) is calculated. While the process of picking off values of an FRF may induce some errors in damping ratio results, the errors are typically small enough such that the method’s straightforward calculation make it a popular tool to use.

2.3.4 DoD Space Experiments Review Board. Philley also initiated the process required to for RIGEX to meet the DoD Space Experiments Review Board (SERB). The SERB meets every year to rack and stack all DoD space experiments. Once this prioritization is established, the DoD Space Test Program (STP) takes over

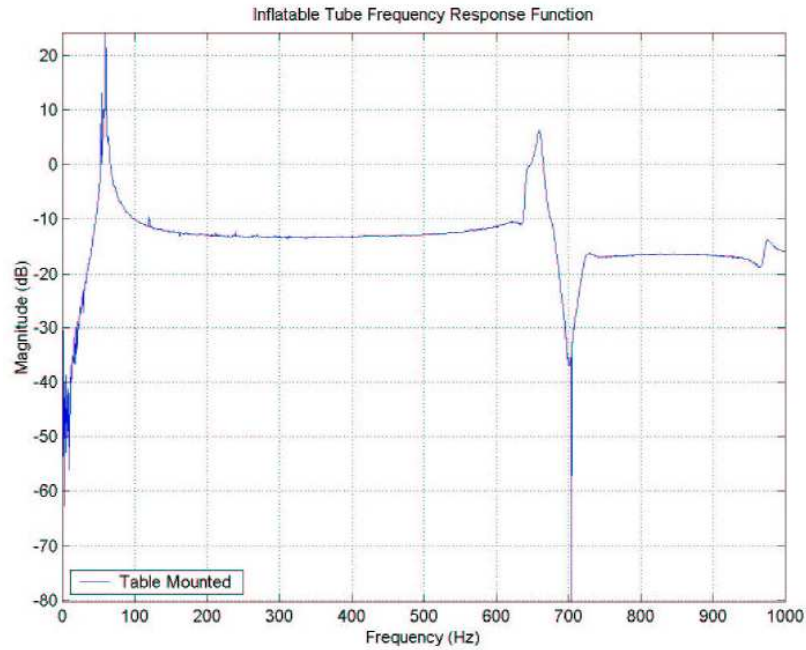


Figure 2.10: Example Tube Frequency Response Function [27, p.4-27].

and determines the best method of access to space for as many experiments as fiscally possible.

As Philley was previously assigned to STP, he and the new faculty advisor (Dr. Richard Cobb) recognized that the key to planning a successful Shuttle mission begins with STP and the SERB. Although it was still too early to get too far in the process, their foresight led to the experiment's SERB approval, which would eventually lead to being manifested on a Shuttle mission.

2.3.5 Section Summary. Philley's efforts concentrated primarily on testing new tubes from L'Garde with a working prototype of the RIGEX payload. While the prototype was only a 1/4 of the actual design, it allowed his tests to be conducted in the AFIT thermal vacuum chamber, providing significant insight into the way the tube will deploy on orbit. This section presented information on his prototype structure, his deployment and vibration tests, and the SERB process.

2.4 *Raymond G. Holstein III, Thesis, 2004*

After Single and Philley had each completed exhaustive vibration analyses of their respective sets of tubes, Captain Ray Holstein decided to do the same for the complete RIGEX assembly. Holstein was one of three students working on RIGEX at the time, alongside Captain Steven Lindemuth and Lieutenant David Moody. Working together, the team helped the RIGEX evolution leap forward, bringing it very close to the point of readiness for the Preliminary Design Review (PDR) with STP. Holstein's efforts on the structural side were a significant catalyst to this advancement.

Specifically, the first of Holstein's contributions was the refined development of the structural design. Using Pro/ENGINEER[®] computer-aided-drafting software, Holstein made models of each of the aluminum plates. Furthermore, since the advantages of using Pro/ENGINEER[®] are in its ability to easily produce drawings for the machine shop, as well as in its portability among other popular engineering software programs, Holstein was able to use his drawings to have the RIGEX structure fabricated and then transfer them into ABAQUS[®] to conduct his structural analyses.

ABAQUS[®] is a powerful Finite Element Analysis (FEA) software package used to analytically conduct several types of structural analyses, including eigen analyses (i.e. finding natural frequencies and their associated mode shapes) and stress analyses (finding areas of high stress concentration). It allows the engineer to adjust boundary and loading conditions, element size and type, material properties, etc, without recreating the entire model.

Once the analyses were complete, he conducted laboratory tests to validate his results. Section 2.4.1 presents his analytical approach, while Section 2.4.2 presents his experimental approach.

2.4.1 Finite Element Analysis. Holstein used ABAQUS[®] to develop both a complete *unmassed* and *massed* finite element model (FEM) for the RIGEX quarter structure and for the full structure. His unmassed model, which is a type of model that is designed to save computation time by only including key structural mem-

bers/components, included the aluminum plates for each assembly. Once they were complete, he massed the models, adding in the mass of the ovens, inflation system, inflatable tubes, and computer. He also varied the size of his elements used, giving him the ability to compare the results of a *coarse* mesh with those of a *fine* mesh. Finally, for his stress analysis, he also varied the loading conditions, simulating loads from 1g all the way up to 20g's. Figure 2.11 shows his completed massed model of the full structure.

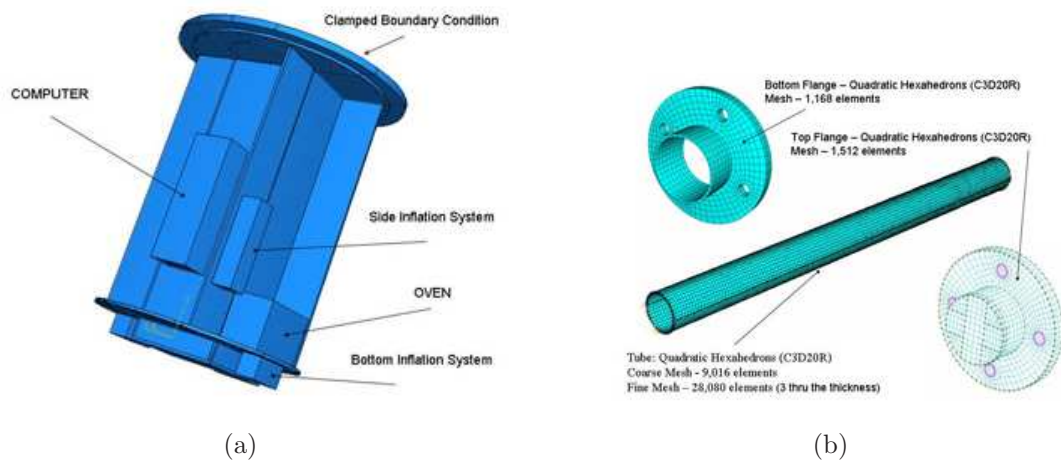


Figure 2.11: Holstein's Finite Element Models.

- (a) Massed structure, including mass simulators for the ovens, inflation system, inflatable tubes, and computer [19, p.45].
 (b) Inflatable Tube Finite Element Model [19, p.36]. Shown in the figure are the types of elements he used.

In addition to the FE models of the complete payload, Holstein also built a detailed model of the inflatable tubes, shown in Figure 2.11(b). Using this model, he was able to compare his results with those found by Single and Philley under varying boundary conditions (specifically, simply supported and clamped).

The tube's analysis showed the first and second bending modes correlated very closely with earlier tube vibration tests performed by Single and Philley. Recalling from Table 2.10, Philley determined the first two modes of the tube to be 59.688 Hz and 660 Hz, respectively. As shown in Table 2.11, the analytic results differed from

past experimental results by under 2.1%. The mode shapes for each of these modes can be seen in Figure 2.12.

Table 2.11: Holstein's Tube Finite Element Analysis Results [19, p.64].

Mode	Philley's Results	Holstein's Results	Percent Difference
1 st Bending Mode (Hz)	59.688	58.441	2.09%
hline 2 nd Bending Mode (Hz)	660	651.90	1.21%

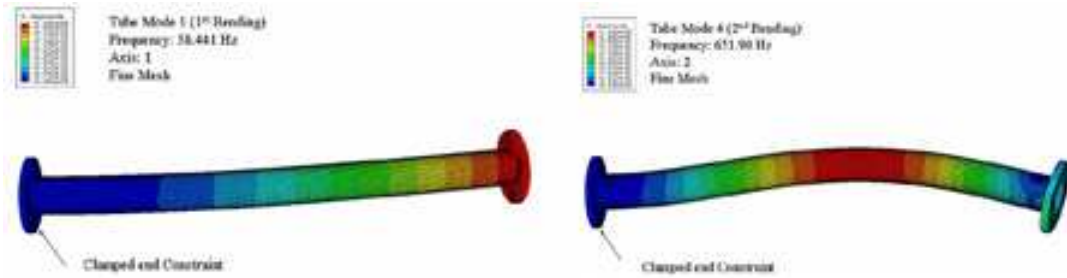


Figure 2.12: Holstein's Tube Finite Element Analysis Results for Inflatable Tube [19, p.61]. Shown here are ABAQUS[®] screen captures for bending modes #1 and #2, calculated to be 58.441 Hz and 651.90 Hz, respectively.

Moving on, his results for the full structure are summarized in Table 2.12 (Note: his results for the analysis of the quarter structure are summarized on page 69 of his thesis). In the table, drastic differences in the first mode of the structure are shown. These are expected, as each model represents an increase in accuracy as model parameters are chosen. Specifically, 3-dimensional elements are typically more precise than 2-dimensional elements, quadratic interpolation is more precise than linear interpolation, and accuracy generally increases as a model's mesh size is refined.

Furthermore, the natural frequency of the massed model is expected to be significantly lower than those of the unmassed models. As mass is added to a model, while stiffness is not, natural frequencies will decrease. A simplified example can be seen in the case of an undamped spring-mass system, where a frictionless mass is connected to a spring, which is also connected to a wall. The system's natural frequency can be calculated by the equation, $\omega_n = \sqrt{\frac{k}{m}}$ where k is the spring stiffness coefficient, and m is the mass. As mass is increased, the natural frequency goes down.

Table 2.12: Holstein’s Structural Finite Element Analysis Results [19, p.79].

Model	Mode 1 (Hz)
2-D element, linear, coarse mesh, unmassed	178
2-D element, quadratic, coarse mesh, unmassed	147.17
3-D element, quadratic, fine mesh, unmassed	113.4
3-D element, quadratic, fine mesh, massed	54.35

Figure 2.13 shows an example of ABAQUS[®] screen captures for the structure’s deflections when excited at its first mode (i.e. the mode shape of the first mode). A structure for both 2-dimensional and 3-dimensional elements is included (Note: the 2-dimensional model is shown inverted from the 3-dimensional model). Both images show the structure cantilevered from the top end (bottom end is identified with the box protruding from the bottom plate). While difficult to see in the image, the max displacement of the bottom end is predicted to be 1.074 inches for the unmassed model, and 1.218 inches for the massed model. This was expected as well, since a significant amount of mass is located at the free end of the structure.

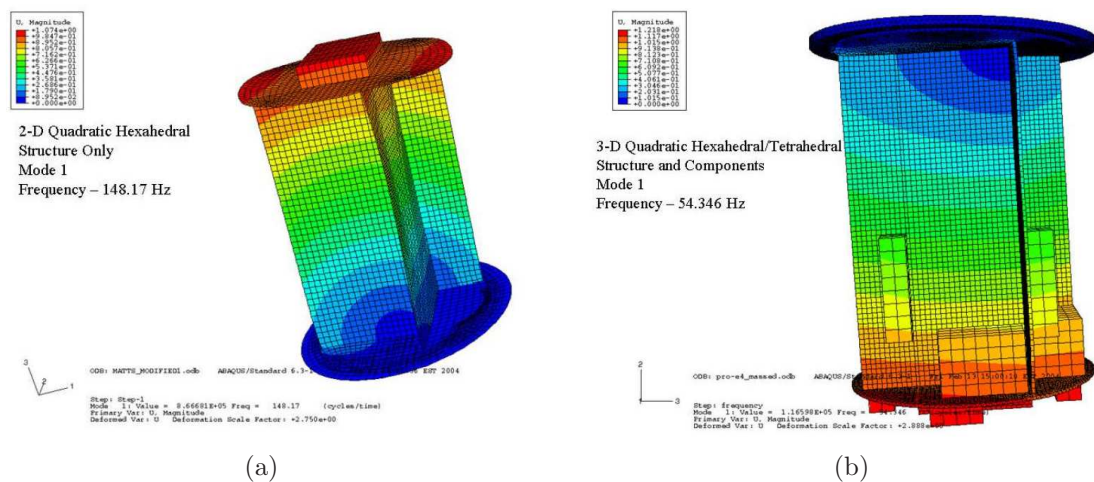


Figure 2.13: Full Structure Finite Element Analysis Results [19, p.73,77].

- (a) Structure created with 2-dimensional elements and quadratic interpolation
- (b) Structure created with 3-dimensional elements and quadratic interpolation

Next, the *most critical result* came not from his eigen analyses, but rather from his stress analysis. When applying a load of 20g’s to RIGEX, Holstein found that there

was a small stress concentration of 50 ksi on the top plate. Unfortunately, according to Military Handbook 5H, the yield stress of this type of aluminum (AL-6061 T-6) is only 36 ksi [6]. To combat this, two changes were made to RIGEX:

- Eliminate computer access hole on top plate
- Increase thickness of top plate

Holstein did not have time to analyze the structure with these changes; however, Lieutenant Sarah Helms picked up where he left off and conducted an analysis of her own. Her thesis [17] is currently being written, however, so specific information is not available at this time.

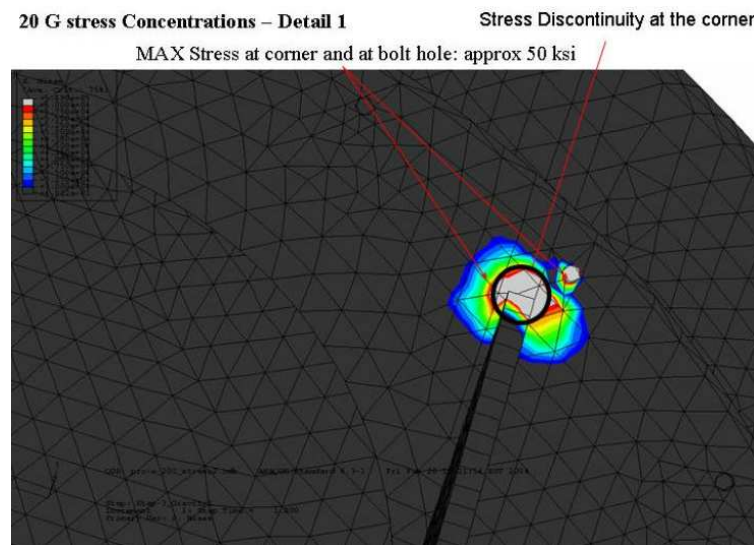


Figure 2.14: Holstein's Full Structure Stress Analysis Results for Full Structure [19, p.86]. The image shows a significant stress concentration at one of the holes on the top plate.

Next, with the structure fabricated and the results of the FEM analysis complete, Holstein set out to compare his analytical results with some experimental data. The next section describes the experimental setup he used for his tests.

2.4.2 Experimental Testing. Holstein expected his model that included 3-dimensional elements, quadratic interpolation, and a fine mesh to be the most accurate model, but he still needed to verify this hypothesis. To do this, he decided to conduct

ping testing on the structure in the lab using a ping hammer to excite the structure and the same Polytec Scanning Vibrometer Philley used to record the response. He also conducted ping testing on the inflatable tubes, using an accelerometer to record the response. Figure 2.15 gives the vibrometer's eye view of the full structure test. It also shows the hammer location, which is the spot that was stricken with the ping hammer.

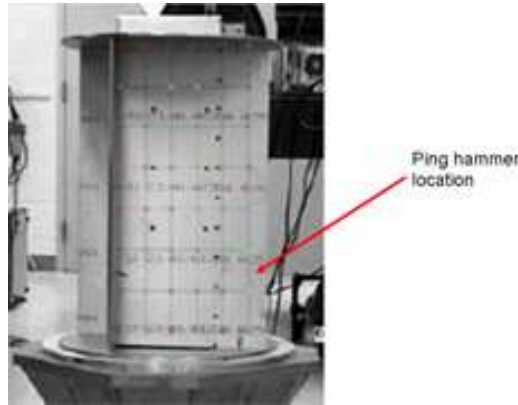


Figure 2.15: Holstein's Ping Test Setup. The hammer location is the spot which was stricken with the ping hammer. The laser vibrometer (PSV) was used to capture the structure's response during the test [19, p.47].

The ping testing showed that his models for the structure were not quite as accurate as his models for the tubes. Shown in Table 2.13, the analytic frequencies were significantly higher than his experimental results. He adjusted the types of elements he used, but that did not present a significant enough change to attribute element type as the cause of error. Therefore, he rechecked his experimental setup and was able to attribute some of the difference to loose fasteners along the top plate. He also recognized that he used an inexact replica of the fastener hole pattern in his model. Unfortunately, however, he did not have the time to correct his model.

2.4.3 Section Summary. This section reviewed Holstein's finite element analysis efforts for the tube and the RIGEX structure. Results for the tube correlated well with experimental results, while those of the structure did not quite correlate so well. Although his analysis may not have been completely accurate, it was close

Table 2.13: Holstein’s Experimental Results [19, p.79].

Model	Mode 1 (Hz)	% Difference from Ping Test
Ping Test	94	–
2-D element, linear, coarse mesh, unmassed	178	89.4
2-D element, quadratic, coarse mesh, unmassed	147.17	58.2
3-D element, quadratic, fine mesh, unmassed	113.4	21.11
3-D element, quadratic, fine mesh, massed	54.35	N/A

enough to give the RIGEX team a general idea of what the first natural frequency of the payload would be.

2.5 Steven N. Lindemuth, Thesis, 2004

In addition to Captain Holstein, Captain Steve Lindemuth also worked on the RIGEX program between 2003 and 2004. While Holstein concentrated his efforts on analyzing and testing the tube and structure, Lindemuth focused his energy on refining the heating and inflation systems. He also worked with STP to get RIGEX accepted by the SERB. This section describes his progress in each of these areas.

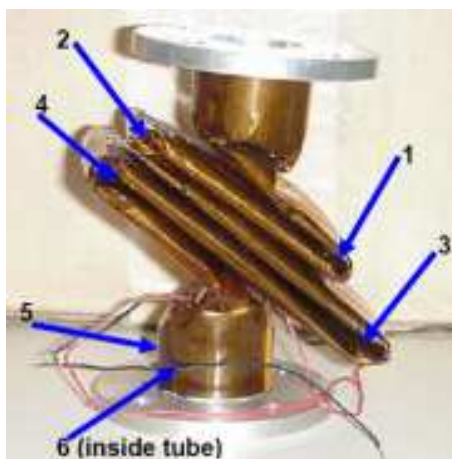
2.5.1 Heating System Testing. Due to the nature of the Sub- T_g tubes, the heating system is a critical system for RIGEX. In particular, knowing the amount of time required to heat the tube *completely* is vital to mission success. For example, if a tube’s heating time is insufficient, some or all of it may not reach $125^\circ C$, and improper deployment like that shown in Figure 2.16 may result.

To counteract this, Lindemuth’s first goal was to characterize the differential heating across the tube. Furthermore, Lindemuth also recognized that the PZT patches made by NASA may not be appropriate for this mission due to temperature limitations. Therefore, he conducted tests to ensure functionality after being exposed to temperature extremes. Both of these tests are described further below.

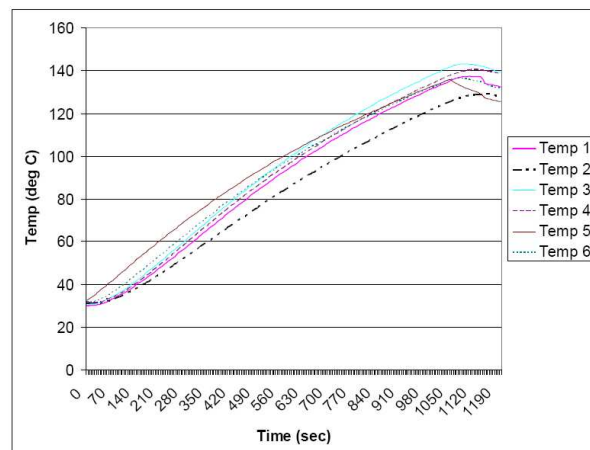


Figure 2.16: Result of Poor Tube Heating [23, p.65].

2.5.1.1 Determination of Tube Heating Profile. The first test Lindemuth conducted was to determine the inflatable tube's heating profile. Using the quarter structure, the vacuum chamber, and a folded tube placed inside one of the experiment's ovens, he recorded the data from six strategically-located thermocouples as he warmed the tube from 30°C to above 125°C . Using this information, he not only determined the heating profile, but the best locations to place the thermocouples for the mission as well.



(a)



(b)

Figure 2.17: Lindemuth's Tube Heating Profile Test [21, p.51].
 (a) Thermocouple locations (each on the inner side of a tube fold).
 (b) Measured thermocouple data throughout test.

Figure 2.17(a) shows the location of the thermocouples. He placed each one on the inside of a tube fold, as they would be blocked the most from the heat of the resistive heaters on each side of the ovens. As seen in Figure 2.17(b), the results of the test show that approximately 950 seconds (roughly 16 minutes) were needed for the tube to reach 125°C . It is important to remember, however, that this does not necessarily represent flight conditions exactly, as the ambient temperature may vary from -40°C to $+70^{\circ}\text{C}$. That being said, the test did provide excellent new insight to the distributional heating of the tube. In particular, the test showed that Location #2 warmed the slowest, while Location #3 reached 125°C the most quickly. For flight, these two locations will be recorded as the tube heats, and will be used by the computer to initiate tube inflation once they are both above 125°C .

2.5.1.2 Determination of Piezoelectric Patch Heat Tolerance. The other heating test Lindemuth conducted was for the PZT patches. The test was needed because their operating temperature ceiling was *lower* than the temperatures needed to bond them to the tube. Furthermore, the bonding material that holds them together is *not* rated to temperatures seen inside the ovens. Therefore, a test was needed to determine their functionality under such extremes. This test included three steps:

1. Bond a PZT to a tube and apply voltage to it to determine functionality before placing the tube in the oven
2. Place the tube in the oven and heat to a point representative of the on-orbit mission
3. Cool the tube and apply voltage again to determine post-test functionality

The tube was placed in the oven, which was then heated to 170°C over 165 minutes. With the completely successful conclusion of the second excitation test, no changes to the PZTs and their installation methods were needed.

2.5.2 Inflation System Testing. The next set of tests Lindemuth conducted focused on integrating the inflation system with the experiment structure and com-

mand & data handling (C&DH) software, using both the quarter structure as well as the full structure. Specifically, because the quarter structure was not completely representative of the full structure's physical layout, he used it to primarily test the inflation software routines and the full structure to correct any physical layout issues. In addition, he also tested the inflation system's ability to maintain pressure over a significant period of time. Section 2.5.2.1 covers the first set of tests, while Section 2.5.2.2 discusses his pressure maintenance test.

2.5.2.1 Full Scale Inflation Test. Lindemuth designed a full scale inflation test to ensure that the tubes would inflate properly with the flight software. He attacked the task first with the quarter structure and a Sub- T_g tube. Although the software worked perfectly, he found that there were significant layout issues that needed to be corrected for the full structure. In particular, as seen in Frame 4 of Figure 2.18, the inflation system was a significant cause of interference for the tube's inflation. To prevent this from happening on orbit, the entire inflation system was relocated from an experiment bay to the computer bay, as shown in Figure 2.19.



Figure 2.18: Lindemuth's Time Phased Inflation [21, p.60].



Figure 2.19: Repositioned Inflation System. Due to interferences the inflation system caused in one of the experiment bays, it was repositioned to the computer bay [21, p.61].

2.5.2.2 Long-Term Pressure Retention Test. The next test Lindemuth focused on was a pressure retention test. He determined that the experiment must contain at least 32.3 psi when the tubes are inflated. Furthermore, since the experiment could wait up to 7 days on orbit before being initiated by the astronauts, it was imperative to understand the inflation system's ability to maintain pressure over time. To do this, he fully charged the system and then made measurements over 5 days to characterize the loss. After post-processing the data, he was able to identify a trend for the loss rate (see Figure 2.20), and made the following conclusions:

- The system is estimated to contain approximately 163 psi after 7 days, which is 500% above the required 32.3 psi
- The loss rate once the pressure inside the cylinder gets below 200 psi is slow enough such that adequate pressure should be maintained even over a potential 90-day launch delay

Even with these conclusions, however, he still recommended improvements to the system. These recommendations included minimizing potential leak points in the system, as well as increasing the size of the pressure cylinder. These recommendations would eventually be followed by Captain Chad Moeller, as discussed in Section 2.7.

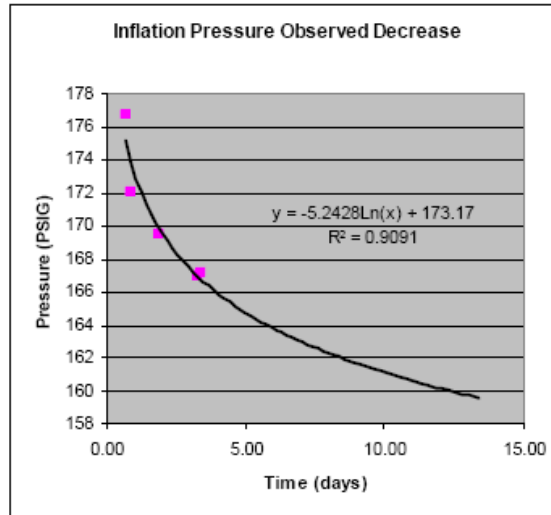


Figure 2.20: Lindemuth's Calculated Loss Rate [21, p.65].

2.5.3 SERB Efforts. In addition to Lindemuth's technical contributions to RIGEX, he also briefed the SERB during his time at AFIT. RIGEX was only ranked 31 out of 41 missions, but most of its competition was not looking for Space Shuttle support. Therefore, it was expected that STP would provide funding and support for the RIGEX launch.

2.5.4 Section Summary. As the second of three students working on RIGEX at the time, Lindemuth was able to concentrate his efforts on the heating and inflation systems, while also working with STP and the SERB. During his time, he determined the heating profile of the inflatable tubes, the best locations for thermocouples on the tubes, and that the PZTs would survive the heat applied to the tubes. Furthermore, he also refined the inflation system, determining that it would retain enough pressure to inflate the tubes even after a 90-day launch delay. Finally, he briefed RIGEX to the SERB, laying the foundation to secure STP funding and support for a future Space Shuttle launch.

2.6 *David C. Moody, Thesis, 2004*

Next, Lieutenant Dave Moody was the third of three students working on RIGEX between 2003 and 2004. With Holstein concentrating on the finite element analysis and Lindemuth concentrating on perfecting the heating and inflation systems, Moody was able to focus on designing the computer and its software. In particular, he separated the computer that was being used into two distinct computers. He dubbed the first the *Data Acquisition Computer* and made it responsible to direct the mission and collect all data, with the exception of the digital camera images. The second computer, dubbed the *Imaging Computer*, received its cues from the Data Acquisition Computer and managed all digital camera operations, including image storage. In order to make the two-computer system work together, he designed the wiring connections between them, as well as their individual software routines. In addition to his computer design, Moody also developed the **Matlab**[®] code to post-process the mission data. Section 2.6.1 discusses his advancements to the computer and software, and Section 2.6.3 discusses his post-processing routine.

2.6.1 Computer Modification. Philley originally laid out the computer design as a single PC-104 computer stack. Unfortunately, he found that a single PC-104 processor board (similar to a motherboard and processor on a home computer) slowed dramatically as more boards were added to the stack, particularly affecting the imaging system and the rate at which images were taken. Therefore, Moody split Philley's design into two computers, but connected them with two timing boards to keep their communication synchronized. The following boards were assigned to the Data Acquisition Computer:

- Power supply board – relays Shuttle power to the Data Acquisition Computer; converts (using DC-DC converters) 28VDC Shuttle voltage to ± 5 VDC and ± 12 VDC to power accelerometers and pressure transducers [8]
- Processor board, including flash memory chip – computer's motherboard and main memory [31]
- Digital/analog (and vice versa) converter board – collects analog accelerometer and pressure transducer data and converts to digital values for storage; also con-

verts excitation signal digital values to analog voltage for exciting the inflatable tube [9]

- Relay board – houses relays used to control experiment [7]
- Thermocouple control board – reads thermocouple data and converts to digital values for storage [3]
- Filter board – filters excitation signal such that no digital aliasing affects input to tube; designed by Moody
- Timer/counter board – used to maintain handshake with Imaging Computer [10]

The boards assigned to the Imaging Computer included the following:

- Power supply board – relays Shuttle power to the Imaging Computer [8]
- Processor board, including flash memory chip – same as above [31]
- Three digital camera control boards – self-explanatory [13]
- Timer/counter board – used to maintain handshake with Data Acquisition Computer [10]

Further information on each specific board may be found in their respective references, or in Chapter III of Moody’s Thesis.

In addition to the board layout, Moody also designed the initial wiring layout. The number of boards and connections makes presenting this information here unreasonable; however, Appendix G of his thesis presents the material completely. Furthermore, as discussed in the next chapter, slight modifications to his wiring layout were made this year, the results of which can be seen in Appendix E.1.

2.6.2 Flight Software Development. With his computer layout, Moody next revised DiSebastian’s Main Event Calendar (shown in Table 2.5) such that each tube would run through its complete heat, inflate, cool, vent, and excitation process before the next tube’s was initiated. Using this updated calendar, his next step was to build and test the experiment code (written in C++).

To build the code, he first built subprograms to test individual functions [24, p.3-47]. These subprograms are listed below, and Appendix D of his thesis provides detailed flowcharts on their functionality.

- Excitation waveform test
- A/D conversion of accelerometer signal
- A/D conversion of thermocouple signal
- A/D conversion of pressure transducer signal
- Single tube experiment in vacuum chamber without imaging (this is the same test as described in Lindemuth’s review, Section 2.5.2.1)
- Imaging Computer test
 - Routine to take pictures on command
 - Accuracy test of height/displacement measurements of tube’s inflation
- Single tube experiment in vacuum chamber with imaging

Each of these subfunctions were successful, allowing him to assemble the complete mission routines for each computer. Furthermore, he was able to simulate his 3-tube test using an Omega Process Calibrator (a simulator used to simulate sensor data) as well as already-inflated tubes, completing every subfunction successfully.

2.6.3 Post-Mission Data Analysis. Perhaps the best testament to the success of Moody’s code is the post-processing of the data he was able to complete. As shown in Figure 2.21, he was able to excite three tubes and calculate each of their frequency response functions (also called transfer functions). While the data is much noisier than seen in Figure 2.10 of Philley’s review, it is clear enough to see each of the tube modes. This demonstrates that Moody’s approach was acceptable, but also that there might be room for improvement to clean up the data. This is discussed further in Chapter III, Section 4.2.

2.6.4 Section Summary. In effect, Moody defined the proverbial nervous system for RIGEX, complete with the brain. This section discussed his improvements to the computer system, as well as his development of the wiring layout, the flight software, and the post-mission data analysis routine. With the conclusion of Moody’s efforts, the design was ready to be implemented on flight hardware.

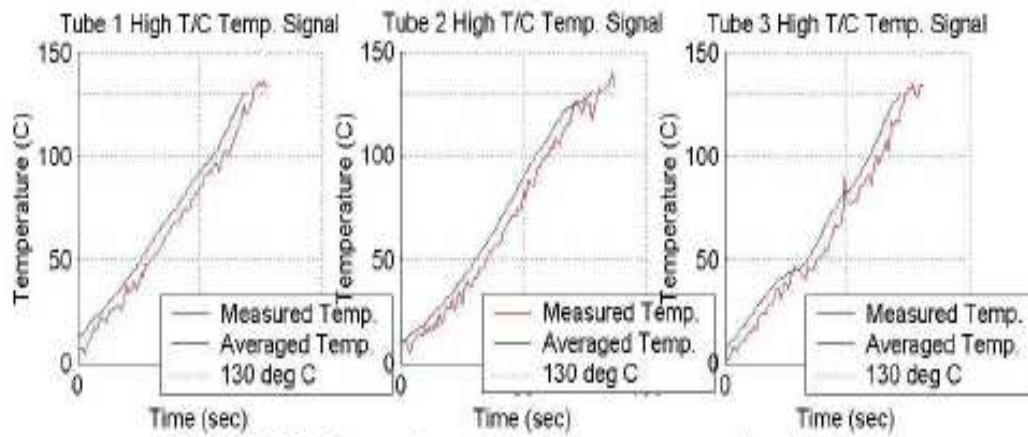


Figure 4.38: Three tube experiment temperature simulations

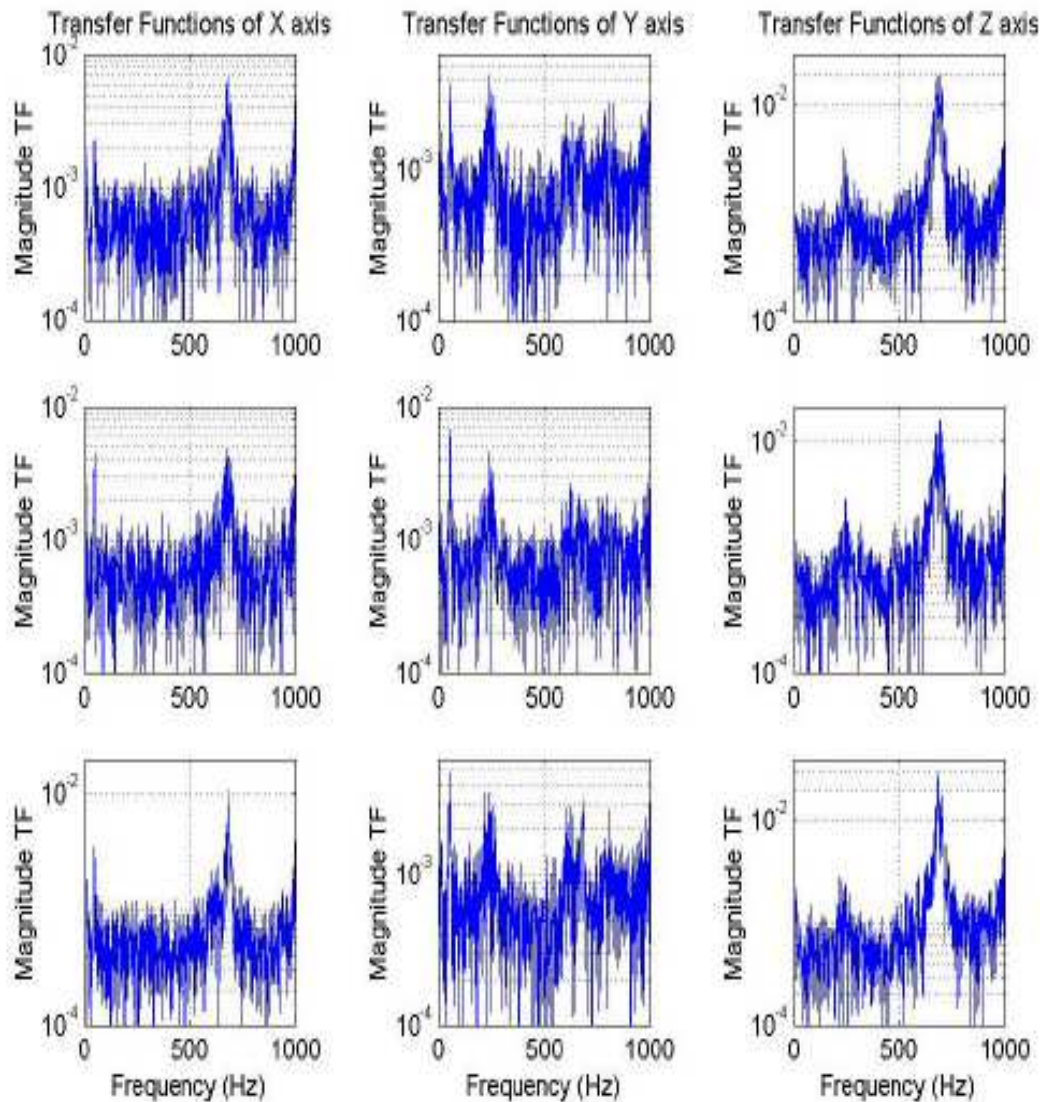


Figure 2.21: Moody's 3-Tube Test Results [24, p.4-48].

2.7 *Chad R. Moeller, Thesis, 2005*

Capt Chad Moeller essentially took over where Lindemuth left off, but with a significant twist. NASA had decided to disband the Get-Away-Special (GAS) program office, which theoretically may have ended the RIGEX program. However, as discussed in Chapter I, STP developed the Canister for All Payload Ejections (CAPE) in place of GAS. As shown in Table 1.2, there are significant advantages to CAPE over GAS. In particular, the weight and size limits previously imposed by GAS were now respectively 175% and 212% higher in CAPE. Furthermore, in addition to CAPE, STP also offered up a connection to Shuttle power, which eliminated 80 pounds of battery weight from RIGEX and opened up 1500 cubic inches in the center of the payload, as shown in Figure 2.22.

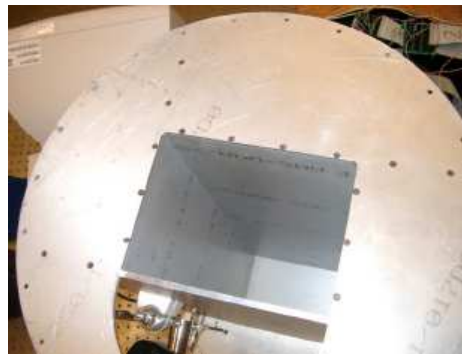


Figure 2.22: Battery Storage Volume [23, p.32]. By transitioning from GAS to CAPE, 80 pounds of eliminated battery weight and 1500 cubic inches of volume were made available for design modifications.

With this substantial change, Moeller initiated a redesign of the inflation system (identified as a high-risk area for mission success). Rather than one high-pressure storage vessel in the computer bay, he investigated using three larger vessels in the middle bay pressurized to a lower pressure. This is discussed further in Section 2.7.1.

In addition to the modifications made to the inflation system, Moeller also analyzed the cooling profile of the tubes. Combining this with Lindemuth's research on the tube's heating profile, Moeller established further insight into how the tube

will behave thermally throughout the entire mission. His specific efforts are discussed further in Section 2.7.2.

2.7.1 Inflation System Modification. First, recall from Section 2.5.2.2 that Lindemuth recommended enlarging the pressure vessel to reduce the pressurization required to fill all three inflatable tubes, thus reducing the tendency of the system to leak. With the middle bay opening up, Moeller took Lindemuth's recommendation one step further, and identified a method of using one large pressure vessel for each inflatable tube. By using one vessel per tube, he could pressurize them at atmospheric pressure (14.7psi, much less than Lindemuth's 400psi) and still have enough gas in the system to inflate the tube. This eliminated the necessity of a pressure regulator and a pressure relief valve, thus eliminating potential leakage points. He also virtually eliminated the storage system's tendency to leak overall, as the vessel's internal pressure would be equalized with the atmospheric pressure outside.

To make his design work, Moeller first had to determine the volume of the pressure system and its components. As shown in Figure 2.23, he dissected the system into two separate components. The first was the storage section, which included the pressure vessel and all tubing and sensors before the solenoid valve. The second was the inflation section, which included the inflatable tube and all tubing and sensors after the solenoid valve. The solenoid valve was the delimiter as it was here that the pressure of the entire system would equalize when the solenoid was operated for tube inflation.

Next, with the volumes of both the inflation and storage sections, Moeller used the ideal gas law ($PV = nRT$) and the combined gas law ($P_2 = \left[\frac{P_1 V_1}{T_1} \times \frac{T_2}{V_2} \right]$) to determine a range of pressure vessel sizes that would fully inflate one tube without over-pressurizing it when the solenoid was activated. After coordinating with a local Swagelok representative (a company popular for its inventory of high-quality fluid system components), and narrowing the range down to either 400 cubic centimeters(cc) or 500cc, he chose the 500cc vessel for its additional capability.

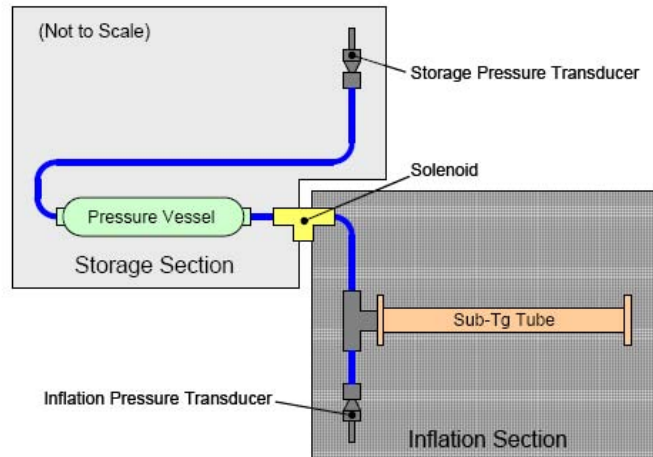


Figure 2.23: Moeller's Pressure System Breakdown [23, p.35]. Using this breakdown, the ideal gas law, and the combined gas law, Moeller determined a range of pressure vessel sizes that would adequately inflate the tubes without the risk of overpressurization.

Once the 500cc vessels arrived, he began testing them with the inflatable tubes. As shown in Figure 2.24, the storage section maintained its 14.7psi until the solenoid was activated. After activation, the two sections equalized at approximately 7.15psi (the brief spike seen in the figure was due to an inadvertent procedural error where the oven latch was not activated on time; no damage was caused to the tube). Then, however, there was a steady leak in the system until the tube was vented. Moeller attributed this leak to the flexible connection between the stainless steel and plastic tubing he used to inflate the tube [23, p.62]. Lieutenant Helms addressed the issue this year by determining better components for the mission. Even with this leak, however, the system maintained enough pressure inside the tubes until they cooled and could be vented.

2.7.2 Determination of Tube Cooling Profile. After modifying the inflation system, Moeller next set out to identify and verify the cooling profile of the inflatable tubes. To identify it, he calculated the heat energy stored in the tube at max temperature, and derived the following analytic expression for its conversion to radiative

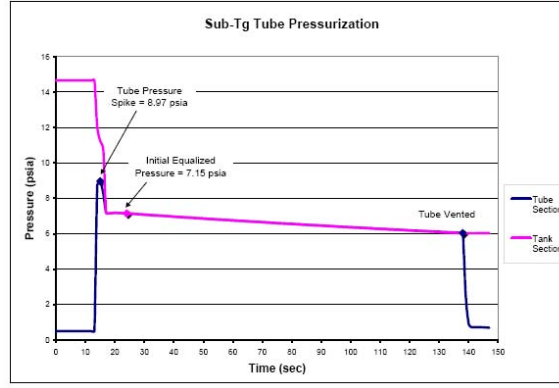
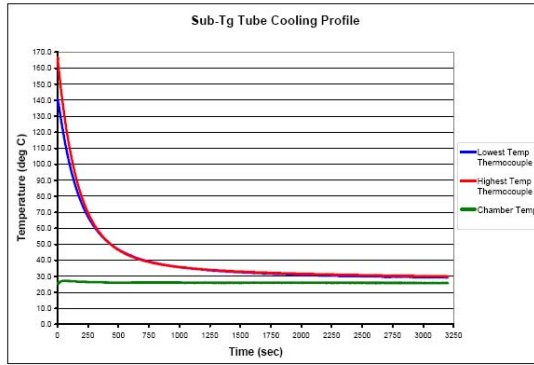


Figure 2.24: Moeller's Inflation Test Results [23, p.63]. While a steady leak in the system is seen after equalization, sufficient pressure to inflate and steady the tube as it cooled/rigidized was maintained until venting.

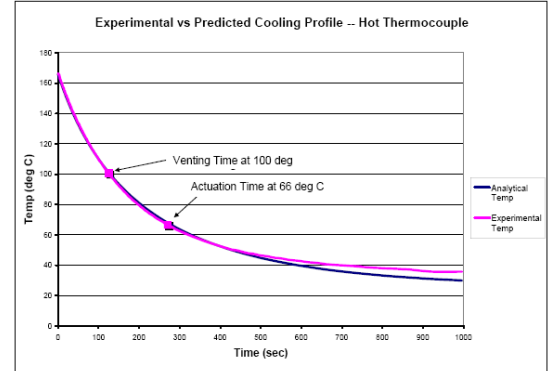
energy (radiation is the driving method of the tube's heat transfer in space):

$$t = \frac{\rho V c}{4 \epsilon A_s \sigma T^3} \left\{ \ln \left| \frac{T_{amb} + T}{T_{amb} - T} \right| - \ln \left| \frac{T_{amb} + T_i}{T_{amb_i} - T} \right| + 2 \left[\tan^{-1} \left(\frac{T}{T_{amb}} \right) - \tan^{-1} \left(\frac{T_i}{T_{amb}} \right) \right] \right\}$$

He then put this equation to the test. Using the same setup Lindemuth used, the results of his cooling profile tests are shown in Figure 2.25(a). Then, when comparing the results from his analytical equation with experimental results, he found that a scaling factor of $16.625K^3$ was needed for them to match up. Applying this scaling factor, Figure 2.25(b) shows the correlated results.



(a)



(b)

Figure 2.25: Inflatable Tube Cooling Profile.

(a) Moeller's cooling experiment results [23, p.68].

(b) Experimental results compared with analytical results [23, p.69]

2.7.3 Section Summary. During Moeller's research, many changes were being made to RIGEX. Transitioning from GAS to CAPE implied significant design changes were needed. Removing the batteries, he initiated the design for an improved inflation system that virtually eliminated the concern of gas leakage while waiting to be launched. Furthermore, he also determined the cooling profile of the tube, thus completing its thermal characterization.

2.8 Chapter Summary

This chapter paints the big picture of the RIGEX evolution. Beginning with DiSebastian's preliminary design, it reviews the methods and results presented in the theses of the seven graduate students that dedicated their AFIT research to its development. In summary, Figure 2.26 illustrates the key efforts of each student. The remainder of this thesis picks up where these students left off as RIGEX is further prepared for flight on the Space Shuttle.

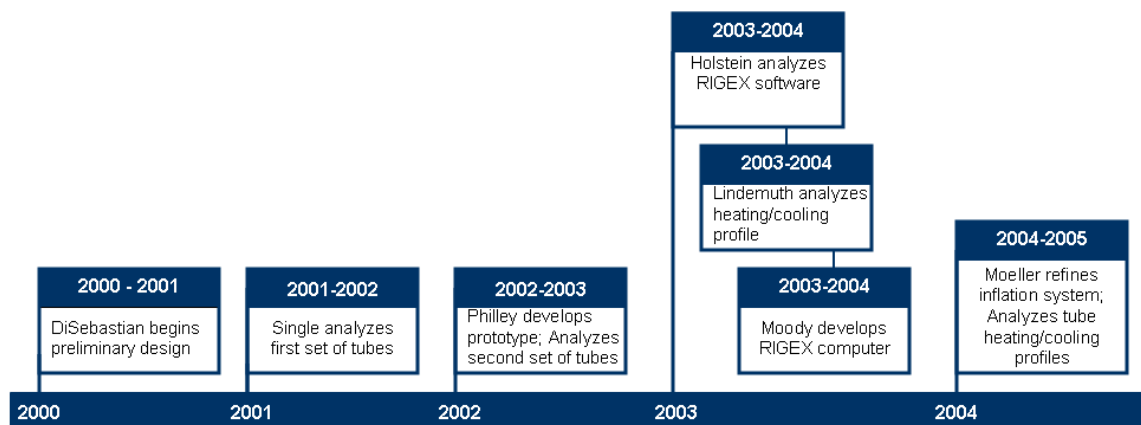


Figure 2.26: Summary of Student Design Efforts

III. Design Modifications

As discussed in Chapter II, the efforts of the past RIGEX students have brought the experiment quite far in its development process. Therefore, although the transition to CAPE carried with it significant requirements that needed to be addressed, their efforts certainly made the process much easier. Still, these requirements have affected the experiment's design, driving modifications to many of its subsystems. This chapter expands on each of the requirements shown in Table 3.1, providing both background information on the requirement itself as well as the detailed design results of the associated modifications.

Table 3.1: Driving Requirements for Design Modifications

Requirement	Origination	Affected Subsystem
Develop protective shroud	STP request	Mechanical
Develop CAPE mounting plate	STP request	Mechanical
Modify Top plate	Mission success (Self-Imposed)	Mechanical
Increase aluminum plate thickness	Derived from NSTS 08307 [2]	Mechanical
Develop bumpers/snubbers	STP request	Mechanical
Develop stabilizing feet	STP request	Mechanical
Develop Shuttle feedback circuit	Previously undeveloped	Electrical
Develop fusing architecture	NSTS 18798B [25]	Electrical
Develop power distribution scheme	Previously undeveloped	Electrical
Develop wiring harness layout	Previously undeveloped	Electrical
Develop inflation system interfaces	Previously undeveloped	Inflation
Increase computer's effectiveness	Mission success (Self-imposed)	Command/data handling

Each of these requirements combine to form the experiment's detailed design. The overall results can be seen in the comparison of DiSebastian's preliminary design assembly with the new detailed design assembly, shown in Figure 3.1.

3.1 Mechanical Subsystem

In this section, the modifying requirements and detailed design for the following structural components are presented:

- Shroud
- Plates/Ribs

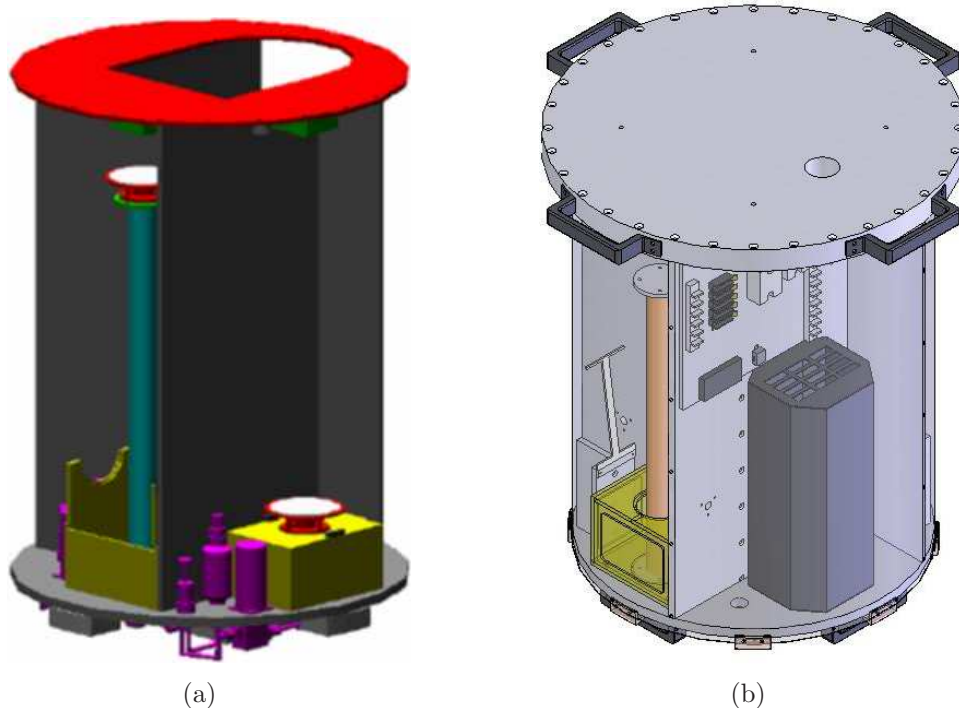


Figure 3.1: Comparison of Preliminary Design with Detailed Design
(a) DiSebastian's preliminary design [11]
(b) New detailed design

- Snubbers
- Stabilizing feet/lifting handles

While some of these components had already been designed, drawn, and manufactured, the electronic files were not kept at AFIT. Therefore, because every structural item needed to be redesigned, and because drawings and models were needed by NASA to satisfy their own requirements and modeling efforts, the original hard copies presented in Holstein's thesis [19] were used as a basis to create the new experiment model in **SolidWorks**® Version 2004 SP3.1. Figure 3.2 illustrates the nomenclature used for each of these structural components. It should be noted here that the RIGEX Critical Design Review has not yet been held (currently scheduled for April 2006); therefore, the potential exists for further modifications to be required.

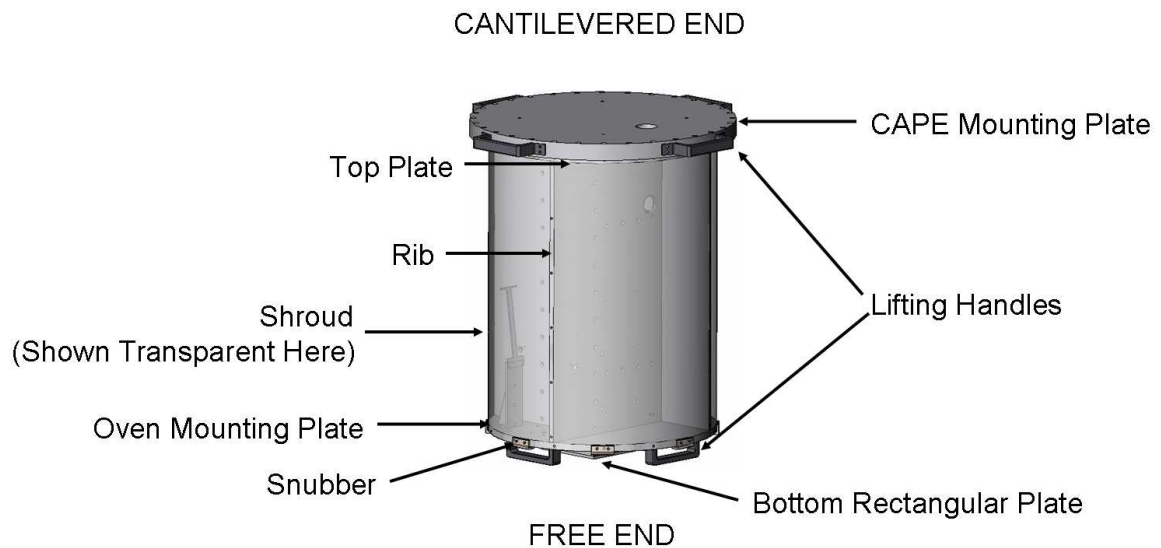


Figure 3.2: RIGEX Structure. Shown here are the experiment plates, ribs, handles, snubbers, and shroud.

3.1.1 Shroud. The first addition to RIGEX was a protective shroud, designed to keep anything happening on the experiment from damaging the CAPE interior. The shroud will also double as a protective covering during shipping and handling, preventing accidental damage as the payload is assembled and disassembled from the shipping container.

3.1.1.1 Requirement Description. During reentry and landing, the Shuttle experiences loads of up to 6.5 times the force of gravity [26]. Since the tubes are cantilevered and fully extended at this point in the mission, these loads may be high enough to cause them to shatter. While the Kapton tape on both the inside and outside of the tubes lessens this possibility, it does not completely eliminate it. Therefore, STP has requested an encompassing shroud be incorporated on RIGEX to prevent any loose parts from damaging the inside of the CAPE. To accommodate this request, the team decided to use a thin sheet of aluminum that will be fastened around the top and oven mounting plates, as well as down each of the vertical ribs. Determining its thickness required a containment analysis to be performed, which along with its results, is presented in Section 4.1.

3.1.1.2 Design. Two initial concepts of the shroud, shown in Figure 3.3, were developed. The first concept included a shroud from the top plate down to the oven mounting plate, and the second included a shroud from the top plate all the way down to an additional 20.5in-diameter (0.52m) plate at the bottom (where the bottom rectangular plate is in the first concept).

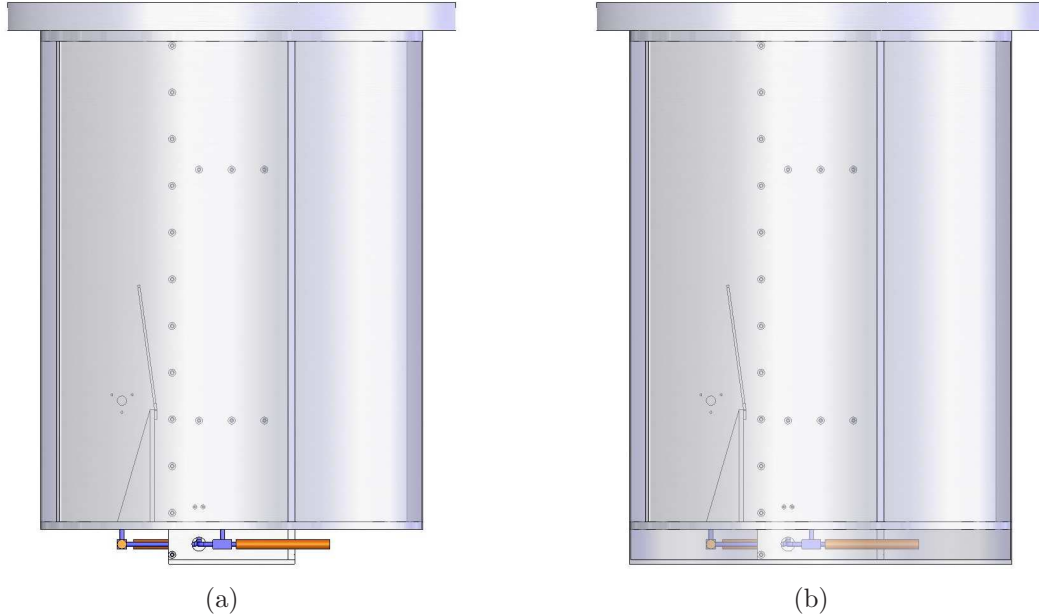


Figure 3.3: Shroud Concepts.
 (a) Concept #1 envelops the payload between the two 20.5in circular plates.
 (b) Concept #2 envelops the entire payload and modifies the rectangular bottom plate into an additional 20.5in circular plate at the bottom (Note: Feet/Handles & Snubbers not shown).

Concept #1 was chosen for a number of reasons, but primarily because Concept #2's additional large plate at the bottom is a significant amount of mass to be added to the experiment. With CAPE's mass capability, this would not normally be a problem. Unfortunately, however, the additional mass would be located at the experiment's free end, therefore potentially causing a reduction to the experiment's first mode. While a structural analysis of this configuration was not performed, a request from STP to keep the first mode above 50Hz was an important factor in the decision.

In addition, because the inflation system's fill valves are located inside the center bay near the bottom of the experiment, Concept #2's large bottom plate would need to be removed at the launch site if the storage cylinders needed to be refilled. Therefore, the lower mass and increased ease of accessibility made Concept #1 much more appealing.

To construct the shroud, a 0.075in (1.91mm) sheet of aluminum will first be sized to fit around the experiment's top plate, including a 1in (2.54cm) overlap. With a 20.5in (52.07cm) diameter, basic geometry ($Circumference = \pi \times Diameter$) is used to determine that the length of the aluminum should be cut to 65.40in (1.66m), including the overlap. Once the aluminum is cut, #8 thru- holes will be drilled for all of the fasteners. Then, the aluminum will be rolled so that it fits snugly around the experiment. Figure 3.4 shows the shroud in both its flat and rolled configurations.

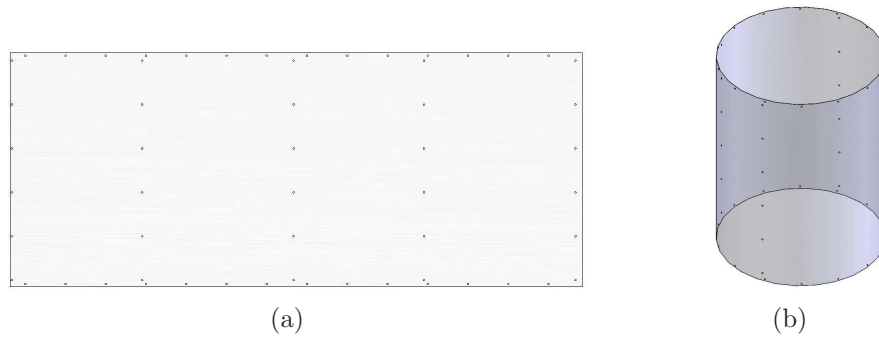


Figure 3.4: Shroud Design

(a) Shroud before rolling (front view)

(b) Shroud after rolling (isometric view; NOTE: Overlap not shown)

For obvious reasons, the shroud will be the last item assembled on to the experiment, but there will be times that it will need to be removed. For example, once it is mounted, RIGEX will be ready for environmental testing (vibration, thermal vacuum, etc.). If the results of this testing present a necessity for accessing the interior of the payload, the shroud will need to be removed. Furthermore, because the access holes used to mount RIGEX to the shipping container are inside the shroud, it will have to be removed as the experiment is prepared for transport to the launch site. To prevent the holes in the plates and ribs from degrading each time the shroud is added

or removed, #8 fasteners with HeliCoil Screw-Lock[®] inserts will be used. This type of insert, shown in Figure 3.5, is a common practice used in space applications to prevent fasteners from loosening during vibration. They can also be easily replaced, if necessary.



Figure 3.5: HeliCoil Screw-Lock[®] Inserts [18]

3.1.2 CAPE Mounting Plate. The CAPE mounting plate was the next new addition to RIGEX. Originally, the GAS program office was going to provide what was called the Experiment Mounting Plate (EMP). However, this provision was lost when RIGEX was transitioned to CAPE.

3.1.2.1 Requirement Description. Because providing an EMP is not yet a service of the CAPE, a new mounting plate was required. Using the CAPE schematics shown in Figure 3.6, (provided by STP), a new CAPE mounting plate was designed.

3.1.2.2 Design. Based on past experience, STP recommended the mounting plate be 1.5 inches (38mm) thick. From the experiment's point of view, there were no adverse impacts from this, so the decision was made to follow the recommendation. In fact, the decision proved to be quite beneficial. Not only did the additional mass bring the center of gravity closer to the experiment's cantilevered end, but the added stiffness of the plate is expected further increase the frequency of the first mode.

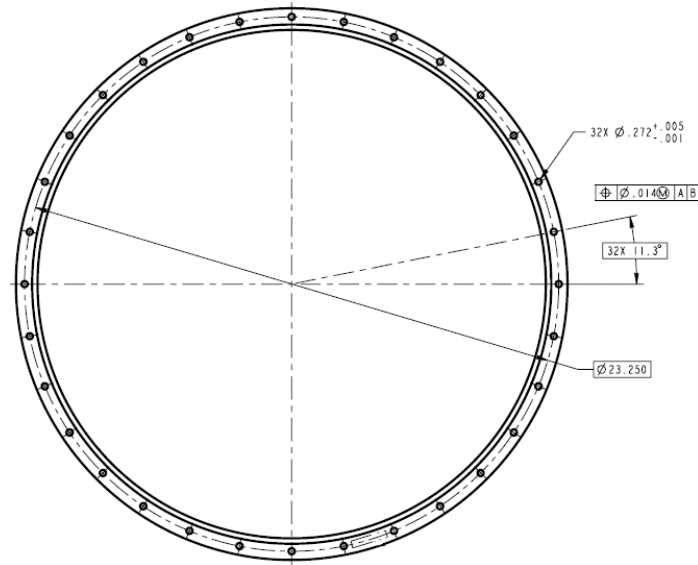


Figure 3.6: CAPE Interface Schematic

The plate's design is shown in Figure 3.7. It's overall diameter is 24 inches (0.61m) to match the outer diameter of the CAPE. On the top, a 23.25in-diameter (0.59m) bolt circle of 1/4in countersunk thru holes is used for the fasteners that mount the plate to the CAPE. Also on the top are four 1/4in x 20 tapped holes, drilled to a depth of 0.54in (13.72mm), for securing a lifting sling to the payload. These holes lie on a 15in-diameter (0.38m) circle.

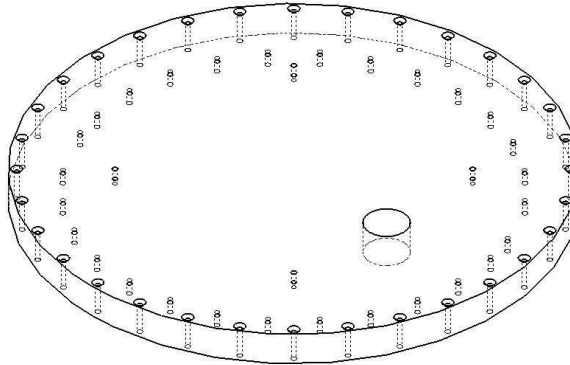


Figure 3.7: CAPE Mounting Plate. On the top of the plate, the CAPE bolt circle and lifting sling mounting locations can be seen; on the bottom, the bolt circle used to mount the RIGEX top plate is shown using hidden (dashed) lines.

On the bottom, a 19.5in-diameter (0.49m) bolt circle of 1/4in x 28 tapped holes, drilled to a depth of 0.54 inches (13.72mm), is incorporated for the fasteners that secure the top plate. These mounting holes are placed on the bottom to facilitate the shipping of RIGEX, which will be bolted upside-down to the bottom of the shipping container. This allows RIGEX to mount to either the mounting plate or the shipping container using the same holes on the top plate. It means, however, that RIGEX will need to be turned upside-down and back again, perhaps multiple times, during processing. Therefore, lifting handles, discussed in Section 3.1.6, were designed to facilitate this handling.

To accommodate these lifting handles, eight 1/4x28in holes drilled to a depth of 0.54in (13.72mm) will be drilled into the side of the mounting plate. The handles will be mounted to the side of the plate such that they can be easily removed (if necessary) once RIGEX is completely inverted.

3.1.3 Top Plate. The top plate is the interface between the main portion of the experiment and the CAPE mounting plate. Attached to it are the four ribs, the three digital cameras (one per bay), and six LEDs (two per bay). While there were no STP or NASA requirements driving any modifications to the design, there were significant technical issues that surfaced in prior analyses, as well as in testing, that required important changes to be made.

3.1.3.1 Requirement Description. Recall from Holstein's stress analysis results, shown previously in Figure 2.14, that a significant stress concentration exists on the corners of the top plate. Vibration testing conducted by Helms verified this stress when seven fasteners on the top plate sheared in half. To prevent this from happening during flight, the following recommendations suggested by Holstein were implemented:

- Computer access port eliminated
- Plate thickness increased

initial assumptions for the plate thickness and fastener size. Once the analysis is conducted, the design can then be modified accordingly. However, with the significant schedule and technical risks associated with another redesign, the team decided to make a conservative change now to improve the results of the bolt analysis later.

3.1.4.1 Requirement Description. A good engineering practice when drilling holes is to keep at least one full bolt diameter between the center of the hole and the nearest edge. For the RIGEX ribs, this means that their thickness would be at least two times the maximum bolt thickness. The original design called for #6 bolts to be drilled into 1/4in (6.4mm) aluminum. Unfortunately, the diameter of a #6 bolt is 0.138in (3.505mm) [22], which is about 10% larger than the ribs should handle. Therefore, some modifications were required.

3.1.4.2 Requirement Description. The conservative measure the team decided upon was to increase the size of the fasteners from #6 to #10, which have a diameter of 0.190in (4.826mm). Following the good engineering practice discussed above, the rib thickness was increased to 3/8in (9.5mm). Although this thickness is actually 0.005in (0.127mm) too small, STP approved the modification.

In addition to increasing the ribs' thickness, each rib was also modified to accommodate the new inflation system. Specifically, holes for the mounting plates, solenoids, and tube pass-through locations were added. Holes were also added to accommodate the wiring harness. The physical layout of each of the new ribs is shown in Figure 3.9.

3.1.5 Snubber Design. A snubber, which can also be referred to as a bumper, is a device typically designed to snugly interface two components together such that one does not vibrate against the other and cause damage. In his preliminary design, Holstein developed a concept for the RIGEX snubbers, but it was actually more complex than it needed to be, as seen in Figure 3.10. Since the snubbers have not been built yet, the opportunity was taken to develop a more simple design.

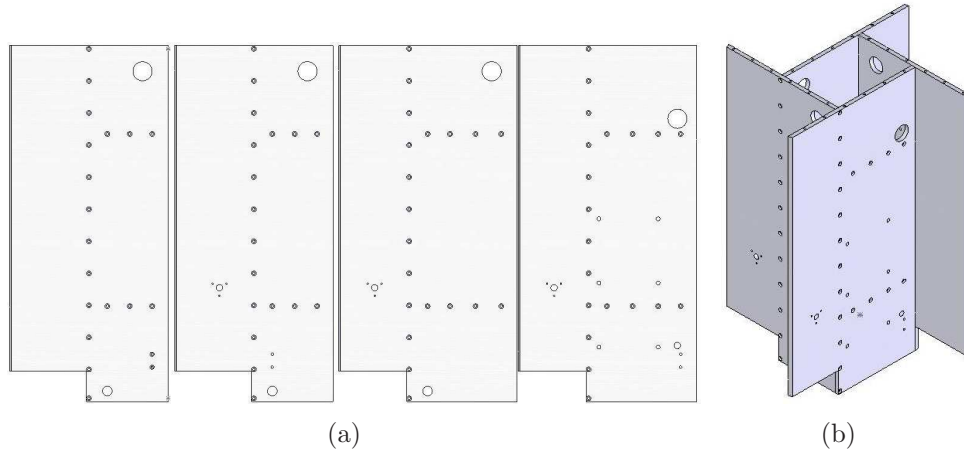


Figure 3.9: Rib Physical Layout
(a) Individual ribs (front view);
(b) Ribs joined as on RIGEX

3.1.5.1 Requirement Description. During the transition to CAPE, the requirement for a snubber changed from needing to be snug against the CAPE interior to needing to protect the interior as the experiment is assembled and disassembled from the canister. Therefore, snubbers made of Delrin plastic were requested for the edge of the oven mounting plate. Delrin, made by DuPont, is a lightweight acetal-resin plastic that is used when low-friction materials capable of being operated in high heat extremes (in excess of $90^{\circ}C$) are required [12].

3.1.5.2 Design. The design, shown in Figure 3.11(a), consists of a crescent-shaped vertical edge that coincides with the outer edge of the oven mounting plate, and a horizontal edge that coincides with the bottom edge of the plate. It is secured to the outer edge with two #10-32 fasteners. As shown in Figure 3.11(b), there will be eight snubbers on the experiment spread 45 degrees apart to minimize the risk of contact with the CAPE interior.

3.1.6 Stabilizing Feet/Lifting Handles. The original RIGEX design included an 8in x 6.5in rectangular protrusion from the bottom of the oven mounting plate that would serve as the experiment's single interface to the ground. During payload

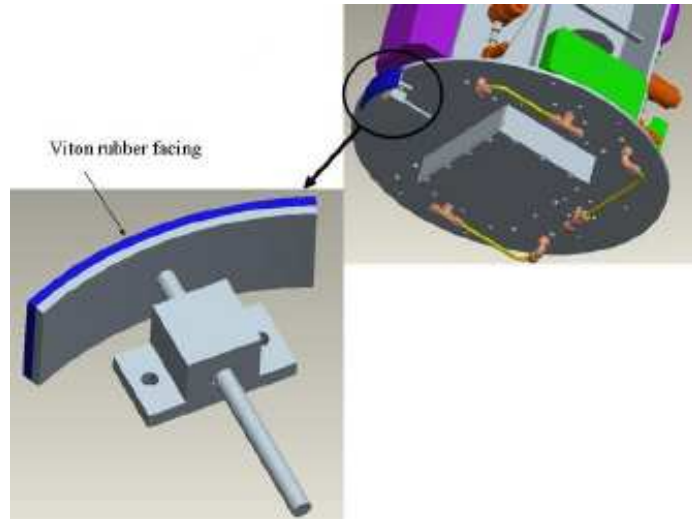


Figure 3.10: Holstein's Snubber Design [19]

processing, this could present an unsafe tipping hazard. In addition, throughout the assembly, integration, shipping, and processing of RIGEX, it will need to be turned upside-down and back again. To safely perform both of these operations, stabilizing feet that double as the experiment's lifting handles were designed for the outer edges of the plate, and are shown in the right image of Figure 3.12 (Figure 3.2 illustrates their interface with the experiment).

There were also handles designed for the CAPE mounting plate, which are slightly different from the oven mounting plate's handles. During assembly and testing, RIGEX will need to rest upside down on its top end. As such, larger handles with curved flanges will be fastened to the *side* of the plate rather than the top face, as shown on the left of Figure 3.12.

Once payload processing is complete and RIGEX is ready to be installed in the CAPE, a lifting sling will be attached to top of the CAPE mounting plate. All handles will then be removed, and RIGEX will be lifted up and installed according to STP's procedures.

3.1.7 Mass Properties. One of the many advantages to using SolidWorks® is its outstanding Mass Properties tool. Using a built-in database of material properties,

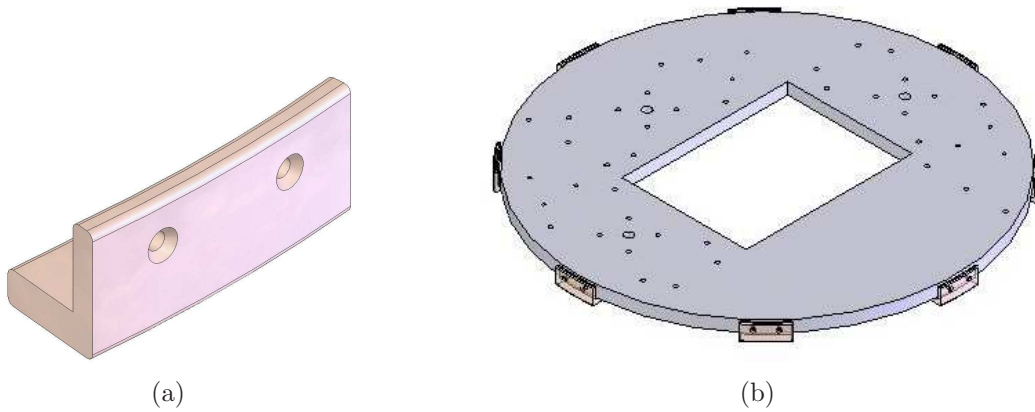


Figure 3.11: Snubber Design and Implementation
(a) Snubber design
(b) Snubber implementation

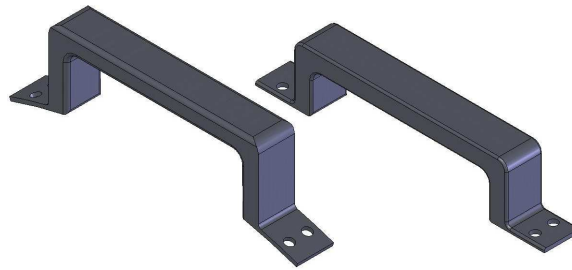


Figure 3.12: Lifting Handles. The handle on the left is the CAPE mounting plate's lifting handle, while the handle on the right will be attached to the oven mounting plate.

or even custom properties entered by the user, it will calculate the mass properties of a part or assembly. Using this tool, the masses of each of the redesigned structural components, as well as the mass properties of the overall structural assembly, have been estimated and are shown in Table 3.2. The total mass of the experiment structure (without handles) is approximately 163.7lb (74.4kg), or about 281% heavier than Holstein's 58.24lb (26.5kg) structure. A significant portion of this weight comes from the addition of the 65.1lb (29.6kg) CAPE mounting plate, while the remaining weight primarily is due to the larger diameter and thickness of the top plate and oven mounting plates.

Table 3.2: Structure Mass Properties

CENTER OF GRAVITY			
<i>(measured from center of CAPE mounting plate top surface)</i>			
x (towards computer bay):	-0.17cm		
z (towards bottom of experiment):	-0.03cm		
y (completing right-hand rule):	25.51cm		
MASS			
<i>Component</i>	<i>Mass (kg)</i>	<i>Quantity in Assembly</i>	<i>Total Mass (kg)</i>
CAPE Mounting Plate	29.646	1	29.646
Top Plate	7.614	1	7.614
Large Rib, w/o computer	6.107	1	6.107
Large Rib, w/ computer	6.093	1	6.093
Small Rib, w/o pinpuller	5.359	1	5.359
Small Rib, w/ pinpuller	5.363	1	5.363
Inflation Mounting Plate	0.773	2	1.546
Oven Mounting Plate	7.270	1	7.280
Bottom Plate	0.665	1	0.665
Shroud	2.848	1	2.848
Handle - Top	0.579	4	2.314
Handle - Bottom	0.536	4	2.143
Snubber	0.013	8	0.106
Oven Bracket	0.602	3	1.806
<i>Total Structural Mass:</i>			78.856

3.2 Electrical Subsystem

In this section, the modifying requirements and detailed design for the following items are presented:

- Shuttle feedback circuits
- Fusing Architecture
- Power distribution plate
- Wiring harness layout

3.2.1 Shuttle Feedback Circuits. The experiment's on-orbit operation is completely autonomous, but it will need to be powered on and off by the astronauts. Before disengaging power, the original intent was for the astronauts to wait a predetermined length of time to ensure the experiment's mission was complete. However,

the variability of the ambient temperature in the Shuttle cargo bay will directly affect the time required to heat the tubes, causing the overall mission duration to be unknown. Therefore, in order to prevent premature shutdown, feedback circuits have now been designed to provide the astronauts further insight to the experiment's state of operation.

A separate feedback circuit was also designed for the environmental heaters, which may be eliminated if the team determines that environmental heaters are not required. This circuit will tell the astronauts when the heaters are powered on.

3.2.1.1 Requirement Description. There is no documented requirement to incorporate the feedback circuits, nor are there documented requirements for their specific design. Since they are important to the success of the mission, however, the following design specifications were developed and agreed upon with STP:

- The system must indicate that the experiment is powered on
- The system must indicate the the experiment has completed its self test
- The system must indicate that the experiment has completed its mission and may be powered off
- If applicable, the system must indicate when environmental heaters are on
- The wiring and fusing of the system must meet NSTS 18798B requirements (discussed in Section 3.2.2)

3.2.1.2 Design. The circuits themselves are relatively simple. They will take power in from the Shuttle (Connector J2), fuse it, and then relay it to the Shuttle's display panel (via Connector J1). As shown in Figure 3.13, each circuit will contain a solid-state relay, which will be the the same type of relay used to route power to the ovens.

To control the relay coils, there are currently two options being considered. The first involves a digital input/output register on the computer's analog/digital converter board, and the second involves a new PC-104 relay board that has recently arrived, but has not yet been installed and tested.

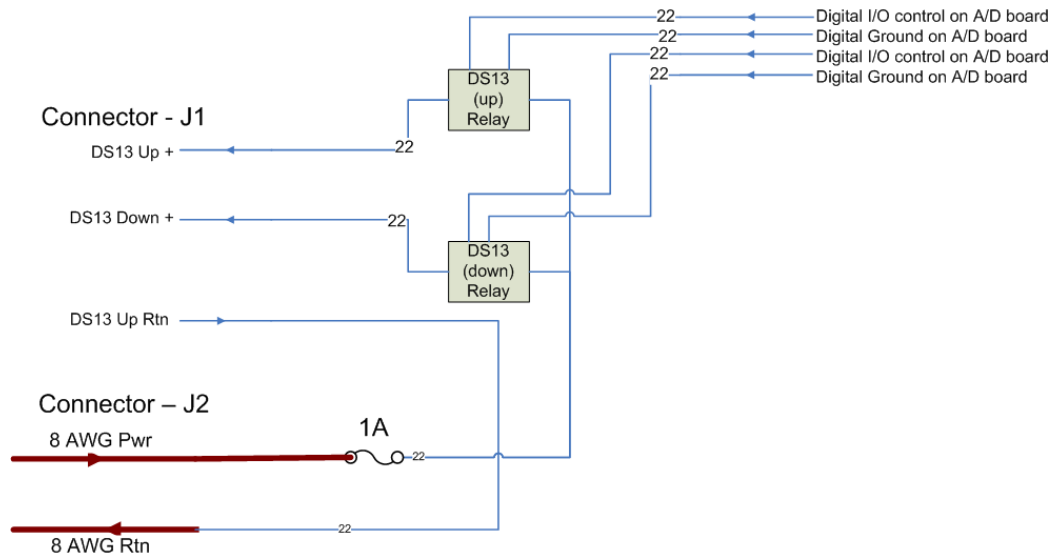


Figure 3.13: Shuttle Feedback Circuit Design

The first method uses one of the two digital input/output registers on the A/D converter board. The first register, addressed at **Base+1**, is shown in Figure 3.14(a). It controls three pins on the J3 analog input/output header, shown in Figure 3.14(b). This is the same header used to record the experiment's analog sensor data. Because only two bits will be needed to control both of the solid-state relays, the J3 header would likely be used if the decision is made to use the A/D board. The other register is a 24-bit register, controlling 24 pins of the J4 digital input/output header, which is on the other side of the board.

As currently planned, the relay controlling power to the display for the environmental heaters would be wired to the **Dout1** pin, and the relay controlling power to the display for the computer status would be wired to the **Dout0** pin. By writing a 1 to either of their respective bits of the register, a high signal of 5V will be sent to the pins, thus activating the relay coils and routing the Shuttle's power to the appropriate display.

The second method to control the solid-state relay coils would take advantage of the increased capability of the new relay board. The existing board contains 16 relays, all of which are used to control some aspect of the experiment's operation. The new

7	6	5	4	3	2	1	0
x	x	x	x	x	Dout2	Dout1	Dout0

(a)

Odd pins, 1-39	⋮	⋮	Even pins, 2-40
...	41	42	Dout 2
Dout 1	43	44	Dout0
Odd pins, 45-47	⋮	⋮	Even pins, 46-48
+5VDC	49	50	Digital Ground

(b)

Figure 3.14: A/D Board Digital Operation [9]

(a) Base+1 register (write operation)

(b) Digital input/output pins on J3 header

relay board will offer up eight additional relays for the team's use, two of which may be used for controlling the feedback circuits. The concept involves relaying +5V from the computer's DC-DC converters on the power supply board to the coil contacts. In fact, since this method is essentially how the rest of the experiment is controlled, it would be in place already if the existing relay board had any excess relays available. Therefore, pending test results of the board, this will likely be the implementation used.

3.2.2 Fusing Architecture. The original electrical power system used payload-provided battery power, which minimized the electrical interface to the Shuttle. As such, a fusing architecture was not part of the original design (though they would have been required for the Shuttle's switching circuits). With STP's offer to provide Shuttle power during the transition to CAPE, however, the interface requirements became significantly more complicated. To accommodate these requirements, a new fusing architecture has been developed.

The voltage supplied to the experiment is expected to be $28\pm 4\text{VDC}$. Therefore, the conservative approach for determining appropriate fuse and wire sizing requires using 32VDC as the supplied voltage, as discussed below.

3.2.2.1 Requirement Description. According to NSTS 18798B [25], any circuit containing a downsizing in wire gauge must be fused. With power from the Shuttle supplied via 8AWG (American Wire Gauge) wire, and all RIGEX wiring not larger than 22AWG, the entire electrical design needed to be fused. This included the oven heater circuits as well, as the Shuttle will be supplying power to them directly.

Complicating matters was a fuse derating requirement. Fuses have thermal properties associated with their operation, heating up as current passes through them. At sea-level conditions, where their rating is typically defined, the surrounding air will cool them through convection. However, in the vacuum of space, the absence of air causes fuses to not only heat faster, but also to blow at a lower current level [15]. Therefore, NASA imposes a strict 50% derating on every fuse used.

Additionally, once fusing is introduced into a circuit, stricter requirements are placed on the current rating of the wire used. Specifically, the current rating must now be at least 35% larger than the rating of the fuse (50% greater for fuses smaller than 3.5A), thereby ensuring the prevention of overheating and fire. All of these requirements were carefully considered as the steps to a new fusing architecture were taken.

3.2.2.2 Design. The first of these steps was to determine the expected current in the circuit. This can either be found by measuring it with an ammeter, or by using Ohm's Law (solved for current):

$$I = \frac{V}{R_{eq}} \tag{3.1}$$

where

$I = \text{Current (A)}$

$V = \text{Voltage supplied to the circuit (V)}$

$R_{eq} = \text{Overall resistance of the circuit (R)}$

Then, to account for the 50% fuse derating requirement, the current is doubled, and the next possible fuse size up is chosen for the design. Once the fuse size is chosen, the current rating of the fuse is then multiplied by 1.35 or 1.5, depending on whether it is above or below 3.5A respectively, and Table 3.3 is used to determine the minimum wire size.

Table 3.3: Maximum Current Ratings for 200°C-Insulated Wire Inside Payload Bay [25].

Wire Gauge	Maximum Current (A)	Wire Gauge	Maximum Current (A)
0	332.0	14	26.0
2	225.0	16	20.0
4	157.0	18	17.0
6	118.0	20	13.0
8	81.0	22	9.5
10	51.0	24	6.8
12	37.0	26	4.8

This process was applied to five main circuits that needed to be fused, with one of those containing the 15 oven heater circuits. Altogether, 20 fuses were added to the design, offering protection for the computer, the feedback circuit discussed in Section 3.2.1, the circuits containing the switches the astronauts will use to power the experiment, the circuit containing environmental heaters (which may be removed), and the main line supplying power to the oven heater circuits. The first four items are discussed here, while more detailed information on the oven heater circuits is provided in Section 3.2.2.3.

The first circuit considered for fusing was the power line to the computer. This circuit also powers the experiment's six pressure transducers, which draw 5mA of

current each. To determine the current drawn by the computer and its associated components, an ammeter was connected in between a 28VDC power supply mimicking Shuttle power (a 32VDC power supply was not available) and the computer's DC-DC converters on the PC-104 power supply boards. Although all components are not available for integration with the computer at this point, the maximum current draw is expected to occur during the modal testing of a tube, which has been done a multitude of times. Therefore, during a modal analysis test, the ammeter was used to identify this max expected current. During the test, the following components are powered by the computer:

- All PC-104 boards, including 8th-order Butterworth filter and four current amplifiers on custom-made filter board
- Step-up transformer
- Piezoelectric actuators
- Accelerometer
- Pressure transducers

With the exception of the pressure transducers, each component was powered, the tube excitation routine was run, and the current was monitored. At its peak, the current did not exceed 1.26A.

Rather than using this value in the fuse determination, however, a more conservative approach was taken using the current consumption data provided in each computer board's specification sheet. Each current value is specified with a DC-DC converted voltage, which means that simple power calculations can be performed to more accurately estimate current using

$$P = VI \tag{3.2}$$

where

$$P = \textit{Power} \text{ (W)}$$

$$V = \textit{Voltage} \text{ (V)}$$

$$I = \text{Current (A)}$$

In addition to the above equation, it is important to remember that DC-DC converters are not perfectly efficient, which means power will be lost during voltage conversion. According to the power supply board's specification sheet, the minimum converter efficiency is 80%, depending on load [8]. Using Equation 3.2 and the 80% efficiency factor, Table 3.4 shows the total predicted current drawn by the computer at 32VDC is 1.48A. As an additional measure of conservatism to account for the pressure transducers and additional components, a 15% margin is added on, bringing the max expected current to 1.7A, which is 35% higher than the highest current measured in the lab. For 1.7A, a 3.5A fuse and 22AWG wire will be used.

Table 3.4: Computer Current Consumption Determination

Computer Board	Specification (A ; V)	Converted Power (W)	Unconverted Power ¹ (W)	Current at 32V (A)
MZ104+ Processor Board (x2) [31]	0.94 ; 12 ²	11.28	14.10	0.441 x 2
Relay Board [7]	0.42 ; 5 ³	2.1	2.63	0.082 x 1
Counter/Timer Board [10]	0.36 ; 5	1.80	2.25	0.070 x 2
Thermocouple Board [3]	0.05 ; 5	0.25	0.31	0.010 x 1
A/D Converter Board [9]	0.20 ; 5	1.0	1.25	0.039 x 1
Camera Board [13]	0.05 ; 5	0.28	0.34	0.011 x 3
	0.21; 12	2.52	3.15	0.098 x 3
TOTALS		19.225	24.031	1.480

1. Assumes 80% DC-DC converter efficiency

2. Actual current for $\pm 5V$ and $\pm 12V$ not supplied; therefore, 12V used in calculation

3. Assumes all relays are activated

The fuse size for the circuits the astronauts use to switch on power was given by STP to be 5A, which was therefore used in the design.

Next, the fuse for the feedback circuits was determined. According to a STP, the resistance of each display panel circuit is 25k Ω . With a 32VDC source, the current through each circuit is only 1.28mA. The smallest readily-available space-rated fuse is 1/10A, but as an overconservative measure of protection, STP approved a 1A fuse and 22AWG wire implementation.

The last circuit discussed here is that of the environmental heaters, which may be eliminated if future testing deems appropriate. Currently, the heaters are included to meet the relay board's specified operating temperature of 0°C . However, the new relay board has an operating temperature range equal to that of the other computer boards, rendering the environmental heaters unnecessary. Assuming the heaters are kept in, however, they will first need to be identified before final design decisions are made. That being said, a 6A fuse and 22AWG wire are currently kept in the design as placeholders. It is recommended to choose heaters such that the current through the circuit is less than 3.5A so that 22AWG wire can still be used.

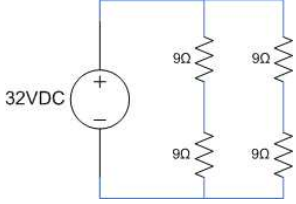
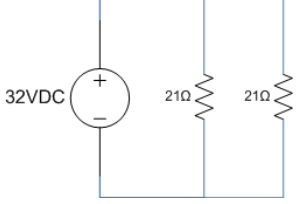
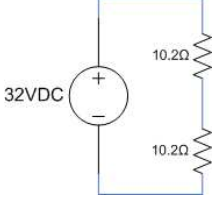
The final fused circuit includes the oven heaters, discussed in the next section.

3.2.2.3 Oven Circuit Design. The initial oven circuit designs met NASA wire sizing requirements. The hookup wire used to connect each heater circuit with its power relay was 22AWG, which according to NSTS 18798B, is rated to handle 9.5 Amps. In addition, the resistive heaters of Circuits #1 & #2 had two 26AWG lead wires soldered to them, and the heaters of Circuit #3 used 24AWG wires. Each of these circuits could handle up to 4.8A and 6.8A, respectively. As shown in Table 3.5, the current in each original circuit met each of these requirements, and there was no cause for concern.

The circuits, however, did not take fusing requirements discussed above into account. As a result, adding fuses in as an afterthought required significant redesign. As an example of an unmet requirement, consider Circuit #1 from Table 3.5. The current in the circuit was 3.56A, or 7.12A once fuse derating was taken into account. This means that at least a 7.25A fuse would need to be used in the circuit. Adding in the additional 35% safety factor for the wire brought the current up to 9.79A. This was above the 9.5A limit of the 22AWG hookup wire already purchased (see Table 3.3), so either the circuit or the wire needed to be modified.

Unfortunately, modifying the hookup wire would not completely solve the problem. Recall that each individual resistive heater has smaller lead wires attached to it.

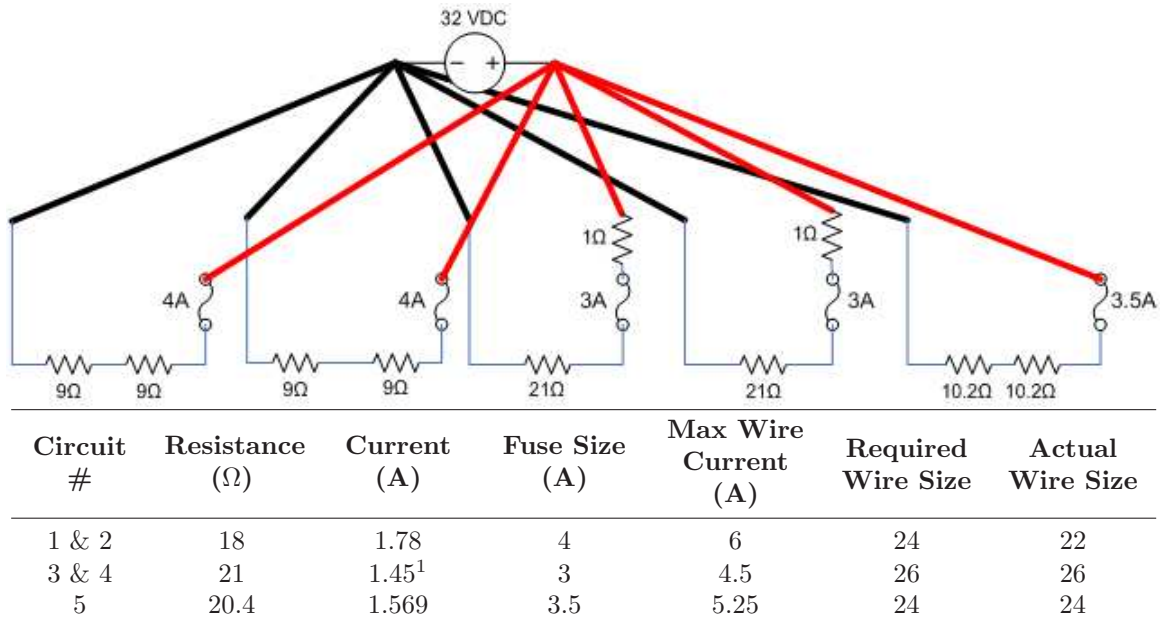
Table 3.5: Previous Oven Circuit Characteristics

Circuit #	Current (A)	Resistance (Ω)	Circuit Diagram
1	9	3.56	
2	10.5	3.05	
3	20.4	1.57	

Running the same analysis discussed in the previous paragraph yielded unacceptable results for these heater wires as well, identifying that new heaters with larger lead wires would need to be purchased if the decision was made to use larger hookup wire.

Ultimately, the team decided on a combination of a new circuit design and purchasing new resistive heaters. First, using the sizing process described above, the new design is shown with its characteristics in Figure 3.15.

When possible, steps were taken to avoid purchasing new heaters. For example, note the resistors used in Circuit #3 & #4. Using 32VDC, the current in the circuit is 1.524A. This requires a fuse of greater than 3A, which further requires a wire size larger than 26AWG. Rather than purchasing new heaters, however, the team decided to incorporate a 1Ω resistor into the circuit, which increases the resistance of the circuit to 22Ω . With this resistance, the current in the circuit is 1.45A, which is low enough for a 3A fuse and 26AWG wire. At a current of 1.45A, the power dissipated by the resistor (found using $Power = Current^2 \times Resistance$) is 2.11W. As with the fuses, the resistor needs to be derated as well, which means that a resistor rated to



1. Circuit #3 & #4 use a 1Ω resistor in series to drop the current below 1.5A such that a 3A fuse and 26AWG wire could be used.

Figure 3.15: New Oven Circuit Design Characteristics.

at least 4.5W must be used. The resistor will likely need to be heat-sinked, as well, which is yet to be determined.

The heaters used in Circuit #1 & #2 were not quite fortunate enough for minor design modifications, however. Their current was also too high for their lead wires, but powering them with the lower acceptable current level would introduce an unacceptable drop in their heating capability. Therefore, the team decided to purchase new versions of these heaters, this time using 22AWG lead wires and eliminating the risk of wire overheating.

3.2.3 Power Distribution Scheme. The distribution of power throughout the experiment begins with a Power Distribution Plate (PDP), which became another new addition to RIGEX. It is designed to take power from the Shuttle, fuse it, and then route it to the appropriate experiment bays. To do this, it consolidates the following electrical components into one central location:

- Primary fuses for Shuttle power; fuses to computer and heater circuits

- Electromagnetic interference filter
- Power relays routing power to Shuttle displays via feedback circuits discussed above
- Latching relay, activated with Shuttle power switch, to supply power to the computer
- Fault bond (ground)

To assist in the routing of signals, the PDP uses terminal strips and wires with closed terminals soldered to their ends. It is important to note here that there are wire size and current rating specifications associated with terminal strips. Therefore, care must be taken to ensure the appropriate hardware is used. Below is a list of the specifications required for each particular location in the design:

- 8AWG 5-pole terminal strip – Routes power from Shuttle to main fuse block
- 8AWG 10-pole terminal strip – Routes experiment returns to Shuttle return
- 14AWG 10-pole terminal strip – Routes Shuttle power to solid-state oven relays (fused from 8AWG to 14AWG)
- 14AWG 5-pole terminal strip – Routes power from oven relays to oven fuse block (to fuse from 14AWG to 22AWG (or higher))
- 22AWG 6-pole terminal strip – holds Schottky diodes that prevent current spikes to computer when solenoids are deactivated

3.2.3.1 Requirement Description. With the exception of the fusing and wire sizing requirements discussed previously, the requirements for the PDP were actually self-imposed *desirements*. They included:

- When possible, consolidate components directly interfacing with Shuttle power into computer bay to minimize wiring harness length
- Components should be consolidated on one plate (separate from rib) to minimize hole requirements in computer bay's rib
- Components should be situated such that wiring bends are minimized

3.2.3.2 Design. The physical layout of the PDP is shown in Figure 3.16. It consists of a 1/4"-thick (6.35mm) aluminum plate. Each component will be secured to the plate, and then the plate is secured to the rib of the experiment. Once all components are secure, the wiring is installed.

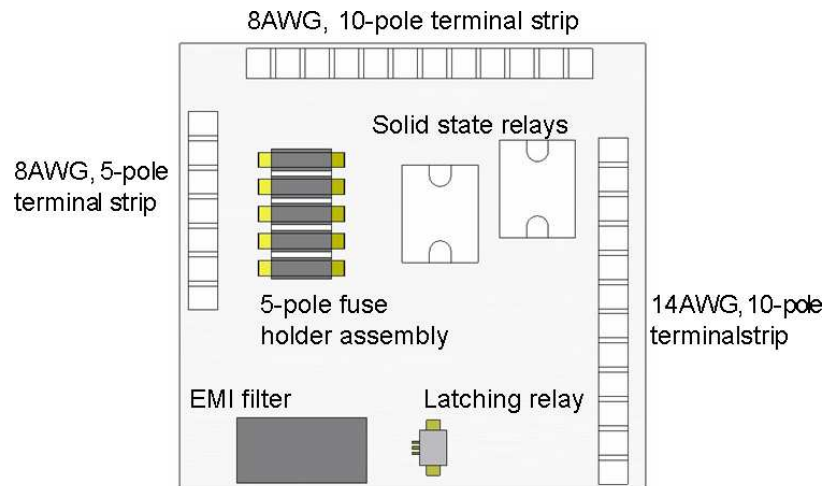


Figure 3.16: Power Distribution Plate

3.2.4 Wiring Harness Layout. The wiring of the experiment is separated into two major areas:

- Computer harness, internal to the computer
- Experiment harness, external to the computer

The interface of the two is the connector plate on top of the computer, which holds twelve 15-pin D-subminiature connectors, as shown in Figure 3.17.

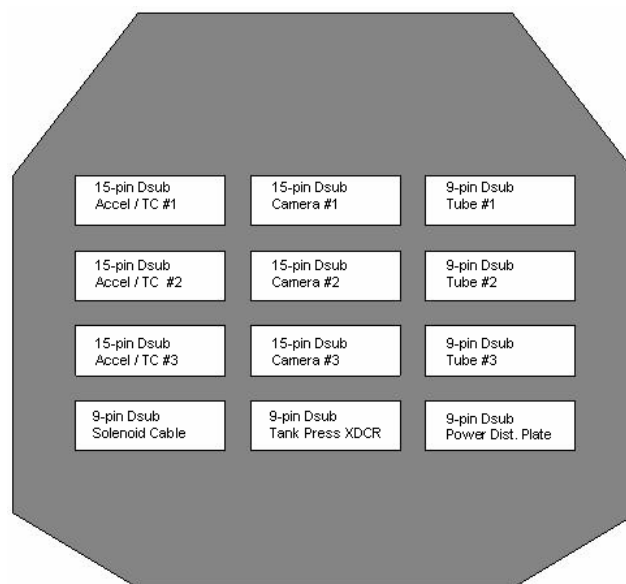


Figure 3.17: Computer Connector Plate

3.2.4.1 Requirement Description. The current rating requirements of the wire have all been discussed previously. However, there were additional requirements as well.

The first of these requirements was the temperature rating of the wire's insulation, which is a significant factor in the wire's current rating. According to NSTS 18798B, the insulation must be rated to a minimum of 100°C [25]. As this insulation rating goes up, so does the allowable current. Therefore, wire rated to 200°C was purchased to minimize the size required of each wire on the experiment.

Another primary requirement for the wire was the type of plating on the conductor. The options available were either nickel or silver plating. Nickel plating is typically better for corrosion resistance, but is difficult to solder. Silver plating, on the other hand, is very easy to solder, but can corrode, developing what is called *red plague* due to its red corrosion characteristics. Based on discussions with STP, and the relative simplicity of soldering silver, the silver plating was chosen. Combining the insulation and plating requirements, the military specification for the wire is MIL-W-22759/11, which will be used throughout the experiment.

The final requirement considered for the wiring was shielding. Most of the wire will not need to be shielded; however, the wiring from both the accelerometers and the pressure transducers will need to be such that noise on the data streams is minimized. Therefore, MIL-W-27500 wire was purchased. This type of wire contains a bundle of multiple MIL-W-22759/11 wires, and then surrounds the bundle with shielding. A free sample was provided by the manufacturer for testing, which was then validated using the experiment's excitation test. The resulting data was acceptable, and the wire was purchased.

3.2.4.2 Computer Harness Design. As part of his research effort, Moody developed an initial concept for the computer harness, and used breakout boards in the lab to verify correct signal routing. Although this signal routing was effective, building the harness for integration with connectors rather than the breakout

boards revealed several areas of potential improvement. In particular, rather than distributing his signal returns among the available return points, he combined many of them together. This worked great for the breakout boards, but created wire junctions in the test harness that were significantly large enough to cause concern over both vibration damage and solder strength. Therefore, where feasible, wires were rerouted to maximize the use of these available return locations. The final pinout of each board and connector is presented in Appendix E.1, and a simplified illustration of the wiring harness from the Shuttle power connectors to the computer is presented in Figure 3.18.

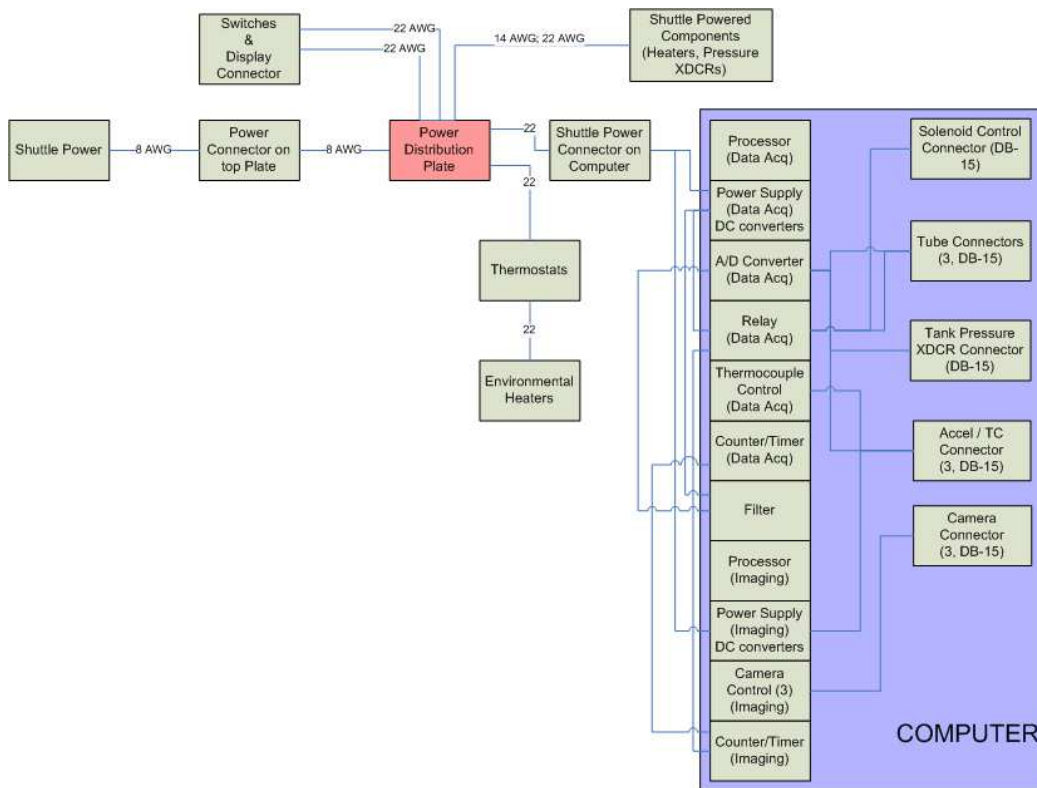


Figure 3.18: Computer Interface Harnessing

3.2.4.3 Experiment Harness Design. The experiment harness begins in the computer bay, combining signals from both the PDP and the computer itself. As illustrated (simplified) in Figure 3.19, the harness branches out to the experiment in a number of different directions.

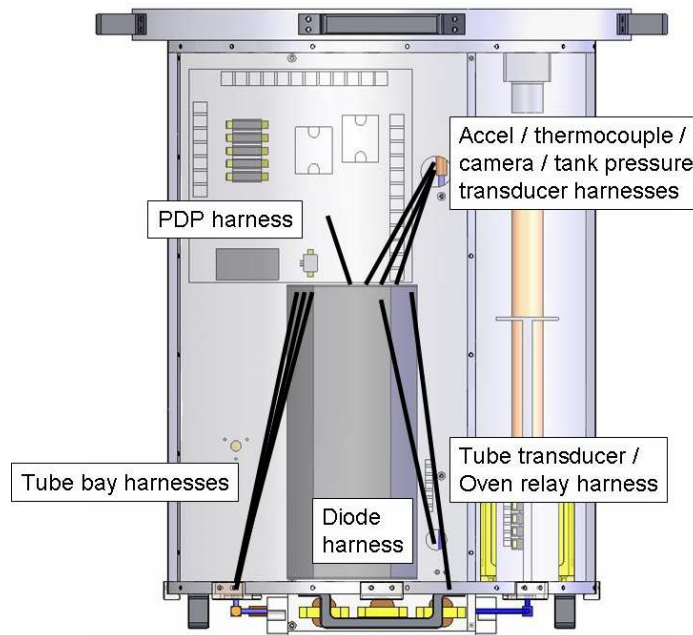


Figure 3.19: Computer Bay Harness Layout

One piece of the harness goes into the top of the center bay, providing power signals *to* and collecting data *from* the pressure transducers. Each rib also has a 1.5in (38.1mm) hole near the top to accommodate the harnessing for the accelerometer, camera, and thermocouples in its bay.

Another piece also goes into the bottom of the center bay, providing power to each of the three inflation system solenoids.

The remaining pieces include the power and data signals to and from the rest of the experiment. For purposes of this discussion, power signals refer to the power lines connecting the high voltage (28V) from the Shuttle to the oven relays and pressure transducers. In the computer bay, these signals are routed down the rib on the right side of the computer, while data signals are routed down on the left. This separation provides added protection from electromagnetic noise spilling over from the power signals and corrupting important experiment data. Each bundle goes through a hole in the oven mounting plate, and is then routed to its appropriate component.

On the data side, the components for the data signals include the three pressure transducers that monitor the internal pressure of the tubes. The third transducer is the final stop for this section of the harness.

On the power side, the solid-state power relays for the ovens, and the step-up transformers used to excite the tubes, are the next stop for the power harness. Power from the transformers and solid-state relays is then routed through a hole in each bay's oven mounting plate real estate. From the transformers, the harnessing is soldered to the hookup wires of the PZTs on the tube. From the oven relays, power is first routed to a terminal strip, then a fuse holder assembly, and finally the resistive heaters in the oven.

3.3 Inflation Subsystem Model

The original inflation gas storage section was mounted in one of the tube bays. However, based on earlier testing as well as his own, Lindemuth moved it to the computer bay. Then, when RIGEX moved to CAPE, Moeller took the first steps in placing a larger system in the interior bay where the experiment's battery once resided. Unfortunately, he did not have sufficient time to completely develop the interface to the experiment. Therefore, when Helms took over for him, she completed the inflation system's design.

Because much of the work done on the system was actually done by Helms, this discussion will be limited to the creation of the SolidWorks® model. The model was created for inclusion into the full assembly, and was further used to identify location and sizes of the required holes in the ribs, as well as the required spacing between components.

3.3.1 Requirement Description. The lack of a physical interface was the driving requirement for developing one. However, there were additional requirements used to develop it as well. Specifically, the larger storage cylinders were required to be mounted inside the interior bay. Further, the lack of a space-qualified, commercially-

available method for securing cylinders of this size required a new, custom development. Finally, the interface needed to leave enough volume inside the bay for wiring, pressure transducers, solenoids, and fill valves. With each of these requirements in mind, the interface was designed.

3.3.2 Design. The interface itself consists of two identical 3/8in (9.53mm) aluminum plates, both containing holes for the ends of the three cylinders. The plates, shown in Figure 3.20(a), will be used to sandwich the cylinders in place, as shown in Figure 3.20(b).

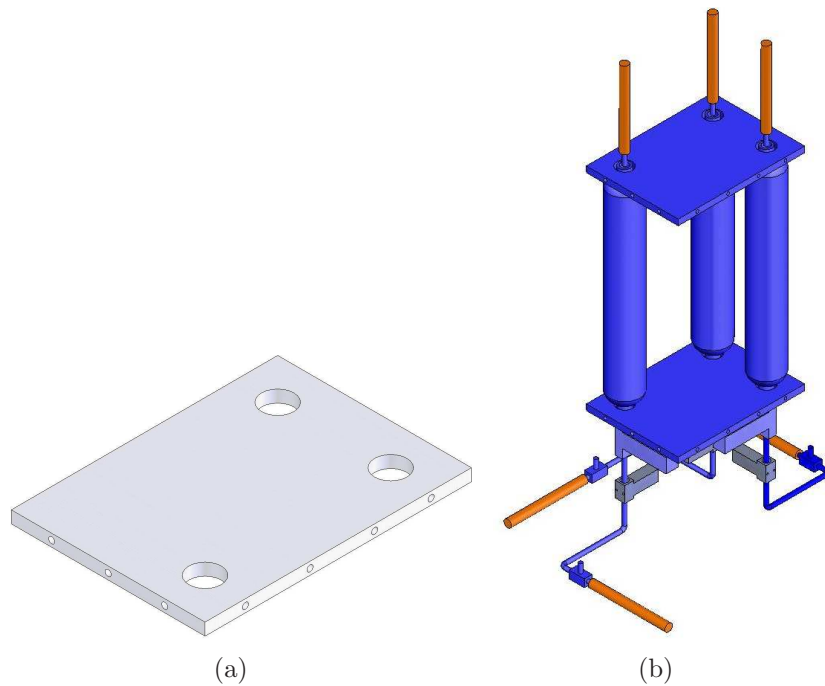


Figure 3.20: Inflation System Design
(a) Inflation system mounting plate
(b) Inflation system physical layout

Each side of the plates will be mounted to one of the four ribs using #10 bolts. Also, to prevent the cylinders from moving, Viton[®] rubber will be used to line each of the cylinder holes. Additional movement prevention will also be provided by components secured to the ribs, such as the solenoids and tubing.

3.4 Command and Data Handling Subsystem

Minor modifications to the Command and Data Handling (CDH) subsystem were made to increase mission effectiveness. Namely, the following components have been purchased to minimize a risk associated with the existing component:

- Relay board
- Power supply board
- Flash memory chips

The new relay board can withstand temperature extremes equal to those of the other PC-104 boards (-40 to 85°C), whereas the existing board is only qualified to operate above 0°C . It also provides an additional 8 relays over the existing board, intended to be used for the Shuttle feedback circuits discussed earlier. The board has recently arrived, but is yet to be tested.

Next, the existing power supply board can only withstand a sustained voltage of 30VDC. Unfortunately, the power supplied by the Shuttle could very well be 32VDC throughout the entire mission (though this is unexpected). Various options were considered for minimizing the risk of over-voltage causing damage to the computer, including the incorporation of Zener diodes across the input lines from the Shuttle. By using three diodes with a Zener voltage of 30VDC or less in parallel, a triple-fault redundant method of ensuring only 30VDC reaches the computer is established. Unfortunately, Zener diodes that are rated for such a high power are not commercial-off-the-shelf items. Therefore, the team decided to purchase new power supply boards from the same supplier as the relay boards. The voltage capability of the new board is 60VDC, thus eliminating the over-voltage risk. Unfortunately, the board has not arrived yet, and has therefore not been tested.

Finally, for the same reasons as the relay board, new flash memory chips have been purchased for the experiment. The new chips can withstand -40 to 85°C , whereas the existing chips were only rated to operate above 0°C . The memory remains the same at 1024MB. The chips have also just recently arrived, but have yet to be installed

and formatted. As Moody discussed in his thesis, significant complications may exist with formatting these chips; therefore, it is recommended they be installed sooner rather than later.

3.5 Chapter Summary

Even with the outstanding efforts of previous RIGEX researchers, no one could anticipate the changes required with the transition to the Shuttle's Canister for All Payload Ejections. With this transition, significant modifications were made to the experiment to not only meet new requirements, but also to take best advantage of the increased capabilities. The majority of these modifications were in the mechanical and electrical subsystems, but there were also minor changes made to the inflation and command & data handling subsystems. Each of these modifications, combined with unmodified efforts of the previous students, create the experiment's detailed design.

IV. Analysis and Results

This chapter presents the results of the analyses performed during this research effort. In particular, the analyses include a shroud containment analysis, used to verify the experiment's shroud thickness. Also, the results of a study on improving Moody's modal analysis procedure are presented.

4.1 Shroud Containment Analysis

A containment analysis was performed to determine the minimum required thickness necessary to ensure the shroud would indeed prevent a separated tube from breaking through and causing damage to the CAPE interior. An overview of this analysis, including pertinent results, is presented below, and the complete calculations can be found in Appendix C.

The analysis itself was developed by NASA, and contains two major equations [26]. The first of these is a velocity determination, shown in Equation 4.1:

$$V = \frac{A_{LF}}{2\pi f_n} + \sqrt{2aS_d} \quad (4.1)$$

where

A_{LF} = *Low Frequency Acceleration* (m/s²)

f_n = *First Fundamental Frequency* (Hz)

a = *Shuttle Acceleration* (m/s²)

S_d = *Maximum Travel Distance of Loose Component* (m)

The second is an energy analysis solved for thickness, shown in Equation 4.2:

$$T_R = \sqrt{\frac{1}{2}mV^2 \cdot \frac{1}{\text{perim} \cdot YS_w}} \quad (4.2)$$

where

$$m = \text{Mass (kg)}$$

$$V = \text{Velocity (m/s)}$$

$$\text{perim} = \text{Perimeter of Object's Smallest Face (m)}$$

$$YS_w = \text{Yield Strength of Wall Thickness (Pa)}$$

Table 4.1 shows the values and assumptions used for the analysis.

Table 4.1: Containment Analysis Assumptions and Values

Item Description	Value
Tube + endcap mass, m	0.170kg (1.165×10^{-2} slug)
Endcap perimeter, perim	0.120m (0.363ft)
Aluminum yield strength, YS_w	2.413×10^8 Pa (5.04×10^6 lbf/ft ²)
Gravity, g	9.807m/s ² (32.17ft/s ²)
Acceleration, A_{LF} & a	Varied (See Table 4.2)
Minimum Natural Frequency, f_n	35Hz (recommended in SSP 52005)
Maximum travel distance, S_d	0.762m (2.5ft)

The complete analysis was conducted for two separate cases, which also contained two separate subcases each. The first case involved the tubes breaking during reentry and landing. For the first subcase, it was assumed that the Shuttle and tube were accelerating at the same rate of 6.5g. The result was a thickness of 0.018 inches (.45mm). Then, for the purposes of over-conservatism, a second subcase assumed the tube and Shuttle were both accelerating at *twice* the Shuttle's maximum acceleration, or 13 times the force of gravity (127.5m/s²). This yielded a required thickness of 0.026 inches (0.66mm).

The second case involved the tube failing due to overpressurization, but further calculations were needed to determine the endcap's acceleration if this occurred. The first step in this determination was finding the maximum expected pressure inside the tubes. Using the ideal gas law ($PV = nRT$), this pressure was determined to be roughly 18 psi (127kPa) [28]. Using this pressure, the endcap's mass and cross-

sectional area, and Newton’s Second Law of Motion (in terms of pressure and area for force: $Pressure \times Area = Mass \times Acceleration$), the endcap’s acceleration was determined to be 195g’s.

Using this acceleration value in place of the low-frequency acceleration (A_{LF} in Equation 4.1), the first subcase was run using 6.5g’s for the Shuttle acceleration, yielding a required thickness of 0.021in (0.53mm). Similar to the first case described above, a second subcase using a 13g Shuttle acceleration, resulting in a 0.027in (0.68mm) thickness.

Table 4.2: Containment Analysis Results

Description	Shuttle Acceleration (g)	Tube/Endcap Acceleration (g)	Shroud Thickness (mm)	Margin over 1.91mm (%)
Shuttle/tube accelerate at 6.5g’s	6.5	6.5	0.55	346
Shuttle/tube accelerate at 13g’s	13	13	0.79	241
Tube overpressurization at Shuttle acceleration of 6.5g’s	6.5	195	0.66	289
Tube overpressurization at Shuttle acceleration of 13g’s	13	195	0.81	236

The design conservatively uses an aluminum sheet that is 0.075 inches (1.91mm) thick. Therefore, as seen in Table 4.2, the results of the analysis show nearly a 300% margin of safety over even the largest calculated thickness. This allows the team flexibility to reduce shroud size if desired, while also providing excess capability for an unexpected catastrophic failure of the tube.

4.2 Tube Modal Analysis

While the inflatable tubes have been studied by numerous students throughout the evolution of RIGEX using a variety of data acquisition systems, as discussed in Chapter II, Moody was the first to use the experiment’s PC-104. To do this, he developed

- **Matlab**[®] code to generate the digital values that the D/A converter would use to create the analog excitation signal

- Experiment's C++ code to convert the digital values to an analog voltage for the excitation signal (D/A converter)
- Experiment's C++ code to record the analog voltage from the accelerometer and convert it back to digital values (A/D converter)
- **Matlab**[®] code to interpret the digital codes to calculate the frequency response functions (FRF)

Building upon these successful FRF's, the opportunity was taken to find methods of increasing the signal-to-noise ratio of the signals used to create them. Specifically, modifications involved experimenting with the following items:

- Changing accelerometers
- Modifying and filtering the excitation signal
- Filtering the accelerometer signals

In this section, the theory behind the calculation of an FRF, a description of the test setup, as well as each of these modifications are presented in further detail.

4.2.1 Frequency Response Function. A frequency response function (FRF), or transfer function, is essentially the ratio of a system's output to an input (or excitation signal) over a given frequency range. The following development is from course notes provided by Cobb [4]:

$$H(s) = \frac{X(s)}{F(s)} \quad (4.3)$$

where

$$H(s) = \text{Transfer function}$$

$$X(s) = \text{Output signal, in frequency domain}$$

$$F(s) = \text{Input signal, in frequency domain}$$

It shows where the frequencies of the system resonances (modes/natural frequencies) are, and can be used to estimate modal damping coefficients. The quality of transfer functions is dependent on both input and output quality; therefore, it is important to

ensure that these two signals are recorded appropriately, with a high enough signal-to-noise ratio (SNR).

In the lab, spectrum analyzers are often used to determine FRFs. To do this, they first record the voltage level (in the time domain) of the excitation and sensor signals throughout the entire excitation process. Then, the Discrete Fourier Transform (DFT) is required to convert the time domain data of both signals to the frequency domain. The DFT is analogous to a Fourier series expansion in the continuous domain, and is calculated with the equation

$$X_k = \frac{1}{T} \sum_{r=0}^{N-1} x_r e^{-\imath \frac{2\pi k}{T} r \Delta} \quad (4.4)$$

where

$k = k^{th}$ harmonic of sampling frequency

$T =$ Period of data block (seconds)

$r = r^{th}$ sample of data block

$N =$ Block size of data

$x_r =$ Value of x at r^{th} sample

$\imath =$ Complex number, $\sqrt{-1}$

$\Delta =$ Sampling period (seconds)

Since the period of the data block is equal to the product of the block size and sampling period ($T = N\Delta$), Equation 4.4 can also be written as

$$X_k = \frac{1}{N} \sum_{r=0}^{N-1} x_r e^{-\imath \frac{2\pi k}{N} r} \quad (4.5)$$

For experiments that record time data and then post-process it, as in the case for RIGEX, **Matlab**® can do this with the command **fft**. FFT actually stands for Fast Fourier Transform, which by definition, requires a data block whose size is a power

of 2. If the block size is not a power of 2, as again in the case for RIGEX, the command actually calculates the DFT of the signal. One important note is that the DFT assumes a signal is periodic, so special care must be taken when performing its calculations. Otherwise, errors in the digital processing can result.

With the DFTs, the next step is to calculate the power spectral densities (PSD) of the signals. **Matlab**® does this with the **psd** or **pwelch** commands, but the basic idea is to take the DFT of the autocorrelation function, which is defined in discrete form (using $T = N\Delta$ substitution) as

$$R_r = \frac{1}{N} \sum_{s=0}^{N-1} x_s x_{s+r} \quad (4.6)$$

where

$R_r = \text{Autocorrelation function}$

$x_s = \text{Value of } x \text{ at sample } s$

$x_{s+r} = \text{Value of } x \text{ at sample } s+r \text{ (time shift implied in } r)$

A cross-correlation function of signals x and y can be calculated with this equation as well:

$$R_r^{xy} = \frac{1}{N} \sum_{s=0}^{N-1} x_s y_{s+r} \quad (4.7)$$

where

$R_r^{xy} = \text{Cross-correlation function}$

$x_s = \text{Value of } x \text{ at sample } s$

$y_{s+r} = \text{Value of } y \text{ at sample } s+r \text{ (time shift implied in } r)$

One source of digital processing errors, namely *leakage* errors, can occur when computing the autocorrelation function if a signal is not periodic (i.e. when x_s is not equal to x_{s+r}). Leakage is a phenomenon where the power in one frequency is math-

ematically leaked into adjacent frequencies, which may not actually be present in the signal. To minimize these errors, windows can be used, where each point in a block of data is multiplied by *multiplication factor*. By using a window, large discontinuities from block to block are minimized, causing the signal to appear more periodic, and resulting in more accurate DFTs.

Next, by plugging Equation 4.7 into Equation 4.5, the general equation for calculating the PSD, S^{xx} , is defined,

$$S^{xx} = \frac{1}{N} \sum_{r=0}^{N-1} \left[\frac{1}{N} \sum_{s=0}^{N-1} x_s x_{s+r} \right] e^{-j \frac{2\pi k}{N} r} \quad (4.8)$$

Then, by separating terms and taking advantage of the fact that $x^s x^{-s} = 1$, Equation 4.8 can be written as

$$S^{xx} = \left[\frac{1}{N} \sum_{s=0}^{N-1} x_s e^{j \frac{2\pi k}{N} s} \right] \left[\frac{1}{N} \sum_{r=0}^{N-1} x_{s+r} e^{-j \frac{2\pi k}{N} (s+r)} \right] \quad (4.9)$$

or

$$S^{xx} = DFT(X^*) DFT(X) \quad (4.10)$$

where

$$\begin{aligned} DFT(X^*) &= DFT \text{ of signal's complex conjugate} \\ DFT(X) &= DFT \text{ of signal} \end{aligned}$$

By using the cross-correlation function instead of the autocorrelation function, this same process is used to calculate the *cross* power spectral density (CPSD). Here, Equation 4.11 becomes

$$S^{xy} = DFT(X^*) DFT(Y) \quad (4.11)$$

Finally, with the PSDs and CPSDs of the signals, the transfer functions can be calculated. Again, **Matlab**® has a command for this called **tfestimate**, but with the

PSDs and CPSDs, it is easily calculated with Equation 4.12:

$$H(s) = \frac{S^{xy}}{S^{xx}} \quad (4.12)$$

where

$H(s)$ = Transfer function

S^{xy} = Cross power spectral density of output and input signals

S^{xx} = Power spectral density of input signal

This entire process is done almost instantaneously with spectrum analyzers, but with the help of post-processing tools like **Matlab**[®], can also be done quickly even if spectrum analyzers are not available.

4.2.2 Test Setup. For the inflatable tubes, the first step in determining the FRF's was recording the voltage level (in the time domain) of the excitation signal, without actually exciting the tube. Typically, accelerometer and excitation data would be recorded simultaneously. Unfortunately, however, by attempting to record the excitation signal while also exciting the tube, too large of an impedance was introduced into the circuit and the transformer would not supply enough power to the PZT's to excite the tubes with a large enough SNR. While current amplifiers could be incorporated into the circuit to eliminate this problem, recording the input signal and using that in the FRF calculations yielded acceptable results. Although not ideal, this method was still an improvement over the previous implementation, which used a mathematically-ideal representation of the signal rather than measured data.

Once the time domain data of the excitation signal is recorded, the transformer was then hooked back up to the PZT's, the tube was excited, and time domain data of the accelerometer was recorded by the A/D converter board. The data was then

pulled off of the computer's hard drive using a standard USB thumb drive, and run through a post-processing **Matlab**[®] routine as described above (written by Moody).

To perform the tests, the following components were needed:

- PC-104 computer (including power supply) to excite tube and record data
- Step up transformer to provide adequate voltage to the PZTs
- Inflated tube, complete with installed PZTs
- Accelerometers
- Moody's **Matlab**[®] post-processing routine

Using the digital/analog conversion scheme of the PC-104 converter board, a 0-1000Hz chirp signal was coded and stored onboard the computer to act as the excitation signal. It is routed from the converter board through an eighth-order Butterworth filter with a cutoff frequency of 1000Hz to minimize digital aliasing, which is a phenomenon that can introduce undesired frequencies in a signal based on the digital/analog conversion rates. It is then routed to the transformer, which is used to actuate two PZTs on the tube, both at opposite polarity. The data from the accelerometer is taken directly into the analog/digital converter, at a sampling frequency of 5000Hz, and stored for post processing. A rough layout of the test is shown in Figure 4.1.

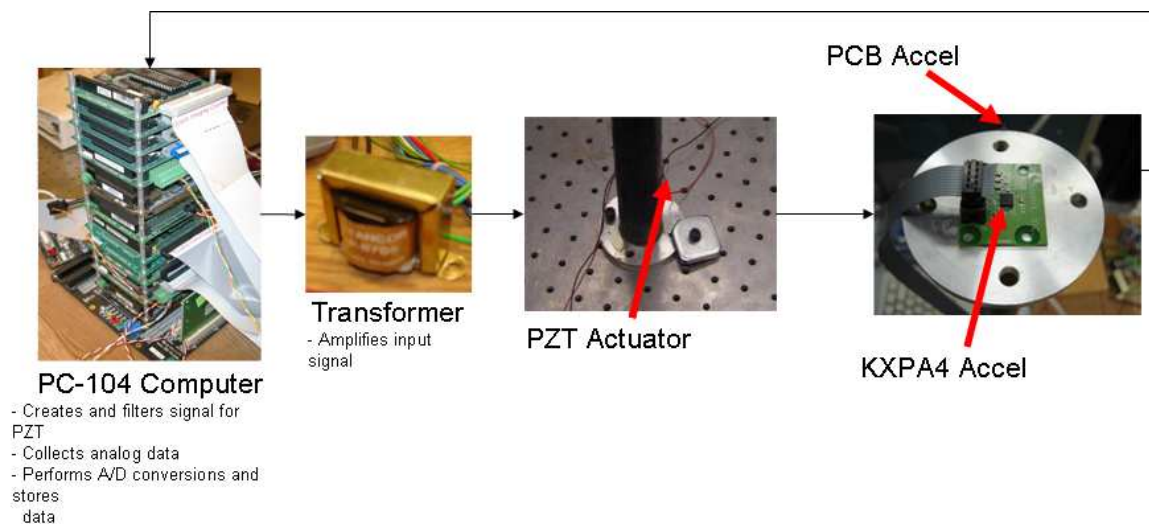


Figure 4.1: FRF Test Layout

During the excitation process, 25 iterations of the chirp signal are used to actuate the tube. The stored data from each axis of the accelerometer, as well as the chirp signal, is windowed using a Hamming window, shown in Figure 4.2.

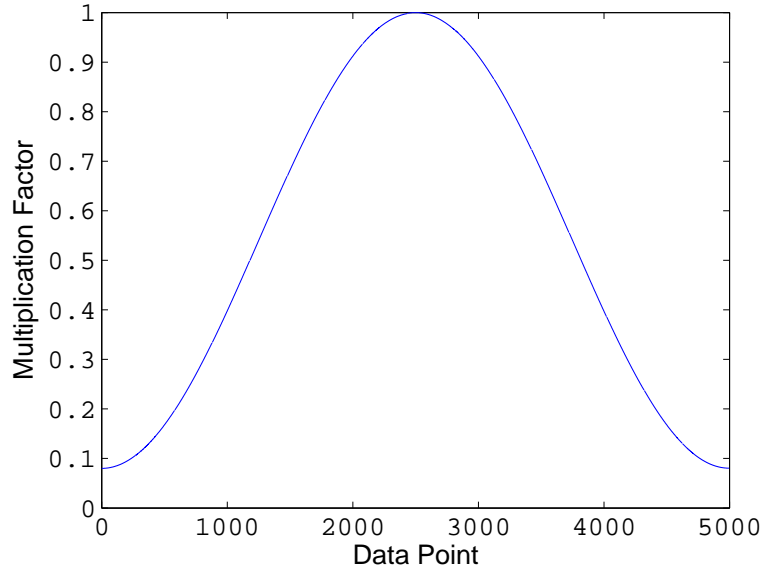


Figure 4.2: Matlab® Hamming Window

While this test setup provided the basis for each of the tests described below, a number of tests also used additional laboratory equipment. In particular, the tests took advantage of SignalCalc and a dSpace system, similar to the system Single used. With dSpace, the signals were interfaced with Matlab® and SimuLink®, which allowed testing to be done on various filtering ideas using software without the necessity of building hardware that might not be used.

4.2.3 Accelerometer. The key advantage of the existing triaxial accelerometer used in the experiment was in its self-contained signal conditioning electronics. As such, a significant disadvantage was in its large size, which Moody concluded was the cause of a reduction in the tube's first two modes from 60Hz and 660Hz to 50Hz and 300Hz, respectively [24, p.4-11]. Figure 4.3 clearly shows the 300Hz mode, which was not seen with the lighter accelerometers used by Single and Philley.

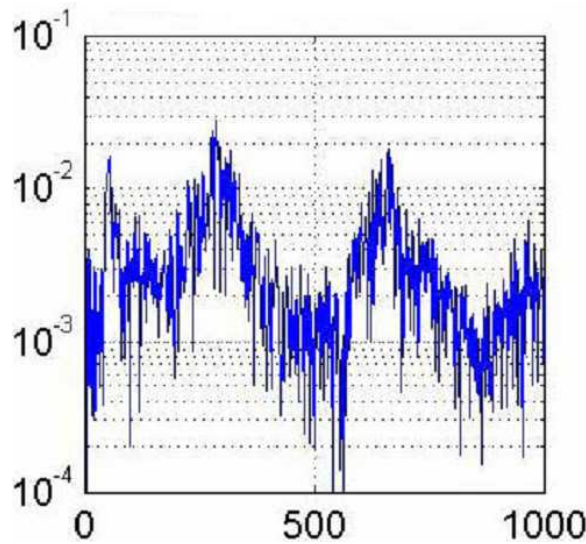


Figure 4.3: Tube FRF as Determined by Moody [24]

Although Moody's results were acceptable to the team, they were not quite ideal. Therefore, when an extremely low-cost, lightweight triaxial accelerometer was identified during the course of testing as a potential solution, the decision was made to look into it further. The accelerometer is the KXPA-4, made by Kionix Incorporated, and consists of a sensing element, an application-specific integrated circuit (ASIC), and a protective silicon cap (hermetically-sealed to minimize environmental damage), all of which are packaged in a tiny 5x5x1.2mm Dual Flat No-lead (DFN) chip. The sensor itself measures differential capacitance, which is proportional to the chip's acceleration. By converting this differential capacitance into an analog voltage, the acceleration can be monitored using any of the data acquisition systems discussed previously.

The accelerometer is designed for easy integration into any circuit board design. However, because they were being looked at as a replacement accelerometer, a circuit board design was not in place. Rather than designing one and potentially determining later that the accel was not right for this implementation, an accel was ordered with an evaluation board from the factory. The accel and this evaluation board are shown in Figure 4.4 next to the original accel.

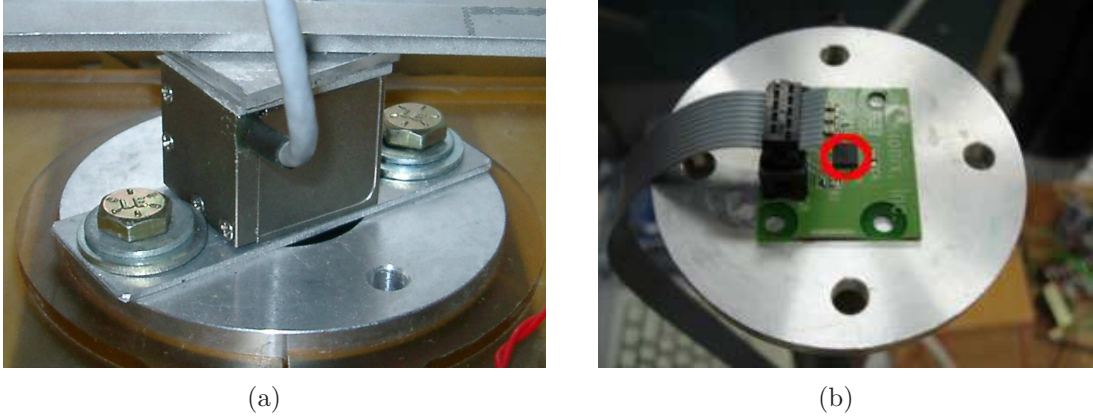


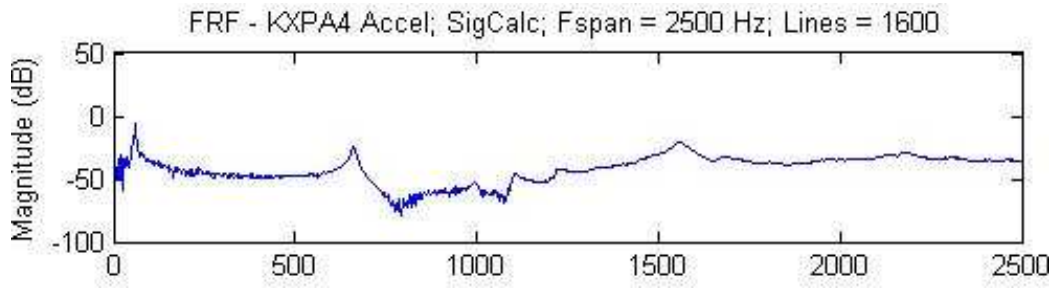
Figure 4.4: Accelerometer Comparison
(a) Original Accelerometer (Summit Instruments PCB 35200a)
(b) KXPA-4 Accelerometer (circled) with Evaluation Board. As a point of reference, the circled accelerometer is roughly the size of the cable connected to the original accelerometer

The evaluation board was wired to a breakout board, which was then used to route the KXPA-4's signals into SignalCalc. The excitation test was run, and the accel performed superbly, as shown in Figure 4.5(a). The signals were then routed into the PC-104 A/D converter, the test was rerun, and acceptable (while noisy) results were again obtained, as shown in Figure 4.5(b). Specifically, the accel did not induce any modes in the 1000Hz frequency span the experiment is concerned with. Therefore, the decision was made to utilize this accel for the flight mission.

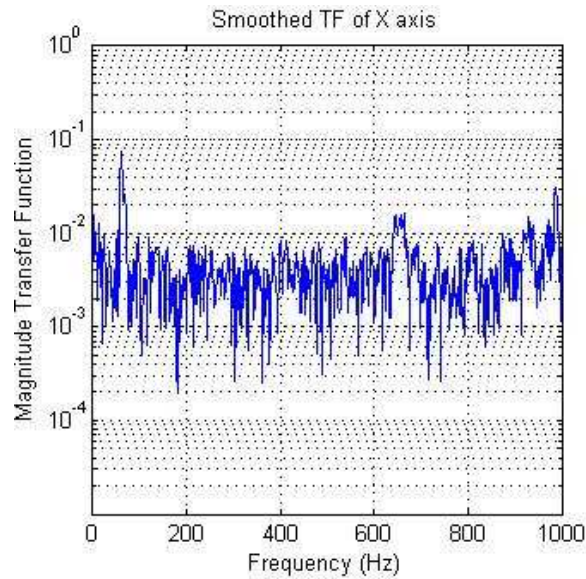
4.2.4 Excitation Signal. As seen in Figure 4.5(b), there was a significant amount of noise recorded on the signal from the KXPA-4. One way to correct this is to boost the power level in the excitation signal.

The general equation used to generate the signal, as defined by Moody, is $\cos(2\pi(5 + 995t)t)$ [24]. Keeping in mind that the output limit of the D/A converter is 5V, the amplitude of this signal was varied from 1-5V, and measured using SignalCalc.

At an amplitude level of 5V, the signal clipped off at 4.4V, which mathematically introduces high frequency (theoretically infinite frequency) components into the



(a)



(b)

Figure 4.5: Results of KXPA-4 Accelerometer Test
 (a) FRF recorded and calculated by SignalCalc software
 (b) FRF recorded by PC-104, and calculated with experiment's post-processing routine

signal. Recall that the signal is recorded in the time domain, and then transformed into the frequency domain with the DFT for use in FRF calculations. Although the 8th-order Butterworth filter on RIGEX has a cutoff frequency of 1000Hz to prevent high frequency from getting to the transformer, it would still affect this method of calculating the FRF. Therefore, the 5V option was discarded.

Next, because the D/A conversion is not perfect, the 4V signal was still clipped at 4.4V, and was therefore also discarded as an option.

The next level attempted was 3V, which was produced without any clipping. The signal still got close to 4V, however, so a 3.5V amplitude was not attempted. Therefore, this portion of the test was concluded, and the next step was to record the signal with the PC-104 A/D converter. Again, no clipping issues were seen, and the decision was made to use 3V as the amplitude for future tests. The power spectral density of this signal, shown in Figure 4.6, is expected to be used to calculate the transfer functions of the tube during the mission.

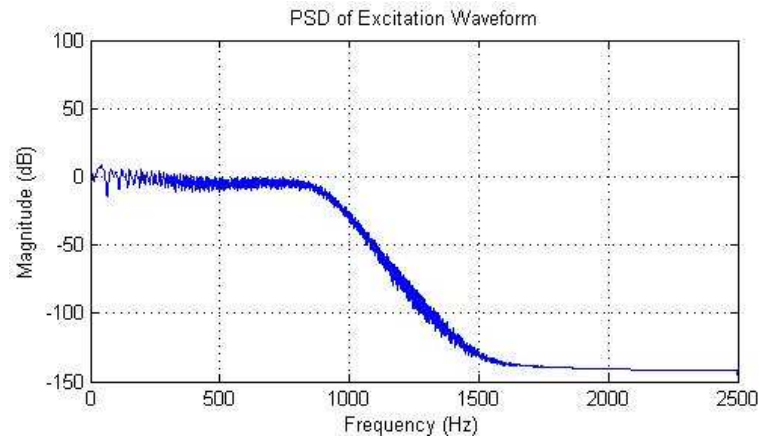


Figure 4.6: Power Spectral Density of 3V, 0-1000MHz Chirp Signal

4.2.5 Filter. After increasing the power in the excitation signal, the next step was an attempt to reduce the power of the noise in the accelerometer signal. To do this, Matlab®, dSpace, and SimuLink were used to create a both a discrete high-pass filter to filter the DC bias out of the accelerometer signal before it could be recorded by the A/D converter, as well as a discrete low-pass filter to reduce its high-frequency noise. Both proved to negligibly improve the FRF, and were therefore not incorporated.

4.2.6 Conclusions. In summary, the following modifications were made to enhance the tube's FRF:

- Change to a new lightweight accelerometer

- Modification to post-processing code to use recorded time-domain data of 3V excitation signal instead of mathematically ideal representation
- Increase excitation amplitude by power of 3

The result of these changes are shown in Figure 4.7.

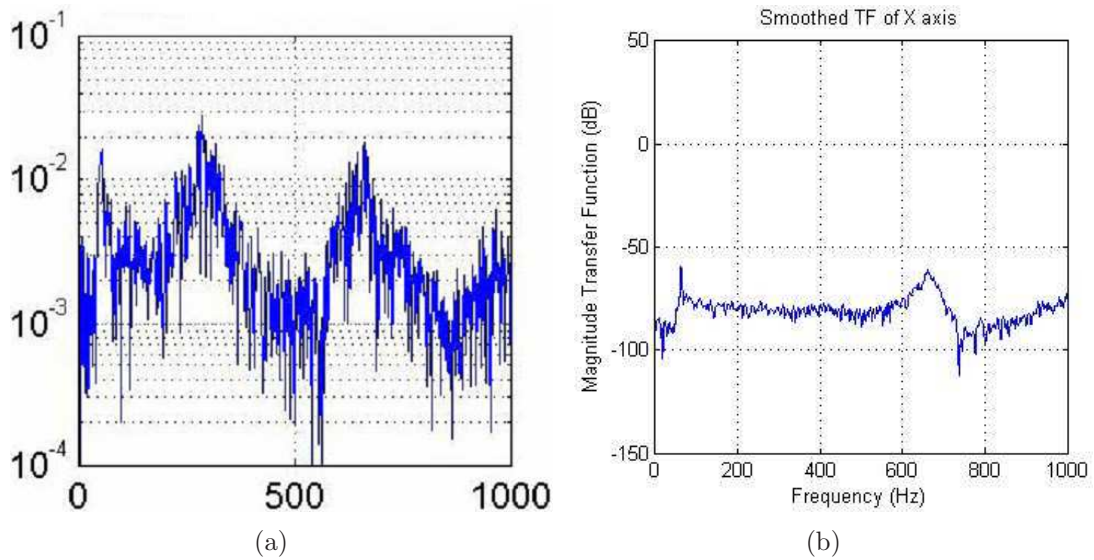


Figure 4.7: Results of Excitation Signal Modifications
 (a) Original FRF, before modifications [24]. Note mode at approx. 300Hz
 (b) Improved FRF (shown in dB magnitude). Note elimination of 300Hz mode

4.3 Chapter Summary

In this chapter, the results of a containment analysis, as well as a study of the tube FRF calculation are presented. The containment analysis shows that the 0.075in (1.91mm) aluminum shroud used on the experiment is 280% larger than the thickness required to contain a broken tube at even its highest predicted velocity. Also, the study of the FRF resulted with a significantly-less noisy calculation.

V. Recommendations and Conclusion

This detailed design represents a snapshot of all the modifications made to the experiment over the last year, and is not quite an exhaustive presentation. Due to the nature of timelines associated with theses, there are still efforts that need to be completed prior to the Critical Design Review (CDR), which is currently scheduled for April 2006.

5.1 Recommendations

A summary of the work to be done to the mechanical and electrical subsystems includes:

- Mechanical Subsystem
 - Mechanical drawings need to be approved and delivered to modeling shop for structural manufacturing
 - Fastener destructive testing needs to occur
 - Environmental testing needs to be accomplished
 - Thermal model needs to be completed
- Electrical Subsystem
 - PC-104 power supply and relay boards need to be integrated and tested with experiment computer
 - Accelerometer board needs to be designed and built
 - Initial verification test needs to be completed
 - The further development of a Shuttle emulator needs to occur
 - Profile of experiment's current drawn during testing needs to be determined and provided to STP
 - Flight wiring harness needs to be built

Each of these items are discussed briefly below.

5.1.1 Mechanical Subsystem Tasks. The first task to be done on the mechanical side is the approval of the structural drawings. This is expected to occur with the CDR. Once approval is established, the drawings will need to be sent to the AFIT modeling shop. Also, due to the safety processes STP must follow, they

have requested that *strict* configuration control is kept throughout the flight hardware build. All drawing revisions will need to be managed, and should be coordinated through their office. Once the components are built by the shop, there will also be requirements on assembling them. One example is the two-person-integrity rule, which means that there will need to be two people present during assembly to ensure quality control.

Next, as part of the CDR, the type of fasteners used for the experiment are expected to be approved. With this approval, the flight fasteners can be purchased. When they come arrive, a strict fastener integrity program will need to be purchased, starting with a non-destructive test run by STP. During this test, a pre-determined number of fasteners from each lot will need to be sent to STP. Also, throughout integration and test, the RIGEX team must know exactly where each fastener on the experiment came from.

Next, once the experiment is built, RIGEX will need to undergo space-qualified environmental testing. Specifically, it will need thermal vacuum (TVAC) testing, vibration testing, electromagnetic interference (EMI) testing. The TVAC and vibration testing can be done at AFIT, but the EMI testing will most likely need to be done in a separate facility. Currently, STP has offered up facilities they have available to them in Houston, but this requires shipping the payload across the country. There may be closer facilities to Wright-Patterson, and should start being planned now to help minimize potential scheduling conflicts later.

Finally, a thermal model of the experiment has been initiated, but due to software licensing complications, has been held up. These complications have recently been removed, so the model can now be finished.

5.1.2 Electrical Subsystem. A task that will slightly change the electrical design that still needs to be completed is the integration and test of the new PC-104 power supply and relay boards. The relay boards have recently arrived, so work can begin on them immediately. The power supply boards have still not arrived, however.

All that should change is the internal wiring of the computer, unless the boards require significantly more power than the existing boards (not available on respective data sheets). Although this is highly unexpected, the fuse and wire sizing of the computer circuit could change.

Next, the initial verification test (IVT) is a subset of the experiment's C-code that will be run every time the computer boots up. In a sense, the IVT is a self-test to help ensure proper operation. However, because the IVT will be run with each power up, there are certain functions that *can not* be included. For example, if the inflation system solenoid is activated when the computer is turned on in space, the ambient vacuum pressure will cause the gas to equalize with the pressure in the tube prior to reaching its glass temperature, and the mission will fail. Before the IVT can be finished, the team will need to determine and decide upon the appropriate activities to be conducted.

As part of the IVT, a Shuttle emulator will need to be developed. The initial design for this emulator exists, but the final decision on connector types has still not been made. STP has offered the flight connectors for RIGEX, but is still in the processing of determining the best way to route power from the Shuttle to the experiment. In the meantime, the emulator is intended to include the two switches for the astronauts (S13 and S15), as well as three LEDs to mimic displays DS13-Up, DS13-Down, and DS15, all of which are the lights on the display panel that the astronauts can watch during the mission. In addition, the emulator will also contain the 28VDC power supply that RIGEX will be powered with during integration and test, as well as two banana jacks for connection with an ammeter.

Then, once the IVT and is completed, the electronic current profile of the computer during the test will need to be determined. This can occur either with the emulator or not. The current profile will also need to be determined for the entire experiment as the astronauts may be monitoring it during the mission.

Lastly, the wire used to build the experiment's harness will need to be sent to STP for flammability testing. Once it returns, the flight harness can be built. In the meantime, since wiring has changed since the construction of the existing test harness, a new one (preferably using non-flight wire as it is a limited resource) can be built. Also, before building the flight harness, it may be beneficial for students and/or technicians to be certified in soldering procedures.

5.2 Conclusion

Working with Dr. Cobb and Lieutenant Helms, the RIGEX payload has come a long way over the last year. Major milestones include the signing of the Memorandum of Agreement and the Program Requirements Document, as well as a successful Preliminary Design Review and Phase 0/I Safety Review. The mechanical and electrical designs have matured as RIGEX was essentially redesigned for flight in the CAPE, and the post-processing of its data has been refined. Remaining tasks, as well as the follow-on students that will complete them, have been identified, and are already in the process of being completed. In short, RIGEX is well on its way to a successful mission, ultimately providing future engineers with a strong foothold on the use of inflatable, rigidizable technology.

Appendix A. Memorandum of Agreement

The following pages include the approved Memorandum of Agreement.

MEMORANDUM OF AGREEMENT
BETWEEN
THE USAF SPACE AND MISSILE SYSTEMS CENTER (SMC)
SPACE TEST PROGRAM (STP)
AND
THE AIR FORCE INSTITUTE OF TECHNOLOGY (AFIT)
FOR THE
RIGIDIZABLE INFLATABLE GET-AWAY-SPECIAL EXPERIMENT
(RIGEX)
S05-2

FOR THE EXPERIMENT SPONSOR:

(SIGNATURE) (DATE)
Dr. Robert Calico, Jr.
Dean, Graduate School of Engineering
and Management
Air Force Institute of Technology

FOR THE SPACE TEST PROGRAM:

(SIGNATURE) (DATE)
David C. Hess, GS-15
Director, DOD Human Spaceflight Payloads Office

1.0 PURPOSE

This Memorandum of Agreement (MOA) delineates the roles and responsibilities among Space and Missile Systems Center's Space Test Program Office (SMC/OLAW) and Air Force Institute of Technology (AFIT) on the terms and conditions for integration and flight of the Rigidizable Inflatable Get-Away-Special Experiment (RIGEX) on the Space Shuttle. The basic guidance for this document is AFI 10-1202(I)/AR 70-43/OPNAVINST 3913.1A, "Space Test Program Management", 01 Apr 98.

2.0 BACKGROUND

2.1 The ultimate objective of RIGEX is to enable the application of large-scale inflatable and rigidized structures for use on operational space systems. Further, the RIGEX experiment will attempt to reduce the risk associated with the operational use of such structures by collecting further data and sharing it with the aerospace industry. In addition to the data collected in orbit, RIGEX will capitalize on the benefits associated with testing space-rigidized structures in a controlled laboratory environment.

2.2 Specifically, the objective of this experiment is to design a system that will collect data on three space-rigidized structures (tubes). The experiment consists of three inflatable tubes that become flexible at a transition temperature of 125°C, expand with air pressure (supplied by the experiment), and then rigidize by cooling. As on-orbit data is compared with ground data, the ground test procedures can be verified, and more complex systems can be developed without full-scale testing in space. Further, the experiment is designed and sized to fly in the Space Shuttle bay in a Canister for All Payload Ejections (CAPE). After the Shuttle astronauts activate the experiment computers, one tube will be heated past its transition temperature, inflated, and re-cooled to a structurally-stiff state. Environmental and video sensors record the inflation and cooling process to verify proper deployment. A modal analysis using an excitation device (piezoelectric patch) at the cantilevered end of the tube will then be done to characterize the mechanical properties of the rigidized structure. During the excitation cycle, accelerometers mounted at the free end of the tube are used to collect data on its modal response. This process will then be repeated for the remaining two tubes (all are done sequentially).

3.0 SCOPE

3.1 This MOA establishes the basic working agreements between SMC/OLAW and the RIGEX sponsor, AFIT, for integration, space flight, operations support, and data retrieval (Shuttle only) for the flight of the RIGEX payload. SMC/OLAW shall have final approval for space flight of all experiments and shall have authority to disapprove or remove any experiment should any problems be uncovered which jeopardize the success of the overall mission. The provisions of paragraph 6.0 of this MOA are subordinate to Shuttle primary mission requirements.

3.2 This agreement satisfies the requirements stipulated in the Space Test Program's Program Management Directive and AFI 10-1202(I) for a signed MOA between SMC/OLAW and the experiment's sponsor. This MOA shall be effective upon the date of the final signature by SMC/OLAW and AFIT. SMC/OLAW will be the primary executing agent for STP under this agreement.

3.3 AFIT is the Sponsor for this spaceflight experiment. AFIT will provide the Principal Investigator (PI) and be the responsible party for all required technical and administrative support required under this MOA.

3.4 This MOA will be reviewed annually and amended as required. Contingent upon the availability of Shuttle flight manifesting opportunities, the RIGEX flight will be targeted for 4QCY06. The MOA will automatically terminate upon completion of RIGEX mission objectives, mutual agreement of the signatories, or five years from the date of origination, whichever occurs first. Termination in advance of this agreed expiration date can be made by any signatory but shall require 180 days advance written notification by the withdrawing party to SAF/USA. This MOA is conditional upon:

3.4.1 Approval of the S05-2, RIGEX Space Flight Plan

3.4.2 Release of STP funding for RIGEX integration

3.5 The AFIT shall develop, test, provide space flight hardware, and documentation for RIGEX that conforms to the most recent edition of the NSTS-21000-SIP-DRP (Deployable/Retrievable-Type Payloads SIP), the NSTS-21000-IDD-SML (Small P/L IDD), and ICD-2-19001.

3.6 NASA/Space Shuttle Program (SSP) has the overall responsibility for hardware integration in the shuttle cargo bay. The RIGEX payload will be integrated into the cargo bay using STP provided mounting hardware and interfaces. Both SMC/OLAW and AFIT will be required to provide information to SSP in the format normally used by experimenters utilizing the shuttle cargo bay.

3.7 The final technical agreement for space system support will be as described in the NASA Payload Integration Plan (PIP) documentation, reviewed by AFIT, and approved by SMC/OLAW and NASA/SSP.

4.0 OVERALL RESPONSIBILITY

SMC/OLAW shall have overall program management responsibility for the integration of RIGEX onto the Shuttle.

5.0 SPECIFIC RESPONSIBILITIES

5.1 STP (SMC/OLAW) agrees to:

5.1.1 Provide program management and control as the sponsor's integrating agency with NASA for all manifesting, integration, and space flight activities of the RIGEX payload in the Shuttle cargo bay.

5.1.2 Provide technical support to the PI for requirements definition, experiment definition, design, and development to ensure compatibility with Shuttle cargo bay requirements.

5.1.3 Prepare and submit to NASA the appropriate flight request forms for the RIGEX payload.

5.1.4 Develop and submit all integration documents to NASA based upon technical requirements, documentation, and data provided by the PI.

5.1.5 Develop and submit the safety data packages to NASA, and provide technical support to the PI to complete the safety assessment, documentation, reviews, and certification.

5.1.6 Represent the PI in direct discussions with NASA to baseline, update, and maintain program integration documentation, including the RIGEX Integration Schedule.

5.1.7 Chair and/or support, as required, program working group meetings, technical interchange meetings, and program reviews.

5.1.8 Review certification test plans and coordinate reviews of test results, as required, to certify RIGEX hardware for flight.

5.1.9 Assure overall compliance with safety, quality assurance, reliability, and testing requirements for RIGEX flight hardware.

5.1.10 As necessary, provide training for experimenters in the use of DoD Payload Operations Control Center (POCC) or NASA supplied equipment.

5.1.11 Coordinate with the PI and SSP for crew and flight control team familiarization briefings and any required crew training.

5.1.12 Provide the STP Canister for All Payloads Ejection (CAPE) for use in the integration and launch of the RIGEX flight hardware.

5.1.13 Coordinate with the PI and SSP for the transportation of all RIGEX flight hardware to support final integration.

5.1.14 Provide a Payload Operations Manager to act as the single point of contact to the NASA Flight Control Team during pre-flight and Shuttle/ISS operations.

5.1.15 Notify the RIGEX principal investigator of changes that may have a funding, security, or schedule impact.

5.1.16 Submit the final RIGEX Space Test Program After Action Report (AAR) to SAF/USA within six months of the experiment's mission completion.

5.1.17 Comply with PI provided Export Control and Security Guidance for the RIGEX Payload.

5.2 AFIT agrees to:

5.2.1 Provide a PI to act as the RIGEX point of contact to SMC/OLAW to define: experiment requirements, interface requirements, crew activities, and flight operations to meet established mission planning milestones.

5.2.2 Support appropriate RIGEX working group meetings, telecons, technical interchange meetings, and program reviews.

5.2.3 As directed, provide a Payload Requirements Document (PRD) for RIGEX. The PRD will be based on a template provided by SMC/OLAW.

5.2.4 Provide all technical requirements and data for incorporation into the PIP, RIGEX ICD, and related integration requirements documents.

5.2.5 As required, provide analysis and data to support the flight certification of the RIGEX experiment. The supporting data may include, but is not limited to, payload operational procedures, physical and functional characteristics, and interface data.

5.2.6 Comply with flight and ground safety requirements and provide hazard assessments and data as necessary for flight safety certification. As directed, prepare and submit Shuttle integration and safety documentation (FCP, SVP, and MSVP) to SMC/OLAW for review, approval, and submission to NASA.

5.2.7 Provide RIGEX payload flight qualified hardware that meets:

5.2.7.1 The STP Canister for All Payloads Ejection (CAPE) physical and electrical specifications as outlined in the user's guide.

5.2.7.2 The shuttle cargo bay environmental, physical, and electrical specifications, satisfies SSP safety requirements for cargo bay payloads, and has undergone appropriate testing.

5.2.8 Provide logistic and operational support for the RIGEX payload flight hardware and unique support equipment during integration, test, pre-launch, on-orbit, and post-flight activities.

5.2.9 Provide training support to the crew and flight control team members on experiment operations; include the provision of training hardware (as appropriate) and crew familiarization briefings.

5.2.10 Participate in NASA Joint-Integrated-Simulations (JISs) and NASA/SSP Payload Operations Control Center (POCC) training, as required.

5.2.11 Provide necessary ground support equipment and software to support the integration and preparation of the RIGEX/Shuttle flight hardware for launch.

5.2.12 Provide necessary hardware and software to support remote payload operations at the PI's facility, if required.

5.2.13 Provide progress and status review information, including funding and schedule, to SMC/OLAW, as required.

5.2.14 Provide access to experiment technical information for SMC/OLAW consultants and contractor personnel.

5.2.15 Submit an experiment press release package to SMC/OLAW NLT three months prior to launch for incorporation into the NASA Mission Press Kit, and brief the experiment overview at the pre-launch press briefing when/if requested.

5.2.16 Complete a Space Test Program After Action package including a 1721-2 (see Appendix A), an end-of-mission report, and any documentation (papers, experiment results, etc.) published on the payload. The package should be submitted to SMC/OLAW within six months of completion of mission.

5.2.17 Provide RIGEX security classification guidance in writing to SMC/OLAW as soon as possible after this MOA is signed.

5.2.18 Provide RIGEX export classification guidance in writing to SMC/OLAW prior to the NASA Phase 1 Safety Review.

5.2.19 Complete human reliability/assurance program certification requirements for all personnel, including contractors requiring unescorted access to space launch and/or operations facilities.

5.3 STP and AFIT will:

5.3.1 STP and AFIT management shall meet to develop a recovery plan in the event of: RIGEX experiment delays, changes to or non-compliance with experiment requirements established by this MOA, the PRD, and the approved ICDs, or damage to support hardware caused by improper payload or experimenter actions.

6.0 **TECHNICAL REQUIREMENTS**

The technical requirements listed below form the basis for the integration of RIGEX into the Shuttle cargo bay until completion of the Payloads Requirements Document (PRD). The PRD shall take precedence over these requirements once approved. The SMC/OLAW capability of meeting the integration requirements of RIGEX will be restricted by the physical limitations and safety requirements of the Shuttle cargo bay.

6.1 Weight (lbs):	198.24
6.2 Form Factor:	STP CAPE Launcher
6.3 Power (watts):	heaters 80W (peak), 172W (peak) during exp.
6.4 Volume (m):	0.142 m ³
6.5 Orbiter Altitude:	Orbit Insensitive
6.6 Orbiter Inclination (deg):	Inclination Insensitive
6.7 Orbiter Attitude/Maneuvers	N/A
6.8 Minimum flight duration:	6 hours
6.9 Total Number of Flights Requested:	1
6.10 Minimum interval between flights:	N/A

7.0 **MAJOR EXPERIMENT MILESTONES:** The following projected month milestones may be used for planning purposes.

7.1	Payload Requirements Document (PRD Signature)	L-20
7.2	Phase 0/1/2 Safety Review	L-14
7.3	Phase 3 Safety Review	L-5
7.4	Flight Hardware Shipped to KSC	L-4
7.5	Orbiter Installation	L-3

8.0 **SHUTTLE INTEGRATION SCHEDULE**

The Composite RIGEX Master Integration Schedule shall be established and maintained by SMC/OLAW.

9.0 **PROGRAM MANAGEMENT AND FUNDING/RESPONSIBILITIES**

9.1 STP (SMC/OLAW) will fund/provide:

9.1.1 Nominal integration costs incurred by the incorporation of this experiment on the Shuttle.

9.1.2 Mission/Payload Specialist training when required.

9.1.3 The retrieval of orbiter ephemeris, altitude, flight history, and experiment raw data as available from NASA and required by the PI in support of data analysis.

9.2 AFIT will fund/provide:

9.2.1 RIGEX unique capabilities and integration requirements beyond nominal SMC/OLAW services. These charges will be determined on a case-by-case basis.

9.2.2 Funding for the development, fabrication, and testing of the payload hardware, including initial flight certification testing and/or analysis.

9.2.3 Facilities to include hardware and software for the operation of the RIGEX experiment from a remote payload operations control center, if required.

9.2.4 IAW AFI 10-1202(I), if AFIT makes a good faith effort to meet the launch date and does not succeed for technical or other reasons, STP will not seek a return of its funds. In the event launch service cannot be provided within STP's available budget, AFIT and STP management will meet to develop a new execution strategy for the mission. In accordance with the Anti-Deficiency Act, the obligations of the parties to this agreement are subject to the availability of appropriated funds, and no party to this agreement shall cause an obligation to be incurred in excess of available funds.

9.2.5 Transportation for the RIGEX payload flight hardware and unique support equipment during integration, test, pre-launch, on-orbit, and post-flight activities.

10.0 **POINTS OF CONTACT**

SMC/OLAW: 1st Lt ReAnn Johnson (USAF)
RIGEX Payload Manager
(281) 483-0358

Captain Albert Meza (USAF)
Deputy RIGEX Payload Manager
(281) 483-0361

2101 NASA Parkway
Mail Code: ZR1
Johnson Space Center
Houston, TX 77058

AFIT: Dr. Richard Cobb
RIGEX Principal Investigator
AFIT/ENY
2950 Hobson Way
WPAFB OH 45433-7765
(937)-255-3636 x4559

11.0 **INFORMATION RELEASE**

All public release of information concerning the Spaceflight of the RIGEX payload will be coordinated and approved by STP and AFIT. This includes the release of any information associated with RIGEX space flight experiment integration, operations, or the terms and conditions of this MOA. Release of information will be in compliance with existing DoD directives and security classification

guides. Any public release will include the statement “RIGEX is integrated and flown under the direction of DoD’s Space Test Program.”

12.0 MOA Appendix

This MOA contains one appendix:

12.1 Appendix A: DD Form 1721-2 (Jul 1997), “Space Test Program After Action Report”

Appendix B. Program Requirements Document

The following pages include the approved Program Requirements Document.

SPACE TEST PROGRAM

PAYLOAD REQUIREMENTS DOCUMENT

FOR

Rigidizable Inflatable Get-Away-Special Experiment (RIGEX)

Date: _____

Approved by:

Dr. Richard G. Cobb
Principal Investigator, Department of Aeronautics
and Astronautics

Dr. Bradley S. Liebst
Professor and Head, Department of Aeronautics
and Astronautics

Dr. Robert A. Calico
Dean, Graduate School of Engineering and
Management

Air Force Institute of Technology
2950 Hobson Way
Wright-Patterson AFB, OH 45433

TABLE OF CONTENTS

1. INTRODUCTION.....	3
1.1. PURPOSE	3
1.2. PROGRAM INFORMATION.....	3
1.3. PAYLOAD CONTACTS (AS APPLICABLE):	3
1.4. DESIRED FLIGHT DATE/WINDOW:	3
1.5. ORBIT REQUIREMENTS	3
2. EXPERIMENT OVERVIEW	4
2.1. MISSION OBJECTIVES	4
2.1.1. Program Objectives	4
2.1.2. Key Mission Objectives.....	4
2.1.3. Extended Mission Operations Objectives:	4
2.2. PAYLOAD ENGINEERING DESCRIPTION.....	4
2.2.1. Major Component Descriptions.....	4
2.2.2. Control Mass and Volume Properties.....	4
2.2.3. Mechanical Interfaces.....	4
2.2.4. Electrical Systems:.....	5
2.2.5. Payload/Shuttle Launch and Landing Configurations:	5
2.2.6. Description of Moving Parts:	5
2.2.8. Assembly Overview Drawings/Schematics:	6
2.3. PAYLOAD FUNCTIONAL DESCRIPTION	6
2.3.1. Hardware Subsystems:	6
2.3.2. Software Subsystem.....	7
2.4. EXPERIMENT OPERATIONAL CONCEPTS.....	7
2.4.1. Experiment Operations Description:	7
2.4.2. Operations Modes:.....	7
2.4.3. Mission Profile/Timeline	8
2.4.4. Critical Operations and Procedures.....	8
2.4.5. Minimum Mission Success Criteria:	8
3. RESOURCE REQUIREMENTS.....	8
3.1. PAYLOAD ASSEMBLIES.....	8
3.1.1. Mass Properties, Dimensions	8
3.1.2. Mount Type.....	8
3.1.3. Area/Volume - Pressurized (Cabin Environment):	9
3.1.4. Area/Volume - Unpressurized (Space Environment)	9
3.2. POWER REQUIREMENTS:.....	10
3.3. THERMAL CONTROL	10
3.3.1. Heater Requirements:	10
3.3.2. Cooling Requirements:.....	11
3.3.3. Thermal Constraints:	11
3.4. COMMAND & CONTROL	11
3.4.1. Crew Control Requirements:	11
3.4.2. Ground Control Requirements:	11
3.4.3. Command Requirements:	11
3.4.4. Telemetry Requirements:.....	11
3.5. EXPERIMENT VIDEO DATA REQUIREMENTS	12
3.6. ORIENTATION AND STABILIZATION	12
3.6.1. Attitude Control:.....	12
3.6.2. Attitude Knowledge:.....	12
3.6.3. FOV/Pointing Requirements:	12

3.6.4	<i>Trajectory constraints:</i>	12
4.	ENVIRONMENTAL CONSTRAINTS FOR PAYLOAD OPERATIONS:	12
4.1.	STATIC LOAD CONSTRAINTS:	12
4.2.	VIBRATION CONSTRAINTS:	12
4.3.	SHOCK CONSTRAINTS:	12
4.4.	ELECTROMAGNETIC COMPATIBILITY:	12
4.4.1.	<i>Sensitivity to Radiated emissions:</i>	12
4.4.2.	<i>Sensitivity to Conducted Emissions:</i>	13
4.4.3.	<i>Sensitivity to Magnetic Fields:</i>	13
4.5.	ATMOSPHERIC PRESSURE CONSTRAINTS:	13
4.6.	THERMAL CONSTRAINTS:	13
4.7.	HUMIDITY CONSTRAINTS:	13
4.8.	CLEANLINESS CONSTRAINTS:	13
4.8.1.	<i>Ground Processing:</i>	13
4.8.2.	<i>On-Orbit Operations:</i>	13
4.9.	RADIO FREQUENCY EMISSIONS:	13
5.	GROUND OPERATIONS	13
5.1.	INTERFACE VERIFICATION REQUIREMENTS:	13
5.2.	PRE-LAUNCH REQUIREMENTS AT KSC:	13
5.2.1.	<i>Experiment Processing Activities:</i>	13
5.2.2.	<i>Experiment Processing Services:</i>	13
5.2.3.	<i>Late Access:</i>	13
5.3.	POST-LANDING REQUIREMENTS:	14
5.3.1.	<i>Early Removal:</i>	14
5.3.2.	<i>Hardware Turnover:</i>	14
5.3.3.	<i>Experiment Processing Support:</i>	14
5.3.4.	<i>Experiment Processing Services:</i>	14
6.	MISSION OPERATIONS REQUIREMENTS:	14
6.1.	LAUNCH PHASE REQUIREMENTS	14
6.2.	ON-ORBIT OPERATIONS:	14
6.2.1.	<i>Initialization:</i>	14
6.2.2.	<i>Post Separation Check-Out:</i>	14
6.2.3.	<i>Experiment Operations:</i>	14
7.	GROUND OPERATIONS SUPPORT REQUIREMENTS:	14
7.1.	PRE-FLIGHT SIMULATION REQUIREMENTS:	14
7.2.	DATA RETURN, PROCESSING, AND DISTRIBUTION:	14
7.3.	EXPERIMENT GROUND SUPPORT EQUIPMENT:	14
7.4.	MISSION DATA REQUIREMENT:	14
7.5.	GROUND SUPPORT FACILITIES	14
8.	SECURITY REQUIREMENTS:	15

1. Introduction

1.1. Purpose

This Payload Requirements Document (PRD) conveys the RIGEX experiment requirements to the Space Test Program (STP) which has overall responsibility for integrating this payload onto the Shuttle.

Note: Once the PRD is approved and until official carrier documentation is in place, updates will be made as required to reflect *significant* changes in project scope or requirements.

1.2. Program Information

Payload's Full Name: Rigidizable Inflatable Get-Away-Special Experiment

Payload Acronym: RIGEX

Sponsoring Organization: Air Force Institute of Technology

Funding Organization: Self

1.3. Payload Contacts (as applicable):

All contacts beyond Principle Investigator, listed below, are AFIT students who will be graduating on 21 March 2006.

	Name	Phone #	Fax #	e-mail address
Payload Sponsor	Dr. Richard Cobb	785-3636 x4559	937-656-7053	richard.cobb@afit.edu
Principle Investigator	Same			
AFIT Grad Student	Capt Jeremy Goodwin	937.776.1460	Same	jeremy.goodwin@afit.edu
AFIT Grad Student	Lt Sarah Helms	719.439.4202	Same	sarah.helms@afit.edu
AFIT Grad Student	Lt Anna Gunn-Golkin	856.287.5528	Same	Anna.gunn-golkin@afit.edu

1.4. Desired Flight Date/Window:

Not earlier than 1QTR, 2007

1.5. Orbit Requirements

Orbit Parameters	Desired	Required
	State apogee/perigee if elliptic	State apogee/perigee if elliptic
Altitude (km)	Any LEO	None
Inclination (deg)	Any LEO	None
Mission Duration	Approx. 4 hours	Approx. 4 hours

2. Experiment Overview

2.1. Mission Objectives

2.1.1. Program Objectives

The ultimate objective of RIGEX is to enable the application of large-scale inflatable and rigidized structures for use on operational space systems. Further, the RIGEX experiment will attempt to reduce the risk associated with the operational use of such structures by collecting further data and sharing it with the aerospace industry. In addition to the data collected in orbit, RIGEX will capitalize on the benefits associated with testing space-rigidized structures in a controlled laboratory environment.

2.1.2. Key Mission Objectives

Specifically, the objective of this experiment is to collect data on three space-rigidized structures (tubes). The experiment consists of three inflatable tubes that become flexible at a transition temperature of 125°C, expand with air pressure (supplied by the experiment), and then rigidize by cooling. After the Shuttle astronauts activate the experiment computers, one tube will be heated past its transition temperature, inflated, and re-cooled to a structurally-stiff state. Environmental and video sensors record the inflation and cooling process to verify proper deployment. A modal analysis using an excitation device (piezoelectric patch) at the cantilevered end of the tube will then be done to characterize the mechanical properties of the rigidized structure. During the excitation cycle, accelerometers mounted at the free end of the tube are used to collect data on its modal response. This process will then be repeated for the remaining two tubes (all are done sequentially).

2.1.3. Extended Mission Operations Objectives:

RIGEX will not be deployed from the Shuttle. As such, there are no extended mission operations objectives.

2.2. Payload Engineering Description

2.2.1. Major Component Descriptions

RIGEX consists of 3 inflatable tubes, as well as heating, inflation, and data collection systems for each tube. The RIGEX structure consists of aluminum, Al-6061-T6, sheets fastened together (not welded). In addition, there is a 1/8" aluminum shroud encompassing RIGEX to prevent damage to CAPE. Instrumentation (actuators and sensors) on board includes transformers, piezoelectric patches, triaxial accelerometers, pressure transducers, pressure valves, pin pullers, and resistive heaters.

2.2.2. Control Mass and Volume Properties

The total mass limit of the experiment is expected to be 200 lbs (90 kg).

2.2.3. Mechanical Interfaces

There is one mechanical interface at the top of the experiment that will be used to connect with the CAPE. The interface is a 1.5"-thick aluminum plate featuring countersunk thru-holes matching CAPE's 23.25" bolt circle. The plate will also have blind holes for attaching a lifting sling to RIGEX for handling. The other end of the experiment will be cantilevered inside CAPE (buffers/snubbers will be used at the free end).

2.2.4. Electrical Systems:

RIGEX requires a 24-30VDC power source. This power is fused and then routed to two relays. One relay will control power to the computer, and the other will control power for environmental (keep-alive) heaters. From the first relay, power will be routed to two PC-104 power supply boards (Jupiter power supply boards, JMM512), three inflation solenoids, six pressure transducers, and three power relays for the heaters. The first power supply board provides power for the overall execution of the experiment, while the second focuses on the imaging systems' execution. Both boards operate on 24-30 VDC, and provide power conversion of +/- 12VDC as well as +/- 5VDC. The allowable input range to the power converters is 7-30VDC. One interface connector will be provided for interfacing with Shuttle power, and one interface connector will be provided for interfacing with the Orbiter Standard Switch Panel.

After the second relay, power will be routed through thermostats, which will control the environmental heaters.

The oven heaters will all be powered from Shuttle power, but turned on via the RIGEX computer. Power will enter the computer through the aforementioned interface connector, and then relayed through a harness to each experiment bay. Per tube, there is one relay inside the computer that controls power to a solid state relay outside the computer, which in turn controls the power supplied to the heater assembly. Everything is provided with a common ground.

2.2.5. Payload/Shuttle Launch and Landing Configurations:

RIGEX is carried to orbit on the Space Shuttle inside CAPE. Upon launch, each tube is stowed within their respective ovens. The experiment is carried out inside CAPE (RIGEX is not to be deployed), and returned to earth with the Shuttle. During the return to earth, each tube will be deployed and cantilevered from the bottom end of the experiment (tubes may fail during landing, but this is unexpected; a 1/8th-inch aluminum shroud around the experiment is used to contain any loose components).

2.2.6. Description of Moving Parts:

Prior to activation of the experiment, there are no moving parts. Once the experiment begins, the primary moving parts will be the tubes themselves. They are approximately 20" long when fully deployed. The experiment begins with them in a stowed (z-fold) condition, and ends with them fully deployed (along the RIGEX/CAPE major axis).

There are also two oven doors per tube (6, total) and a spring-loaded latch (3, total) that are hinged to each oven. Each door is approximately 4.25" wide and 3" long. The doors are held closed by the latch & pin-puller system until the tubes are ready to be inflated. When the tubes reach 125°C, the pin-puller is engaged, the latch is released, and the doors open using only the force of the inflating tube.

2.2.7 Command and Control

Upon experiment activation by the astronauts, the computer runs the entire experiment autonomously. The computer will send a signal to the Shuttle's DS13 (up) light identifying that RIGEX is powered on. It will run through a self-test which finishes by sending a signal to illuminate DS13 (down). DS13 (down) will remain powered for 1 minute, shutting off with

the completion of the self test. After 5 minutes, the experiment will turn on its first set of oven heaters, and DS13 (up) will be powered back on signaling this activation. Once the entire experiment is completed, DS13 (down) will be powered on (DS13 up is shut off), and the astronauts will shut the payload down. All post-processing of recorded data will be done on earth.

2.2.8 Assembly Overview Drawings/Schematics:

Updated drawings have yet to be completed; however, an overview is provided below.

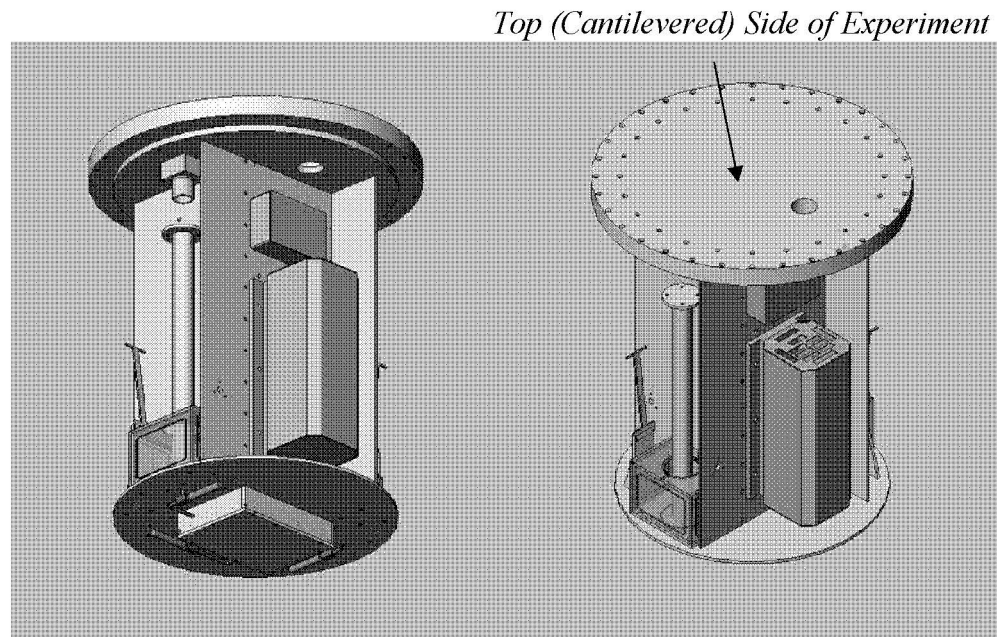


Figure 2.2.8.1 RIGEX Assembly Overview Drawing

2.3. Payload Functional Description

RIGEX consists of a command and control computer, 3 inflatable tubes, 3 ovens, an inflation system, and the necessary instrumentation to capture the experimental data.

2.3.1. Hardware Subsystems:

2.3.1.1. Oven/heater assembly

There are three assemblies onboard the experiment. Each oven is 5" tall, 4.25" wide, and 6" long. They are made of .25" thick Ultem 1000 PEI Polyetherimide material, and contain eight foil-backed Minco resistive heaters to provide heat (flat black paint is applied to each heater in order to increase surface emissivity).

2.3.1.2. Computer assembly

The computer is a PC-104 computer box. It contains essentially two computers in one box (one for overall experiment execution and data collection, and one for controlling the digital cameras). Each computer consists of a processor board, power supply board, and a timer/counter board to ensure correct timing. The primary computer also contains a data acquisition board, relay board, and thermocouple board. The imaging computer also contains three camera boards for interfacing with the digital cameras.

2.3.1.3. Inflation system assembly

In order to provide additional redundancy, each tube has its own inflation system. Each inflation system consists of a pressure vessel, a solenoid (to control airflow into the tube), two pressure transducers (one to measure tank pressure and one to measure tube pressure), and tubing to connect each part. The bulk of each system lies in the center portion of RIGEX, with just a small amount of tubing on the bottom to connect to the inflatable tubes. To inflate the tubes, the computer sends a signal to a relay, which powers a solenoid (valve) that allows airflow from the storage tank into the tube. The computer monitors pressure inside the tube and after inflation, it sends another signal to the relay, which powers off the solenoid.

2.3.2. Software Subsystem

The flight command and control software is an autonomous routine written in C++, and contains failsafe points that allow the experiment to recover in the event the of an inadvertent or deliberate power loss. The software will include a self test that is conducted each time the experiment is turned on. This self test is intended to verify functionality each time the computer is turned on, and to help satisfy interface verification tests (please see 2.2.7 for a more detailed description of feedback signals that the software provides). During interface verification testing, it is important to shut the computer down within 5 minutes of completion of the self test (self-test completion is defined as DS13 (down) being shut off after being illuminated for 1 minute). At this point, the computer must be shut down during interface verification tests (otherwise, the experiment will execute heater turn-on).

2.4. Experiment Operational Concepts

2.4.1. Experiment Operations Description:

The experiment operates autonomously. Once the astronauts apply power to the computer and it boots up, it will run its self test and check the failsafe register to determine where it is supposed to start the routine. If it is the first time the computer is powered on orbit, it will begin the experiment 5 minutes after completion of the self test by applying power to the oven/heaters of tube #1. Once the tube is heated above 125°C, the computer will send a signal to the solenoid of the inflation system, which in turn will inflate the tube. The computer will also send a signal to the first digital camera, which will not only capture the inflation, but also determine the orientation of the tube after inflation (nominally, the tube will be completely vertical). Once the tube cools, it is vented, and the computer sends a drive signal to a piezoelectric patch, which will be used to conduct a modal vibration test (data to be analyzed on the ground). Upon completion of the vibration test, the computer progresses to tube #2, and the process is repeated (and again for tube #3). Once the computer will has routed through its complete routine, it will signal the astronauts to terminate power to the experiment.

2.4.2. Operations Modes:

There are two operation modes for RIGEX: self-test and full operation. When the computer is in full operation mode, it runs the routine described above. Should the routine need to be stopped for any reason, power will need to be cutoff from the computer.

2.4.3. Mission Profile/Timeline

The mission profile is described above in 2.4.1. A rough timeline is presented below:

Computer turns on (CTO) and begins boot-up	CTO
DS13(up) gets +18V & Self-test begins	CTO + 180 s
Self-test ends; DS13(up) off; DS13(down) gets +18V for 60s	CTO + ~380 s
DS13(down) off; 5-min wait period starts (no lights on)	CTO + 440s
Oven #1 heating initialized, DS13(up) gets +18V	CTO + 740 s
Tube #1 deployment initialized	CTO + 4340 s
Tube #1 is fully deployed/begins cooling	CTO + 4360 s
Tube #1 is cooled to vent temp/vents	CTO + 4960 s
Tube #1 actuation	CTO + 4970 s
Tube #1 complete; Begin heating Tube #2	CTO + 5000 s
Tube #2 deployment initialized	CTO + 8600 s
Tube #2 is fully deployed/begins cooling	CTO + 8620 s
Tube #2 is cooled to vent temp/vents	CTO + 9220 s
Tube #2 actuation	CTO + 9230 s
Tube #2 complete; Begin heating Tube #3	CTO + 9260 s
Tube #3 deployment initialized	CTO + 12860 s
Tube #3 is fully deployed/begins cooling	CTO + 12880 s
Tube #3 is cooled to vent temp/vents	CTO + 13480 s
Tube #3 actuation	CTO + 13490 s
Tube #3 complete; DS13(up) off, DS13(down) gets +18V	CTO + 13520 s
<i>Total time:</i>	<i>13520 sec (225 min)</i>

2.4.4. Critical Operations and Procedures

The only critical operation is that power is supplied to the experiment, and the experiment be allowed to run through its entire routine. Should, for some reason, the tubes not deploy, there is no requirement for the astronauts to attempt to fix the experiment.

2.4.5. Minimum Mission Success Criteria:

Minimum success requires at least one tube to fully deploy and be actuated with the piezoelectric patch. Further, minimum success requires the data acquisition system to collect the actuation data for post-processing on the ground.

3. Resource Requirements

3.1. Payload Assemblies

3.1.1 Mass Properties, Dimensions

The total mass is not known at this point, but it is not expected to be more than 200 lbs (90kg). The experiment is 28" tall and 20.5" in diameter. Center of gravity properties are noted below:

- x: 0.7" from centerline
- y: 0.1" from centerline
- z: 7.9" from RIGEX/CAPE interface

3.1.2 Mount Type

The 1.5" mounting plate at the top of RIGEX will need be fastened to the CAPE bolt circle. As such, the appropriate interface drawing(s), as well as a fit check (if possible), are required.

3.1.3 Area/Volume - Pressurized (Cabin Environment):
None.

3.1.4 Area/Volume - Unpressurized (Space Environment)

The RIGEX outer diameter, including shroud, is 20.5 in. With a height of 28in, the volume is roughly 150,000 cc (151.45L).

3.2 Power Requirements:

Experiment Mode	Nominal Power	Power Source	Peak Power (Watts)	Duration (continuous, % of experiment operation, minutes daily)
Pre-Mission (Environmental heaters)	TBD	Shuttle Power	TBD	TBD
Computer Operation	24VDC, .95A	Shuttle Power	22.8	100 %
Heater/Oven Operation	24 VDC, 5.2A	Shuttle Power (relayed through RIGEX computer)	124.8	80 %
Inflation Solenoids	24 VDC, .5A	Shuttle Power (relayed through RIGEX computer)	12	1% (5-10 seconds/tube)
Pressure Transducers	24 VDC, TBD A	Shuttle Power	TBD	100%
Transformers	5 VDC	Shuttle Power (relayed through RIGEX computer)		1% (30 seconds per tube)
Cameras	TBD	Shuttle Power (relayed through RIGEX computer)	TBD	100%

NOTE: Max current draw will be with computer, pressure transducer, and heater/ovens.

3.3 Thermal Control

3.3.1 Heater Requirements:

The table below illustrates the operating temperatures of the computer boards and the on-board cameras. Clearly, the operating ranges of these components do not fully envelop the potential extremes seen on the Shuttle. Therefore, Shuttle-provided power dedicated to environmental heaters is required. These heaters are keep-alive heaters, and as such, power is needed even when the RIGEX computer is not on.

Computer Board	Low Temp (°C)	High Temp (°C)
Processor	-40	+85
Data Acquisition	-40	+85
Counter/Timer	-40	+85
Relay	0	+70
Thermocouple Control	-25	+85
Cameras	0	+43 (110°F)

3.3.2 Cooling Requirements:

N/A

3.3.3 Thermal Constraints:

The thermal storage requirements range from -60 to +85°C. The operations thermal requirements of most of the thermally-critical components range from -40 to +85; however, with heaters incorporated around these components, the experiment is expected to operate from -60 to +85°C .

3.4 Command & Control

3.4.1 Crew Control Requirements:

Activate power to the environmental heaters (using switch S15). Activate power to the experiment (using switch S13). When DS13 (down) illuminates (approximately 4 hours after turning the experiment on), terminate power to the experiment.

3.4.2 Ground Control Requirements:

N/A

3.4.3 Command Requirements:

N/A

3.4.3.1 Command Interface:

N/A

3.4.3.2 Command Data Rate:

N/A

3.4.3.3 Command Uplink Requirements:

N/A

3.4.4 Telemetry Requirements:

3.4.4.1 Telemetry Interface:

N/A

3.4.4.2 Telemetry Data Rate:
N/A

3.4.4.3 Telemetry Downlink Requirements:
N/A

3.4.4.4 Telemetry Data Storage Requirements:
N/A

3.5 Experiment Video Data Requirements

RIGEX has onboard cameras that will capture the required video data.

3.6 Orientation and Stabilization

3.6.1 Attitude Control:
N/A

3.6.2 Attitude Knowledge:
N/A

3.6.3 FOV/Pointing Requirements:
N/A

3.6.4 Trajectory constraints:
N/A

4. Environmental Constraints for Payload Operations

Note: Payload must be designed to meet Shuttle launch/landing constraints.

4.1. Static Load Constraints:

N/A

4.2. Vibration Constraints:

The RIGEX payload requires as much free drift as possible for the time period the experiment is active (approximately 4 hours), therefore OMS and PRCS thrusters should be inhibited. It is also highly desired to inhibit VRCS thrusters for this timeframe. The payload requires post-flight thruster data to correlate any attitude control firings that are necessary while the experiment is operating.

4.3. Shock Constraints:

N/A

4.4. Electromagnetic Compatibility:

4.4.1. Sensitivity to Radiated emissions
TBD.

4.4.2. Sensitivity to Conducted Emissions:
TBD.

4.4.3. Sensitivity to Magnetic Fields:
TBD.

4.5. Atmospheric Pressure Constraints:
N/A

4.6. Thermal Constraints:
With heaters or an appropriate work-around to the thermal issues mentioned under Section 3.3.1, there are no additional thermal constraints.

4.7. Humidity Constraints:
N/A.

4.8. Cleanliness Constraints:

4.8.1. Ground Processing:
Generally clean.

4.8.2. On-Orbit Operations:
Generally clean.

4.9. Radio Frequency Emissions
N/A.

5. Ground Operations

5.1. Interface Verification Requirements:
Either the Lid bolt pattern or drill template will be required in order to ensure mechanical fit. Further, the electrical interface with the Shuttle will need to be determined and verified that 24-30 VDC and 10A is provided on the pins expected.

5.2. Pre-launch Requirements at KSC:

5.2.1. Experiment Processing Activities:
N/A.

5.2.2. Experiment Processing Services:
AFIT will pressurize the system prior to shipping to KSC; however, the pressure vessels may need to be pressurized to at least 14.7psia with nitrogen (fill procedure will be required as a backup). It is desired that RIGEX receives an alcohol/pre-wipe cleaning (and other normal ops) prior to integration with the CAPE. Further, it is also desired that the RIGEX/CAPE assembly receives a nitrogen purge prior to launch to remove any humidity in the experiment.

5.2.3. Late Access:
N/A.

5.3. Post-landing Requirements

5.3.1. Early Removal:
N/A.

5.3.2. Hardware Turnover:
The experiment will need to be deintegrated from CAPE, have a post-mission functional test conducted (same as pre-mission functional test), and returned to the Air Force Institute of Technology for post-processing, preferably within 2 weeks.

5.3.3. Experiment Processing Support:
N/A

5.3.4. Experiment Processing Services:
N/A

6. Mission Operations Requirements:

6.1. Launch Phase Requirements

N/A

6.2. On-Orbit Operations:

6.2.1. Initialization:
Initialize heater power ASAP after orbit insertion.

6.2.2. Post Separation Check-Out:
N/A.

6.2.3. Experiment Operations:
Initialize power to RIGEX computer by engaging power relay. Power off when indicated by panel lights (DS13 down).

7. Ground Operations Support Requirements:

7.1. Pre-flight Simulation Requirements:

N/A.

7.2. Data Return, Processing, and Distribution:

N/A.

7.3. Experiment Ground Support Equipment:

N/A.

7.4. Mission Data Requirement:

N/A. All mission data is captured onboard the RIGEX computer.

7.5. Ground Support Facilities

Offline facility for CAPE integration/deintegration.

8. Security Requirements:

The experiment and its data are unclassified; however, the tube material is proprietary and must be handled as such. Otherwise, the experiment is completely academic and not export controlled. There are no uplinks/downlinks onboard; thus, there are no encryption requirements.

Appendix C. Containment Analysis

This containment analysis follows the equations outlined in NASA SSP 52005 Revision C [26] to determine the thickness of an aluminum shroud required to contain an inflatable RIGEX tube that breaks under the following conditions:

- Max Shuttle acceleration (reentry)
- 2x max Shuttle acceleration (used to find conservative safety margins)
- Overpressurization at max Shuttle acceleration (reentry)
- Overpressurization at 2x max Shuttle acceleration (used to find conservative safety margins)

C.1 Background Information

The first equation in SSP 52005 is used to determine the velocity of the component to be contained:

$$V = \frac{A_{LF}}{2\pi f_n} + \sqrt{2aS_d} \quad (C.1)$$

where

A_{LF} = *Low Frequency Acceleration* (m/s²)

f_n = *First Fundamental Frequency* (Hz)

a = *Shuttle Acceleration* (m/s²)

S_d = *Maximum Travel Distance of Loose Component* (m)

The second is an energy analysis solved for thickness:

$$T_R = \sqrt{\frac{1}{2}mV^2 \cdot \frac{1}{\text{perim} \cdot YS_w}} \quad (C.2)$$

where

$$m = \text{Mass (kg)}$$

$$V = \text{Velocity (m/s)}$$

$$\text{perim} = \text{Perimeter of Object's Smallest Face (m}^2\text{)}$$

$$YS_w = \text{Yield Strength of Wall Thickness (Pa, or N/m}^2\text{)}$$

In order to perform the analysis, the following values and assumptions were used:

Tube + endcap mass, m	0.170kg (1.165×10 ⁻² slug)
Minimum perimeter, perim	0.120m (0.363ft)
Aluminum yield strength, YS _w	2.413×10 ⁸ N/m ² (5.04×10 ⁶ lbf/ft ²)
Gravity, g	9.807m/s ² (32.17ft/s ²)
Acceleration, A _{LF} & a	Varies
Minimum Natural Frequency, f _n	35Hz (recommended in SSP 52005)
Maximum travel distance, S _d	0.762m (2.5ft)

C.2 Analysis Calculations

During the first condition, the tube is assumed to be accelerating at the Shuttle's maximum acceleration. According to SSP 52005, this can be as high as 6.5g's during landing. Therefore, using this value for the two accelerations in Equation C.1, the velocity of the tube is found:

$$V = \frac{6.5g(\frac{9.807m/s^2}{g})}{2\pi \times 35(1/s)} + \sqrt{2 \times 6.5g(9.807\frac{m/s^2}{g}) \times 0.762m}$$

$$V = 10.15m/s \quad (33.29ft/s)$$

Then, using this velocity in Equation C.2, the thickness is determined:

$$T_R = \sqrt{\frac{1}{2}(0.170kg)(10.15m/s)^2 \times \frac{1}{0.120m \times 2.413 \times 10^8 N/m^2 \left(\frac{1 \text{ kg}\cdot m/s^2}{N}\right)}}$$

$$T_R = \mathbf{0.55mm} \quad (\mathbf{0.022in})$$

For the second condition, both a and A_{LF} were assumed to be twice the expected maximum Shuttle acceleration, or 13g's. Therefore, the new velocity is:

$$V = \frac{13g\left(\frac{9.807m/s^2}{g}\right)}{2\pi \times 35(1/s)} + \sqrt{2 \times 13g(9.807\frac{m/s^2}{g}) \times 0.762m}$$

$$V = 14.51m/s \quad (47.63ft/s)$$

and the new thickness increases to:

$$T_R = \sqrt{\frac{1}{2}(0.170kg)(14.51m/s)^2 \times \frac{1}{0.120m \times 2.413 \times 10^8 \frac{N}{m^2} \left(\frac{1 \text{ kg}\cdot m/s^2}{N}\right)}}$$

$$T_R = \mathbf{0.79mm} \quad (\mathbf{0.031in})$$

For the third and fourth conditions, the tube cap's acceleration due to overpressurization was found using Newton's Second Law (in terms of pressure rather than force):

$$P \times A = mA_{LF} \tag{C.3}$$

where

$$P = \text{Pressure (Pa, or N/m}^2\text{)}$$

$$A = \text{Area (m}^2\text{)}$$

Incorporating the equation for the area of a circle (for the tube cap) and solving Equation C.3 for acceleration yields

$$A_{LF} = \frac{P \times \pi r_{tube}^2}{m} \quad (C.4)$$

The tube's maximum design pressure (MDP) is 1.241×10^5 N/m² (or 18psi) and the smallest radius of the endcap is 0.019m (or 1.5in). Also, in order to determine the maximum acceleration, *only the mass of the endcap itself* is included in the calculation, whereas the endcap plus the entire mass of the tube was assumed in previous calculations. The endcap's mass is 0.074kg, yielding an estimated acceleration of:

$$A_{LF} = \frac{1.241 \times 10^5 \frac{N}{m^2} \left(\frac{1 \frac{kg \cdot m}{s^2}}{N} \right) \times \pi \times (0.019m)^2}{0.074kg}$$

$$A_{LF} = 1.912 \times 10^3 m/s^2 \quad (125g)$$

Plugging this, along with a Shuttle acceleration, a , of 6.5g into Equation C.1 yields a velocity of:

$$V = \frac{1.912 \times 10^3 m/s^2}{2\pi \times 35(1/s)} + \sqrt{2 \times 6.5g(9.807 \frac{m/s^2}{g}) \times 0.762m}$$

$$V = 18.55m/s \quad (60.86ft/s)$$

and a required thickness of:

$$T_R = \sqrt{\frac{1}{2}(0.074kg)(18.55m/s)^2 \times \frac{1}{0.120m \times 2.413 \times 10^8 \frac{N}{m^2} \left(\frac{1 \frac{kg \cdot m}{s^2}}{N} \right)}}$$

$$T_R = \mathbf{0.66mm} \quad (\mathbf{0.026in})$$

Finally, the last condition is the same as the third, with the exception of a larger assumed Shuttle acceleration of 13g's. Therefore, the velocity is:

$$V = \frac{1.912 \times 10^3 m/s^2}{2\pi \times 35(1/s)} + \sqrt{2 \times 13g(9.807 \frac{m/s^2}{g}) \times 0.762m}$$

$$V = 22.63m/s \quad (74.26ft/s)$$

and the required thickness is:

$$T_R = \sqrt{\frac{1}{2}(0.074kg)(18.55m/s)^2 \times \frac{1}{0.120m \times 2.413 \times 10^8 \frac{N}{m^2} \left(\frac{1 \frac{kg \cdot m/s^2}{N}}{N} \right)}}$$

$$T_R = \mathbf{0.81mm} \quad (\mathbf{0.032in})$$

C.3 Summary of Results

The current plan is to conservatively use an aluminum sheet that is 0.075in (1.905mm) thick. Therefore, the safety margins are tabulated in Table 1.

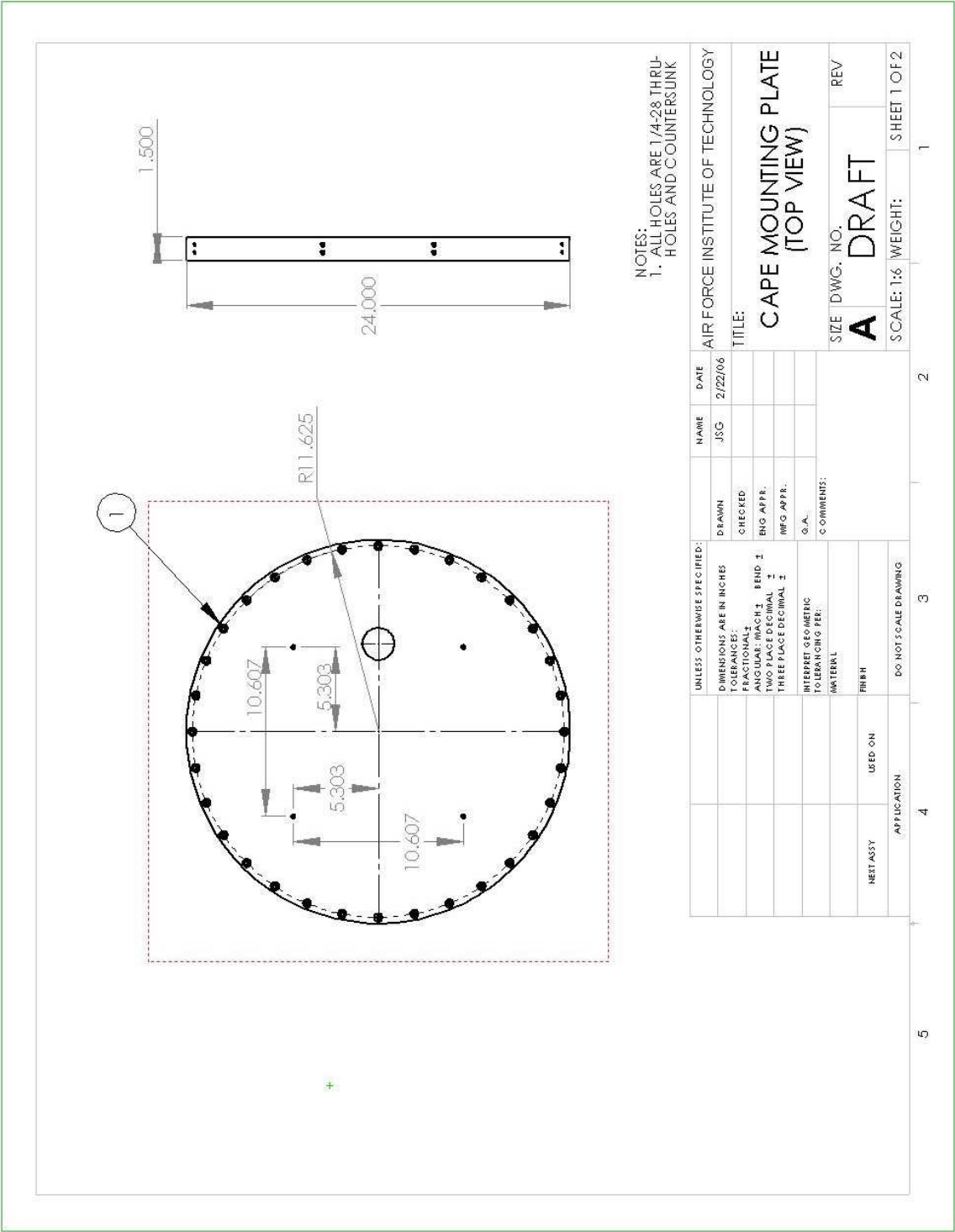
Table 1. Containment Analysis Results

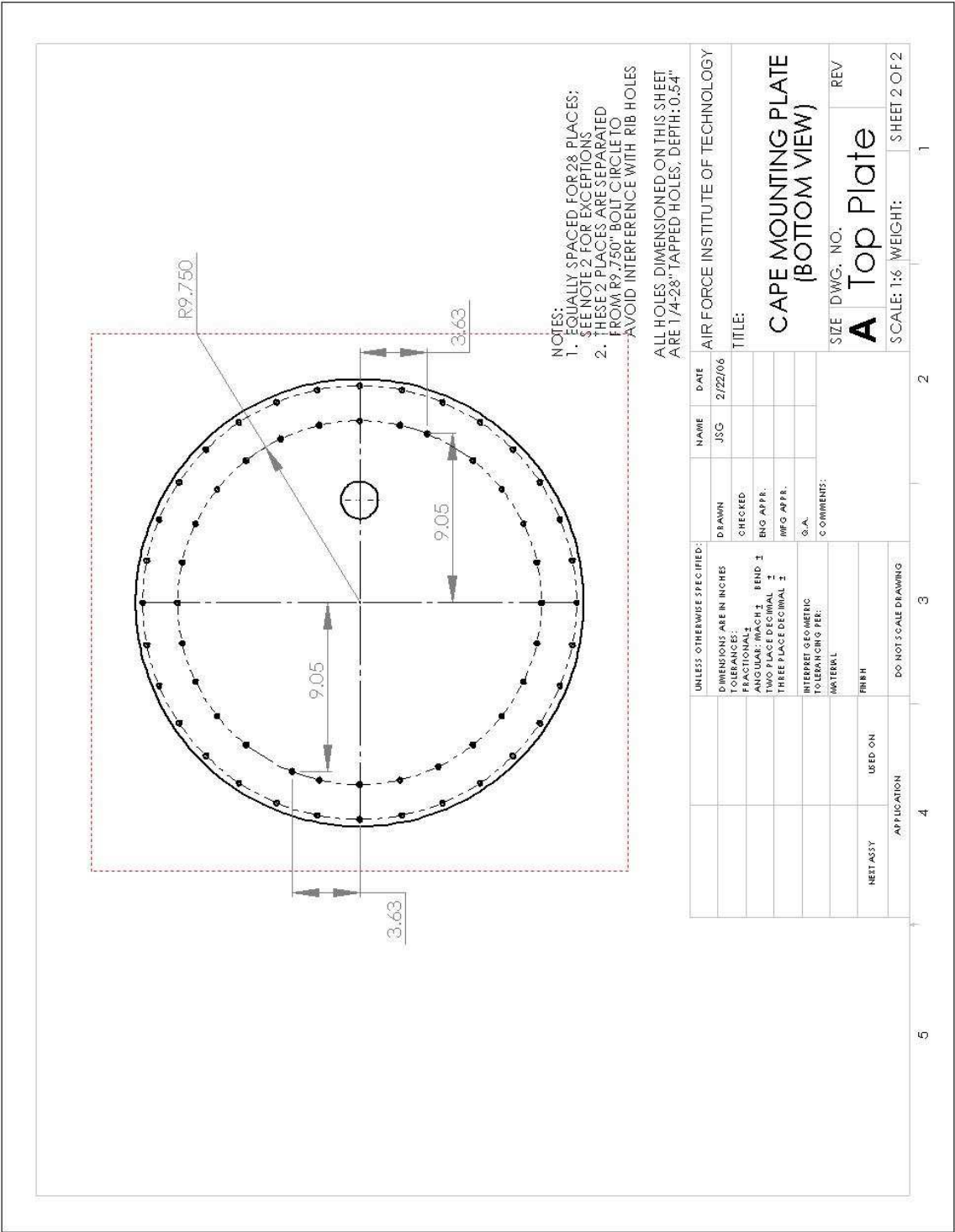
Description	Shuttle Acceleration (g)	Tube Acceleration (g)	Shroud Thickness (mm)	Margin over 1.91mm (%)
Shuttle/tube accelerate at 6.5g's	6.5	6.5	0.55	346
Shuttle/tube accelerate at 13g's	13	13	0.79	241
Tube overpressurization at Shuttle acceleration of 6.5g's	6.5	195	0.66	289
Tube overpressurization at Shuttle acceleration of 13g's	13	195	0.81	236

Appendix D. Drawing Package

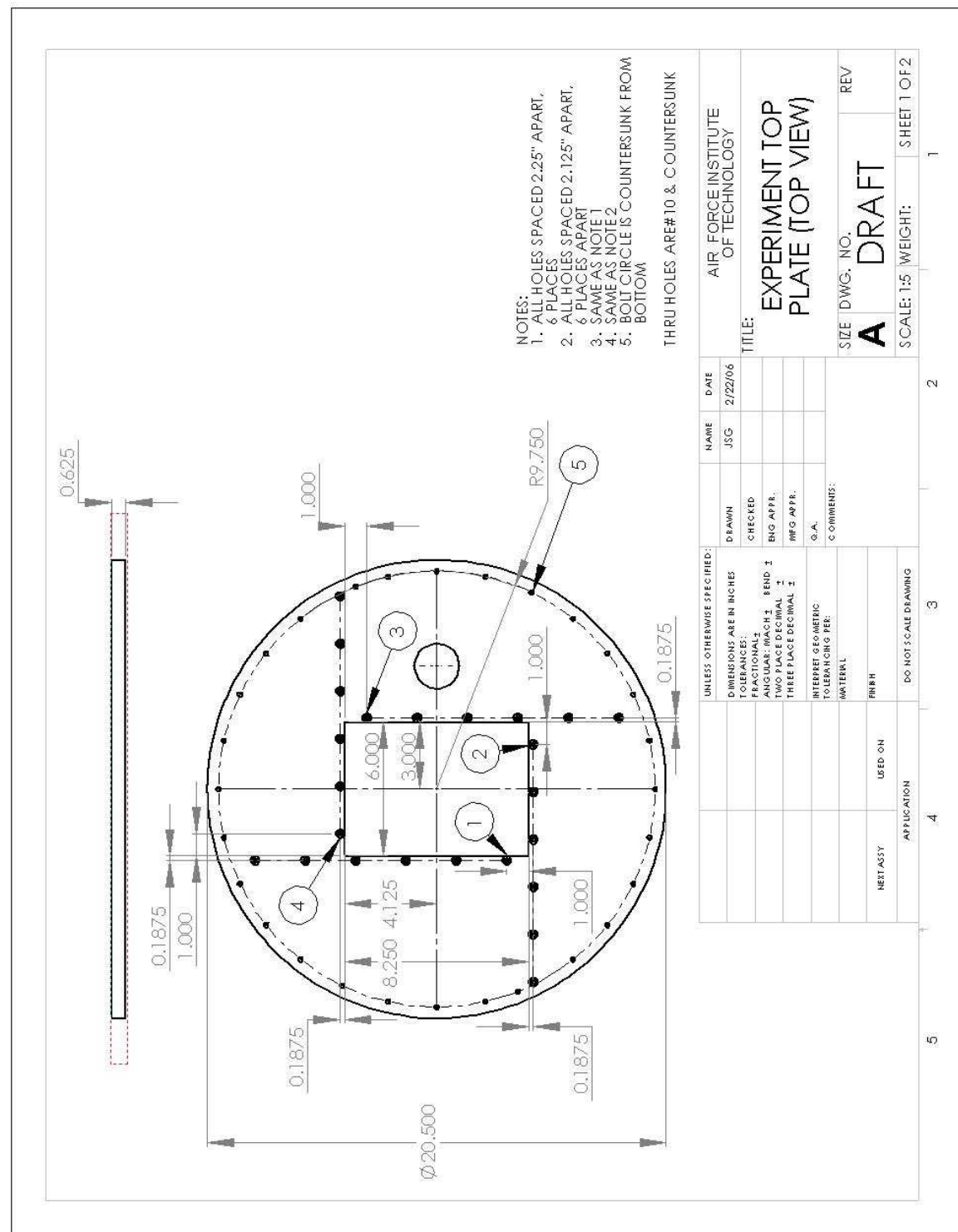
This appendix contains drawings of each structural component. Each will be marked “DRAFT” until approved at the Critical Design Review.

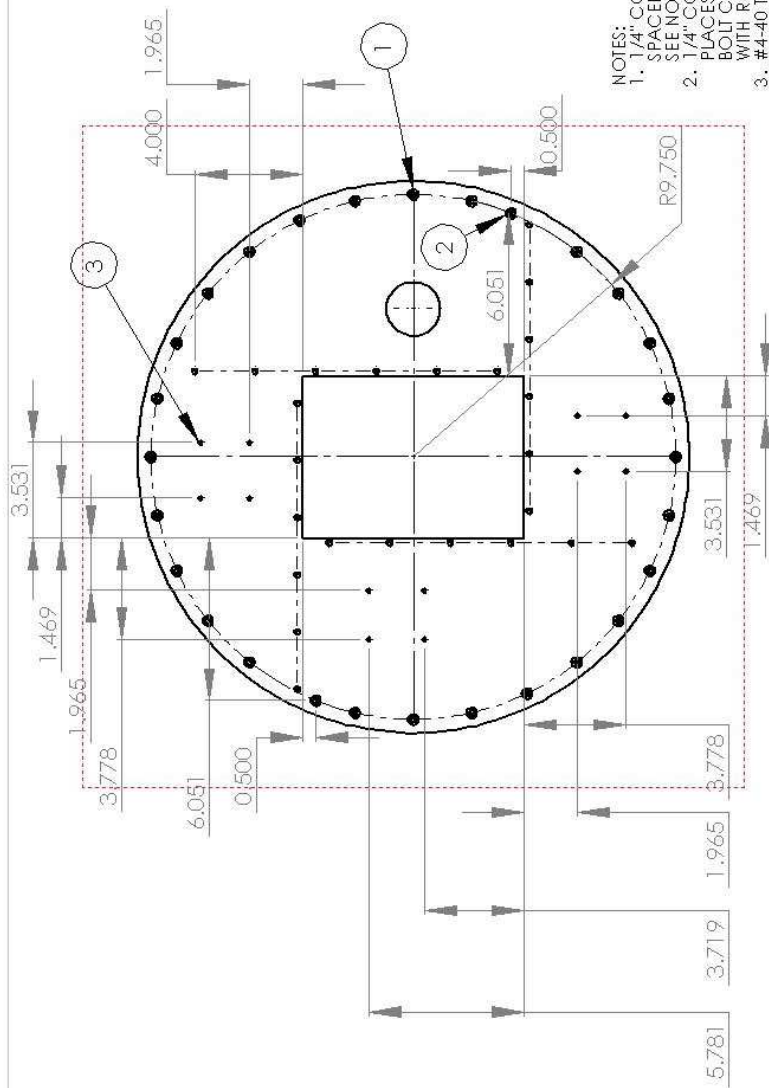
D.1 CAPE Mounting Plate





D-4

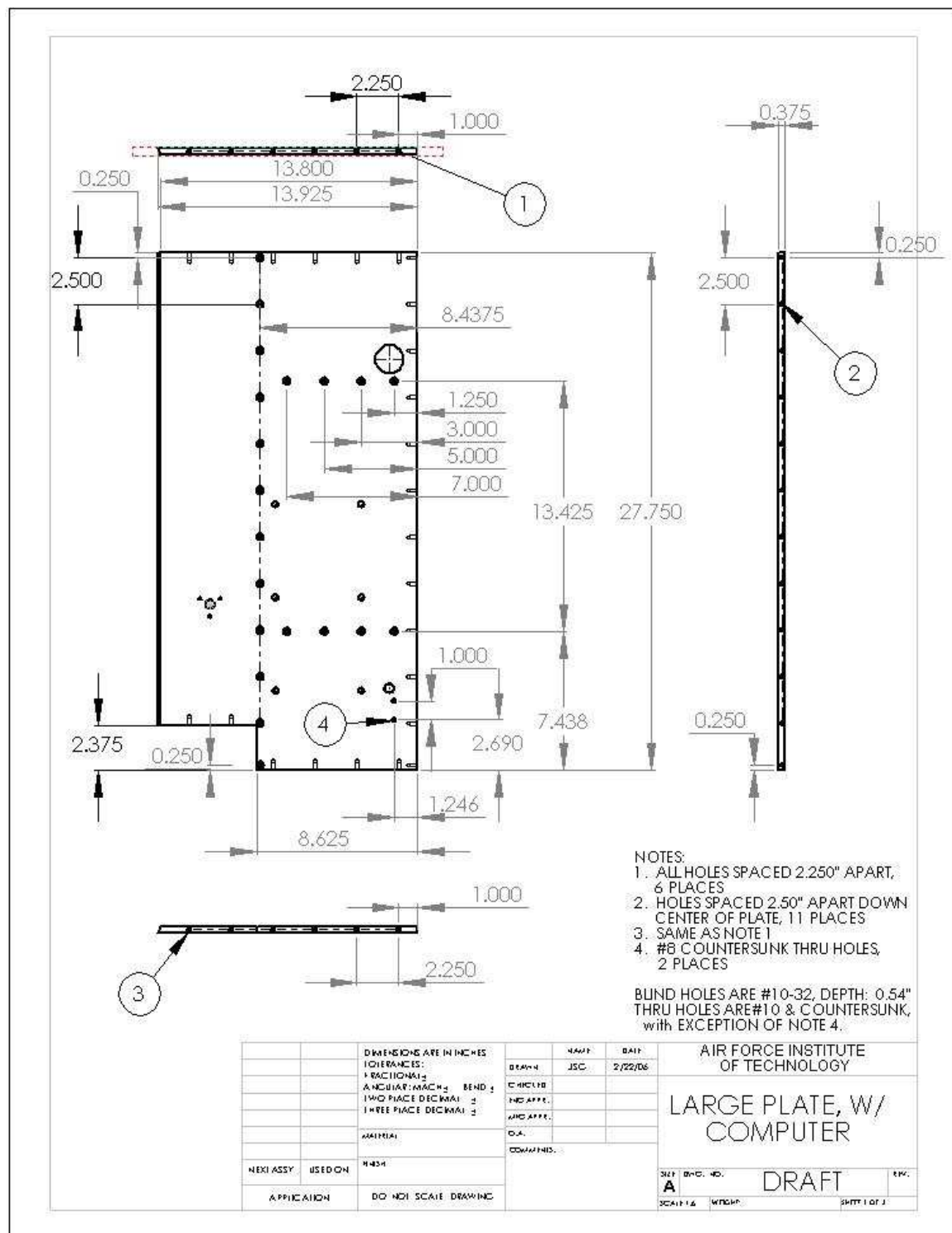




- NOTES:
1. 1/4" COUNTERSUNK HOLES, EQUALLY SPACED FOR 28 PLACES. SEE NOTE 2 FOR EXCEPTIONS.
 2. 1/4" COUNTERSUNK HOLES, THESE 2 PLACES ARE SEPARATED FROM R9.750" BOLT CIRCLE TO AVOID INTERFERENCE WITH RIB HOLES.
 3. #4-40 TAPPED HOLES, DEPTH: 0.54", 12 PLACES.

NAME		DATE		AIR FORCE INSTITUTE OF TECHNOLOGY	
JSG		2/22/06		TITLE:	
DRAWN		CHECKED		EXPERIMENT TOP PLATE (BOTTOM VIEW)	
FRACTIONAL:		ANGULAR: MACH 1		BEND 1	
TWO PLACE DECIMAL 1		THREE PLACE DECIMAL 1		ENG APPR.	
INTERPRET GEOMETRIC TOLERANCING PER:		O.A.		COMMENTS:	
MATERIAL		FINISH		DO NOT SCALE DRAWING	
NEXT ASSTY		USED ON		APPLICATION	
SCALE: 1:5		WEIGHT:		SHEET 2 OF 2	
SIZE DWG. NO.		REV		DRAFT	
1		2		3	
5		4		1	

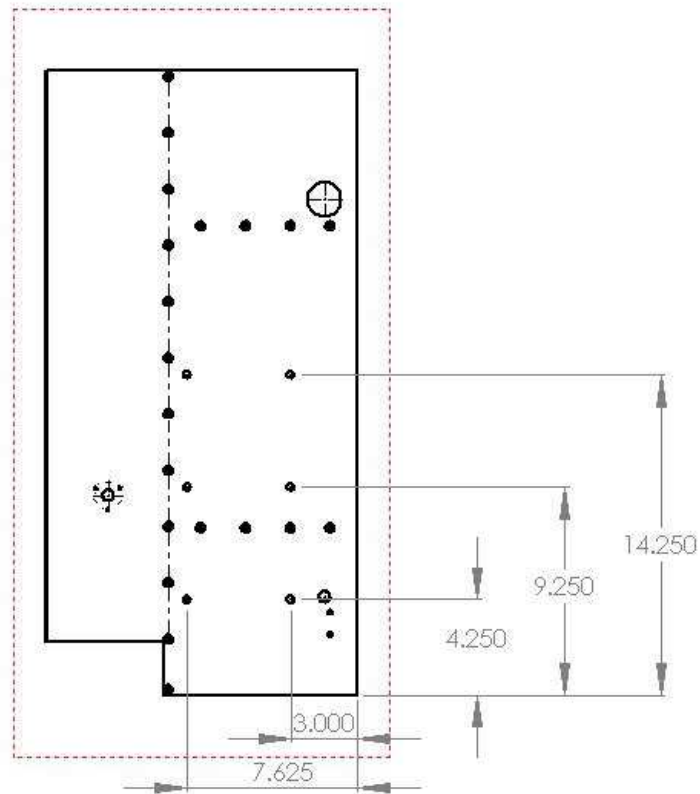
D.3 Large Rib with Computer



AIR FORCE INSTITUTE
OF TECHNOLOGY

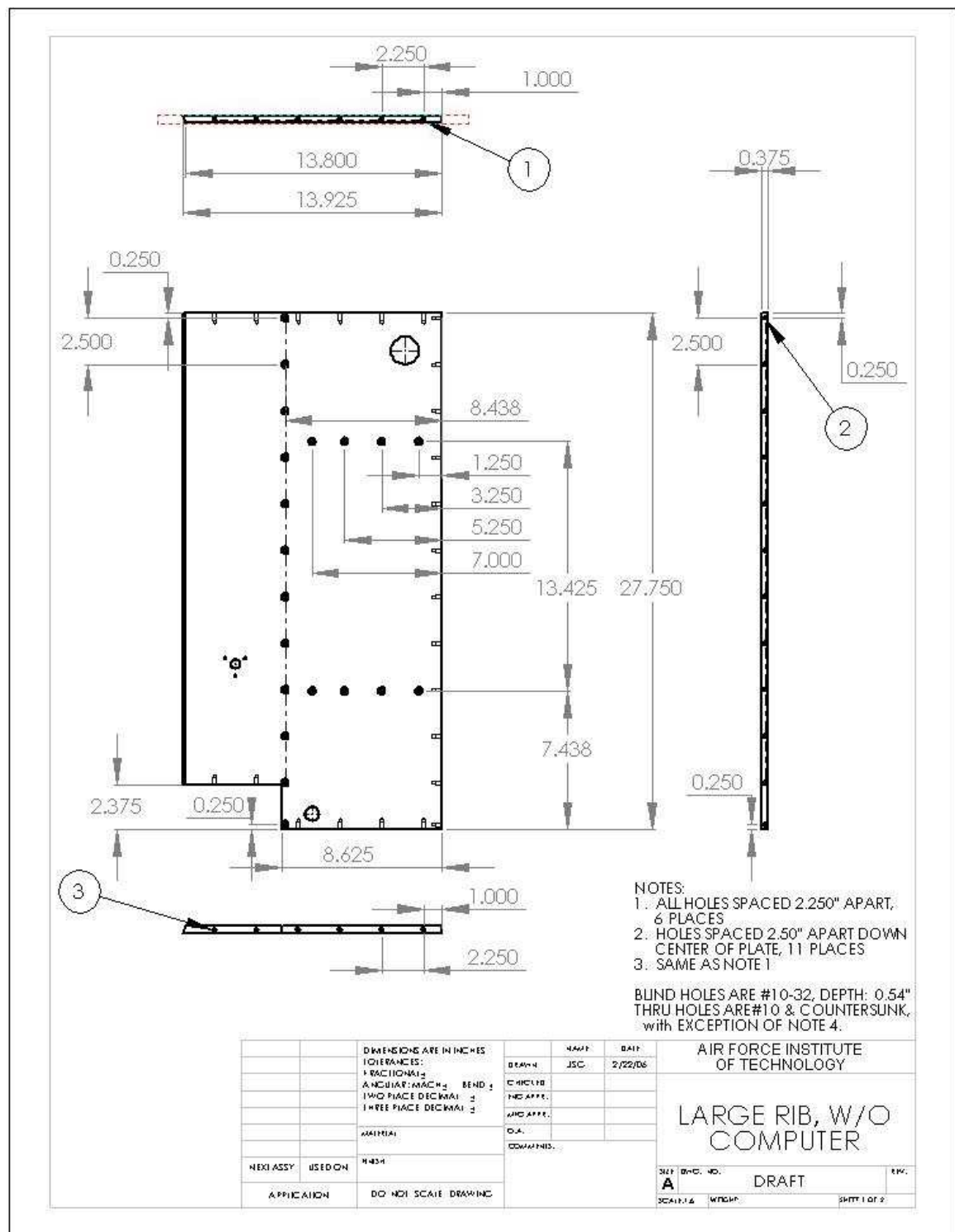
LARGE RIB, W/
COMPUTER

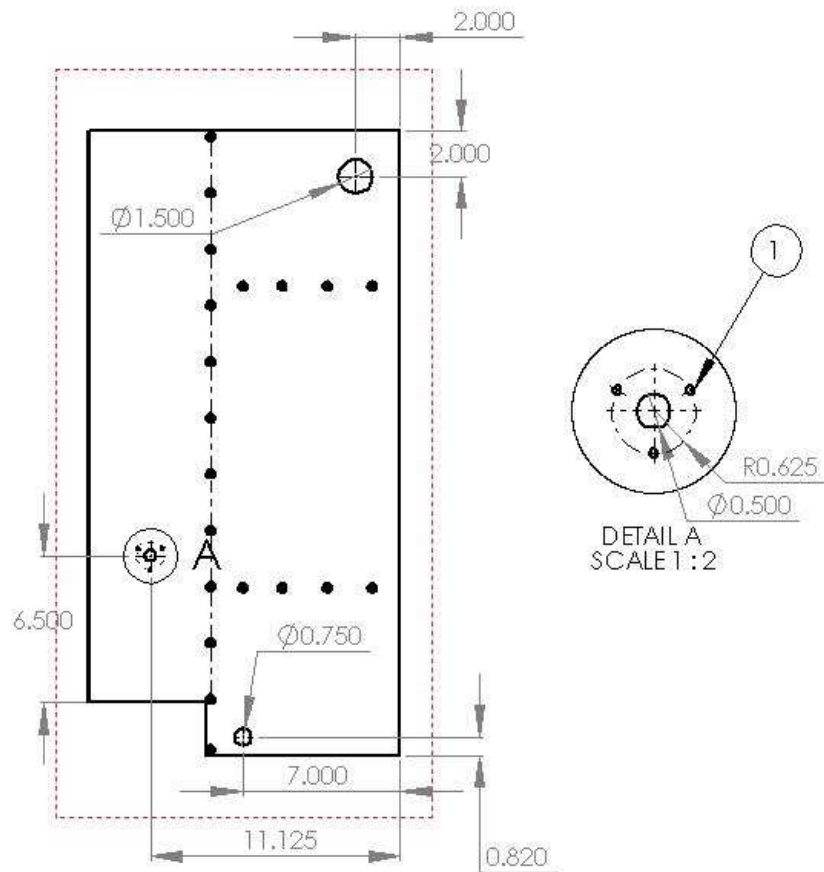
SET A	DRG. NO. DRAFT	REV.
SCALE 1:6	WORKSHEET	SHEET 2 OF 3



		DIMENSIONS ARE IN INCHES TOLERANCES: FRACTIONAL ± ANGULAR/MACH ± BEND ± TWO PLACE DECIMAL ± THREE PLACE DECIMAL ± MATERIAL FINISH NEXT ASSY USED ON APPLICATION	NAME JSC DATE 2/22/06 CHECKED INC APP. INC APP. D.A. COMMENTS	AIR FORCE INSTITUTE OF TECHNOLOGY		
				LARGE RIB, W/ COMPUTER		
				SHEET NO. A	DRAFT	REV.
				SCALE 1:1	INTERIOR	SHEET 1 OF 1

D.4 Large Rib without Computer

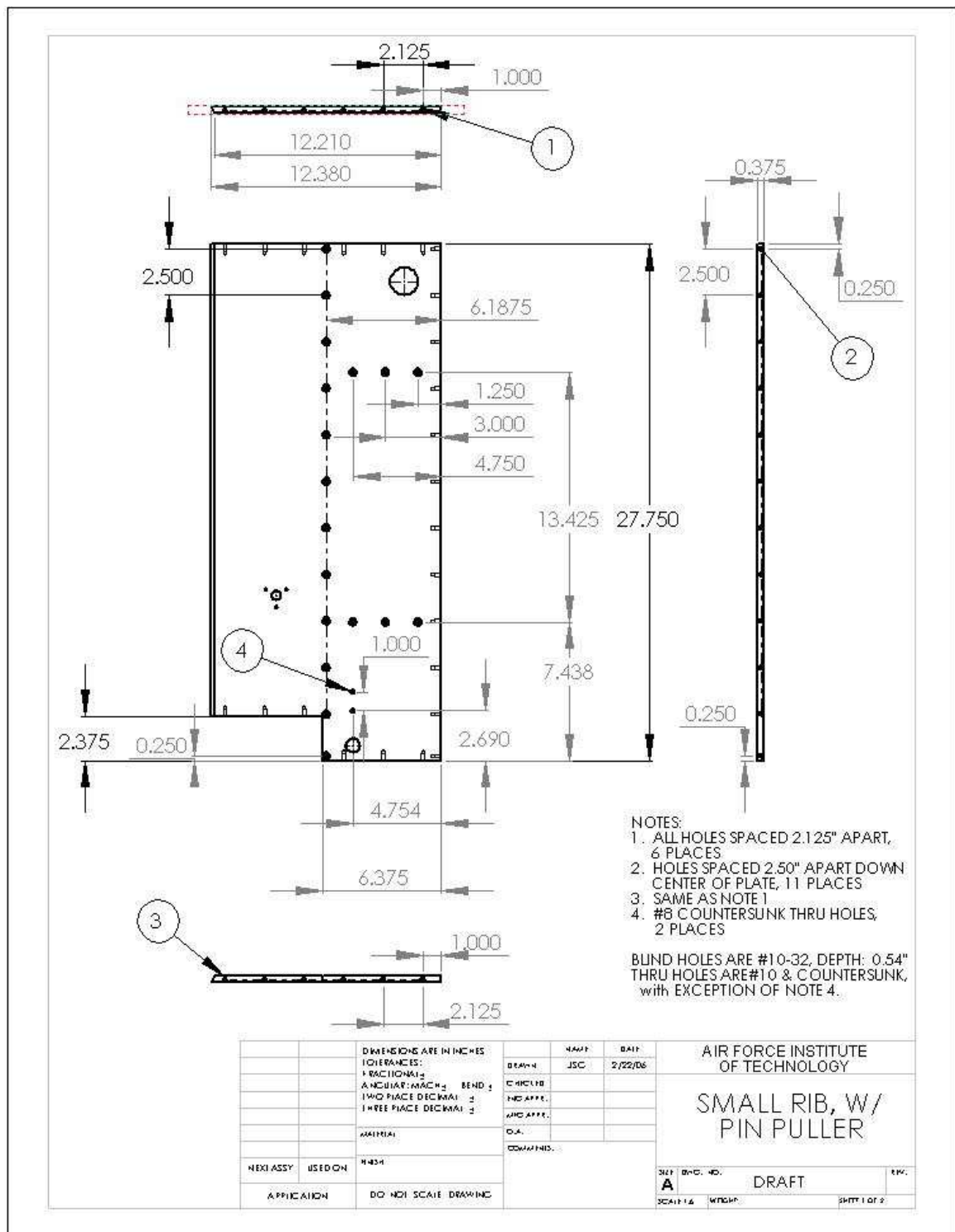


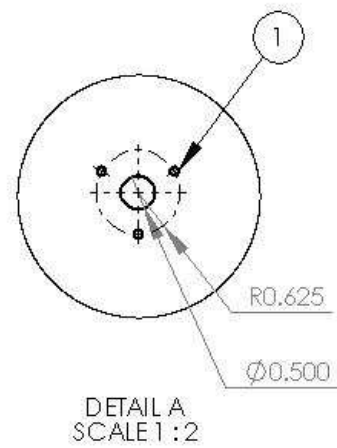
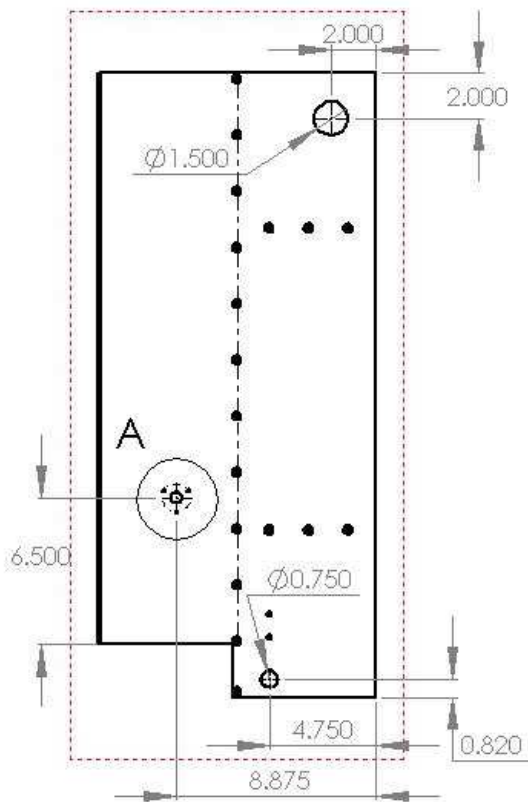


NOTES:
1. 1/8" DIA. THRU-HOLES, EQUALLY SPACED

		DIMENSIONS ARE IN INCHES TOLERANCES: FRACTIONAL ± ANGULAR: MACH ± BEND ± TWO PLACE DECIMAL ± THREE PLACE DECIMAL ± MATERIAL FINISH	NAME	DATE	AIR FORCE INSTITUTE OF TECHNOLOGY LARGE RIB, W/O COMPUTER	
			DRAWN	JSC		2/22/06
			CHECKED			
			AND APPR.			
			D.A.			
			COMMENTS			
NEXT ASSY	USED ON				SHEET NO. DRAFT	REV.
APPLICATION		DO NOT SCALE DRAWING			SHEET 2 OF 2	

D.5 Small Rib with Pin Puller Hole

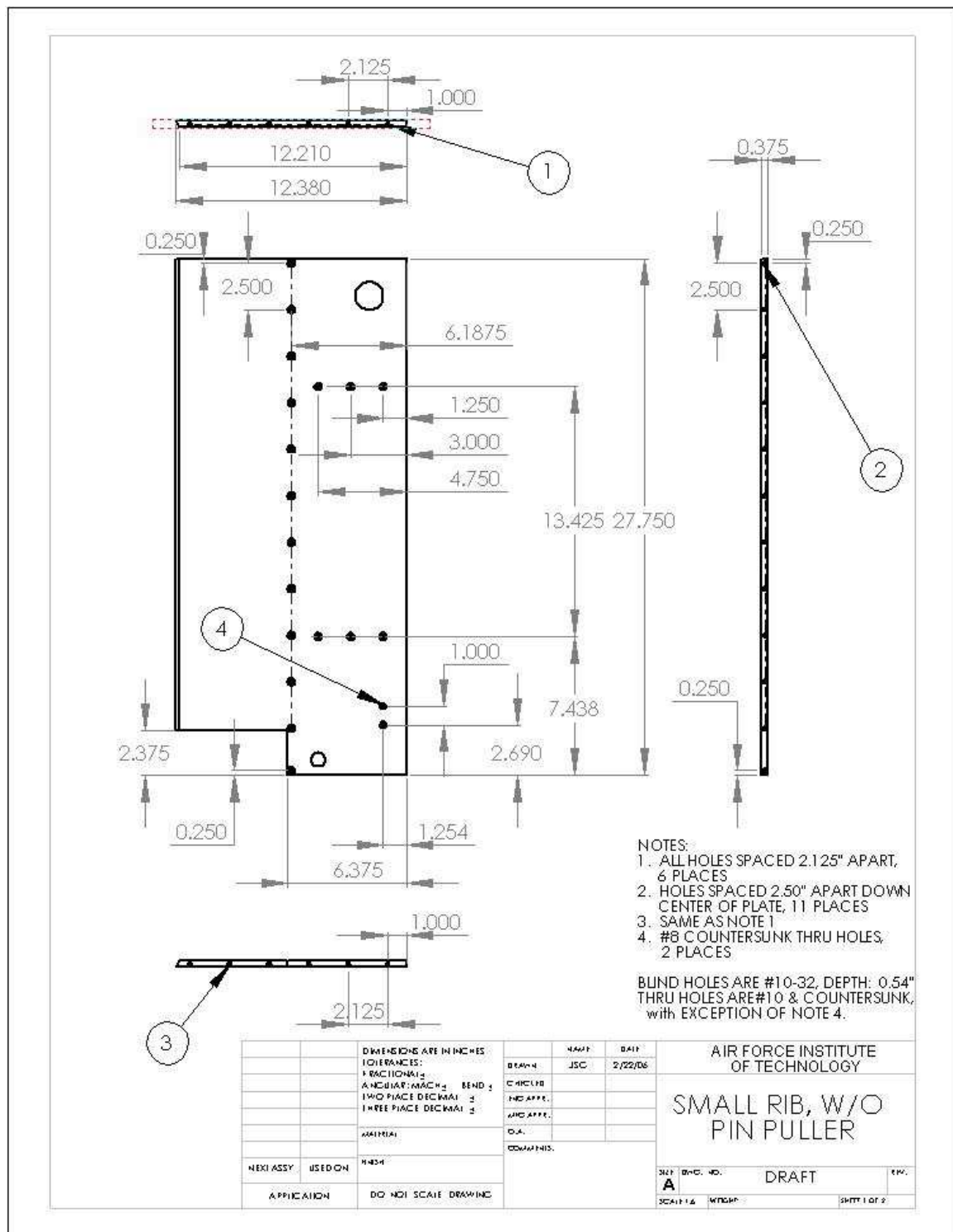


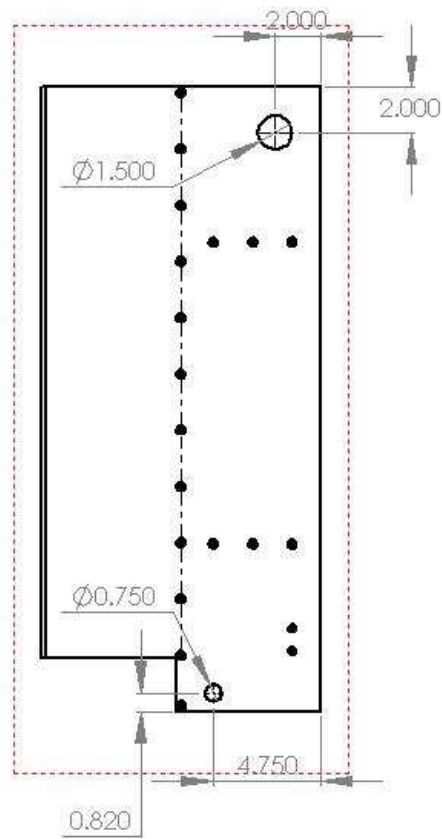


NOTES:
1. 1/8" DIA. THRU-HOLES, EQUALLY SPACED

		DIMENSIONS ARE IN INCHES TOLERANCES: FRACTIONAL ± DECIMAL: MACH ± BEND ± TWO PLACE DECIMAL ± THREE PLACE DECIMAL ± MATERIAL FINISH NEXT ASSY USED ON APPLICATION			AIR FORCE INSTITUTE OF TECHNOLOGY	
			DRAWN JSC	DATE 2/22/06	SMALL RIB, W/ PIN PULLER	
			CHECKED JSC			
			APPR. JSC			
			COMMENTS		SHEET NO. A DRAFT REV.	
					SCALE: 1:2	SHEET 2 OF 2

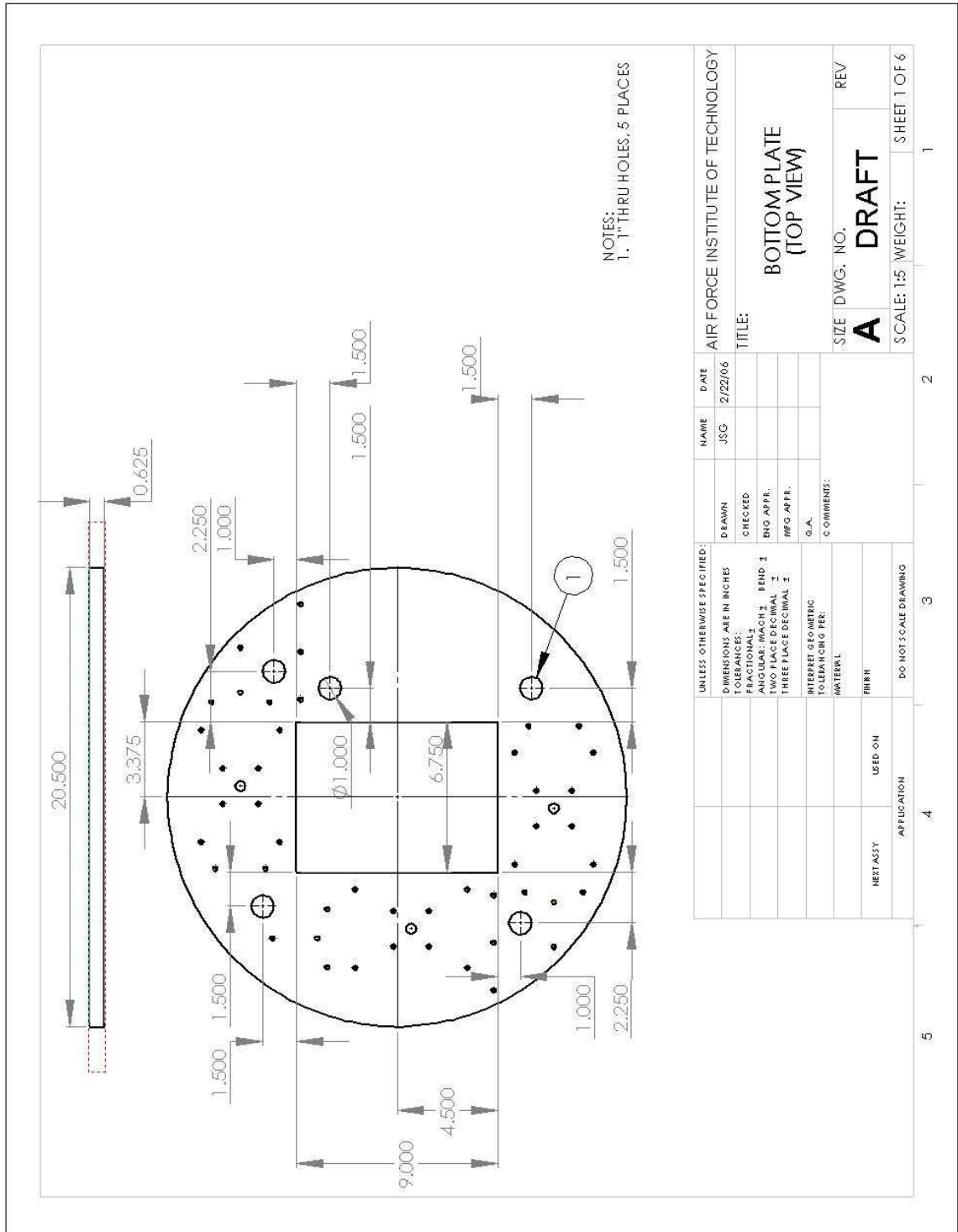
D.6 Small Rib without Pin Puller Hole

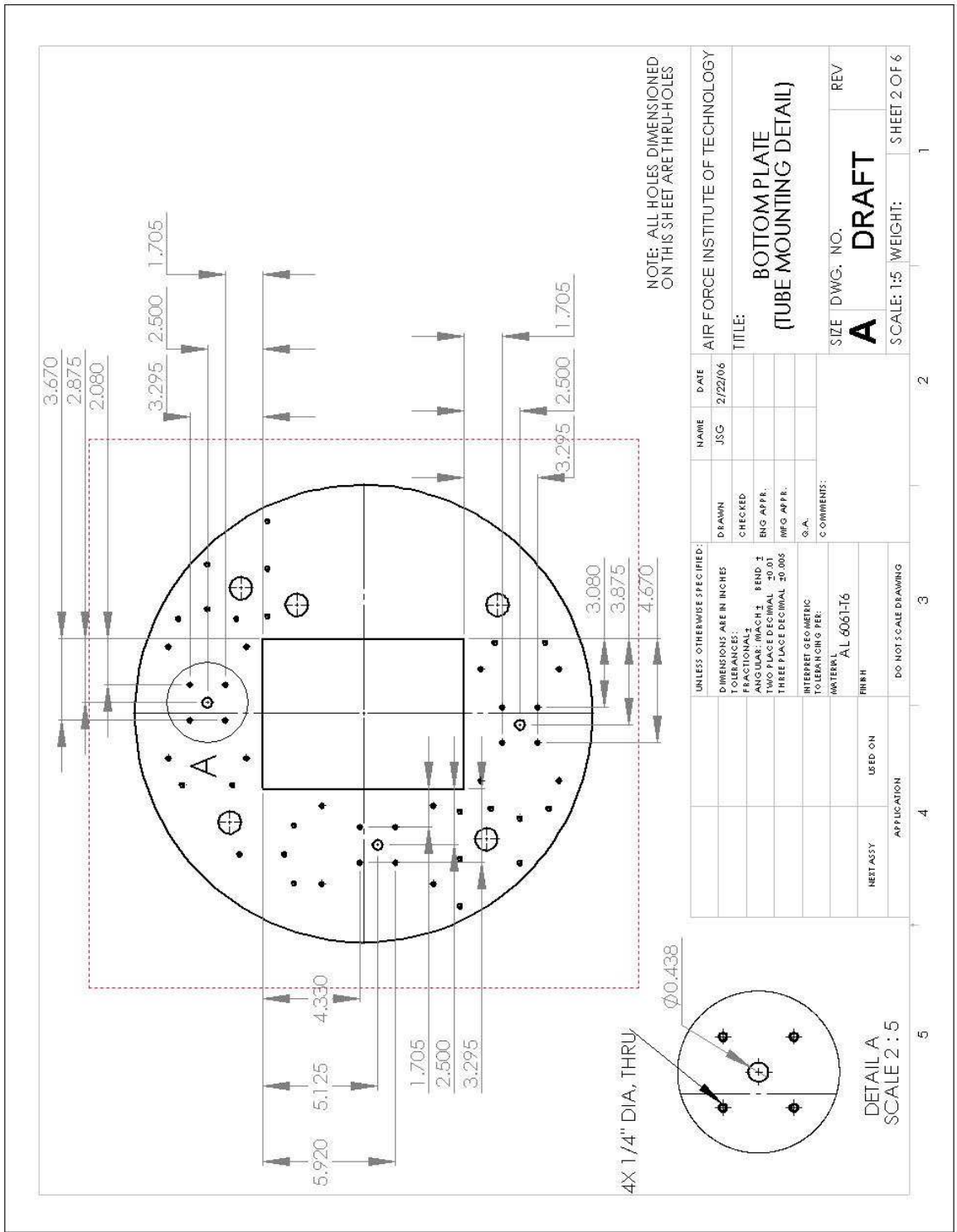


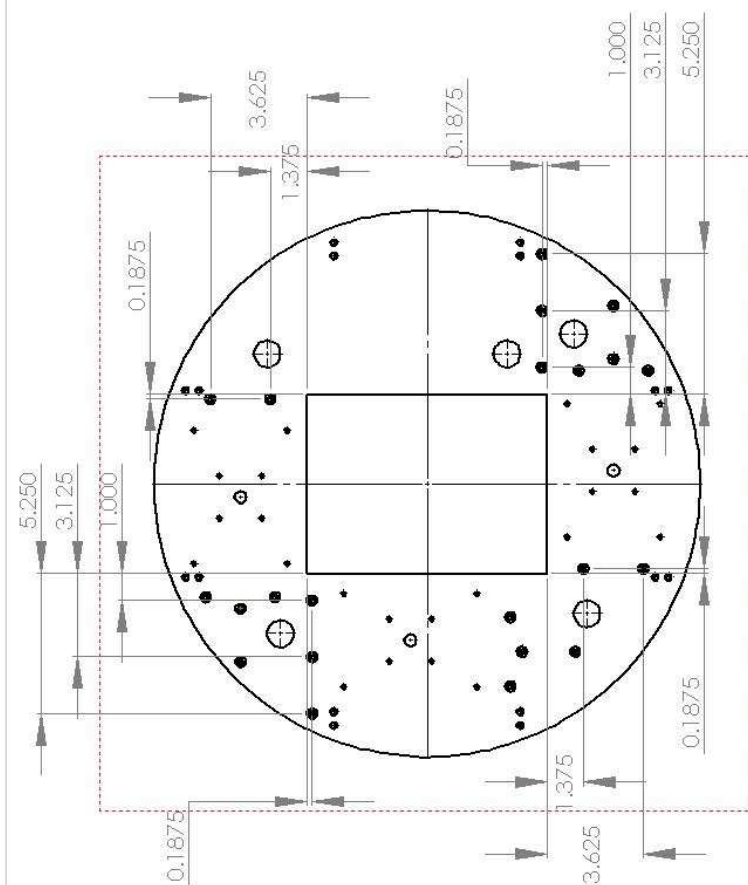


		DIMENSIONS ARE IN INCHES	NAME	DATE	
		TOLERANCES:	DRAWN	JSC	2/22/06
		FRACTIONAL ±	CHECKED		
		ANGULAR: MACH ±	NO APP.		
		TWO PLACE DECIMAL ±	NO APP.		
		THREE PLACE DECIMAL ±	D.A.		
		MATERIAL	COMMENTS		
		14-34			
NEXT ASSY	USED ON				
APPLICATION	DO NOT SCALE DRAWING				
			SMALL RIB, W/O PIN PULLER		
			REV. NO.	DRAFT	REV.
			SCALE 1:1	W/NO	SHEET 2 OF 2

D.7 Oven Mounting Plate

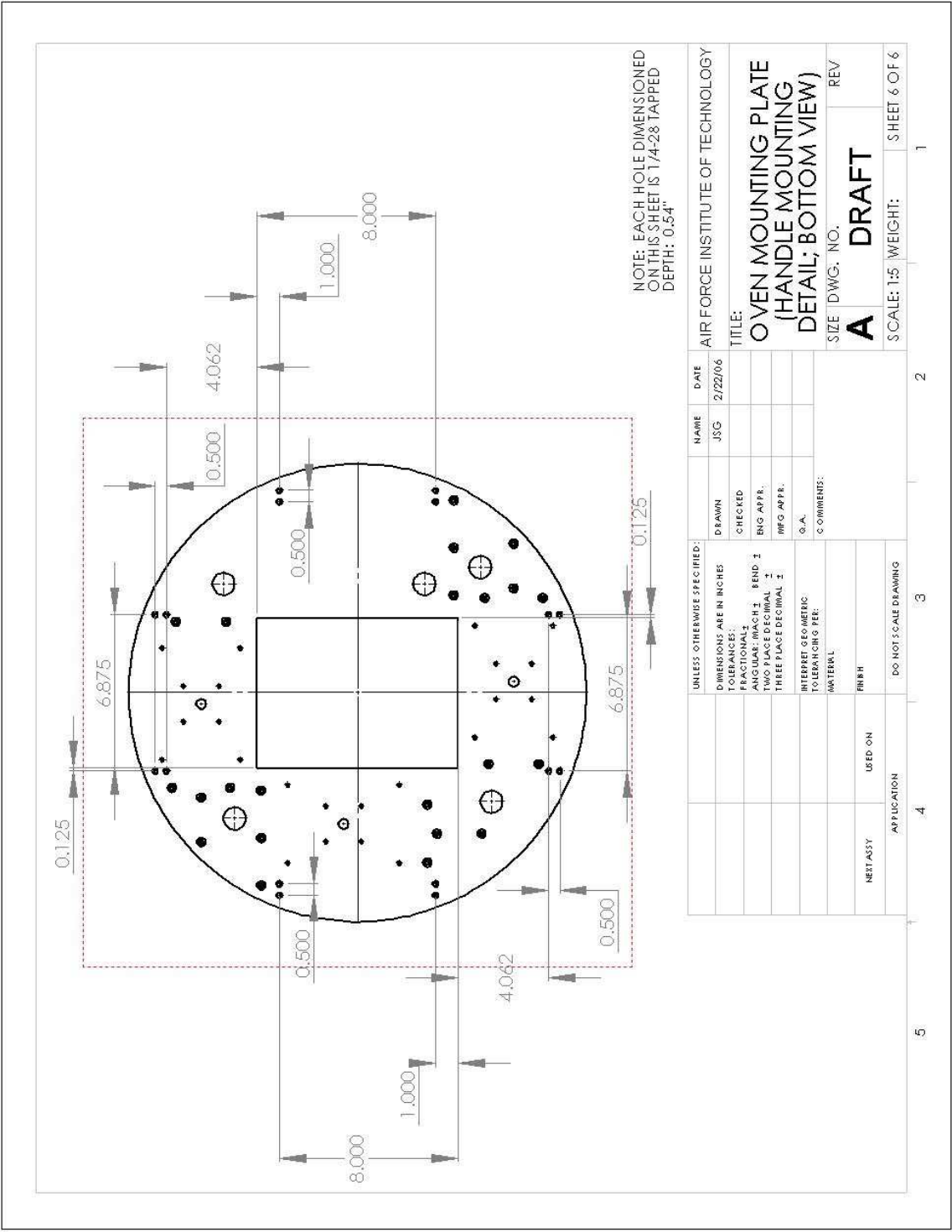






NOTE: EACH HOLE DIMENSIONED
ON THIS SHEET IS #10 THRU-HOLE
AND COUNTERSUNK

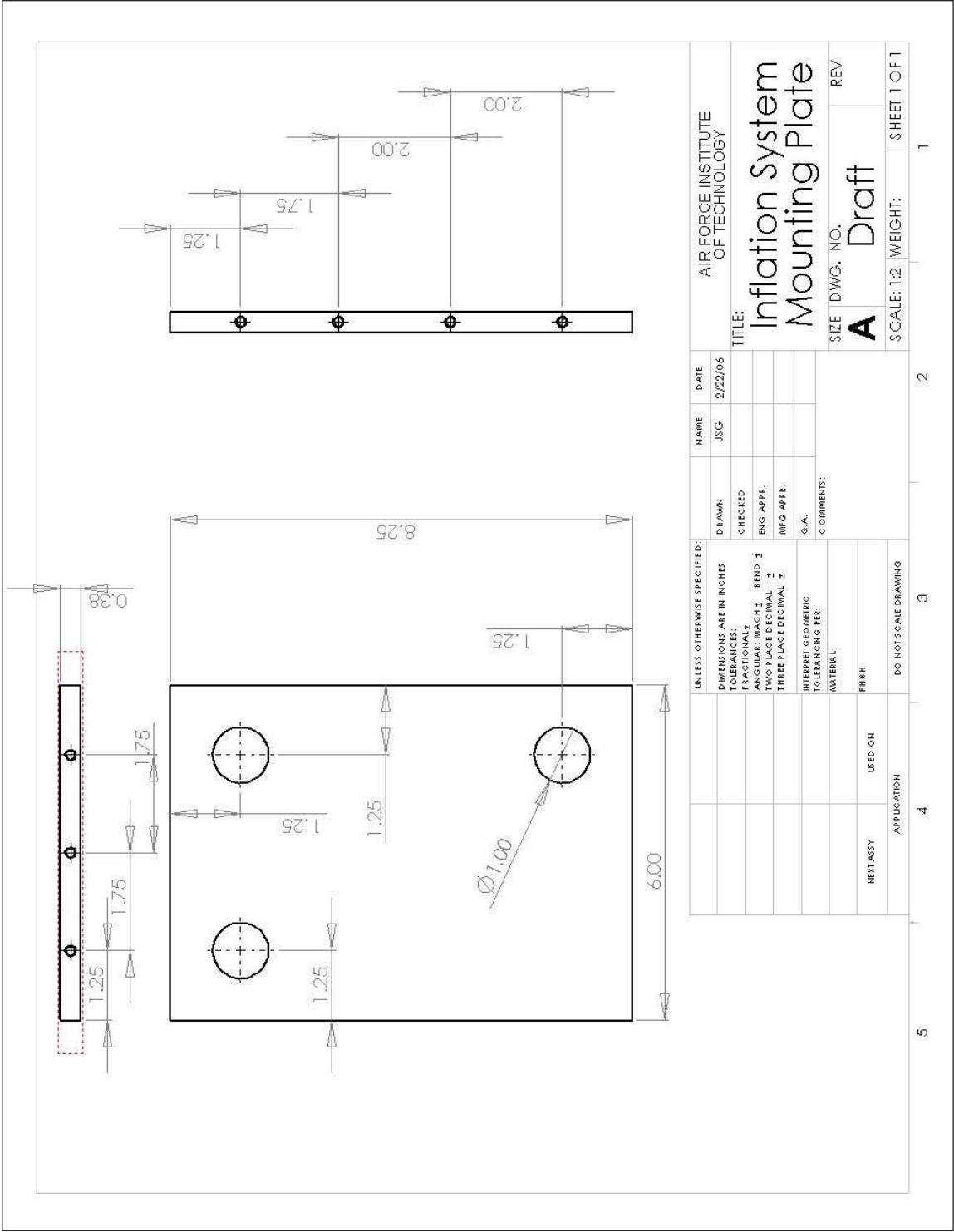
AIR FORCE INSTITUTE OF TECHNOLOGY		TITLE:		OVEN MOUNTING PLATE (RIB MOUNTING DETAIL; BOTTOM VIEW)		SIZE DWG. NO.		REV	
NAME		DATE		A		DRAFT		SHEET 4 OF 6	
JSG		2/22/06						SCALE: 1:5 WEIGHT: 1	
DRAWN		CHECKED		ENG APPR.		INFO APPR.			
DIMENSIONS ARE IN INCHES		FRACTIONAL: 1		ANGULAR: 1		BEND: 1			
TOLERANCES:		TWO PLACE DECIMAL: 1		THREE PLACE DECIMAL: 1					
INTERPRET GEOMETRIC TOLERANCING PER:		AS PER L							
FINISH		USED ON							
APPLICATION		DO NOT SCALE DRAWING							



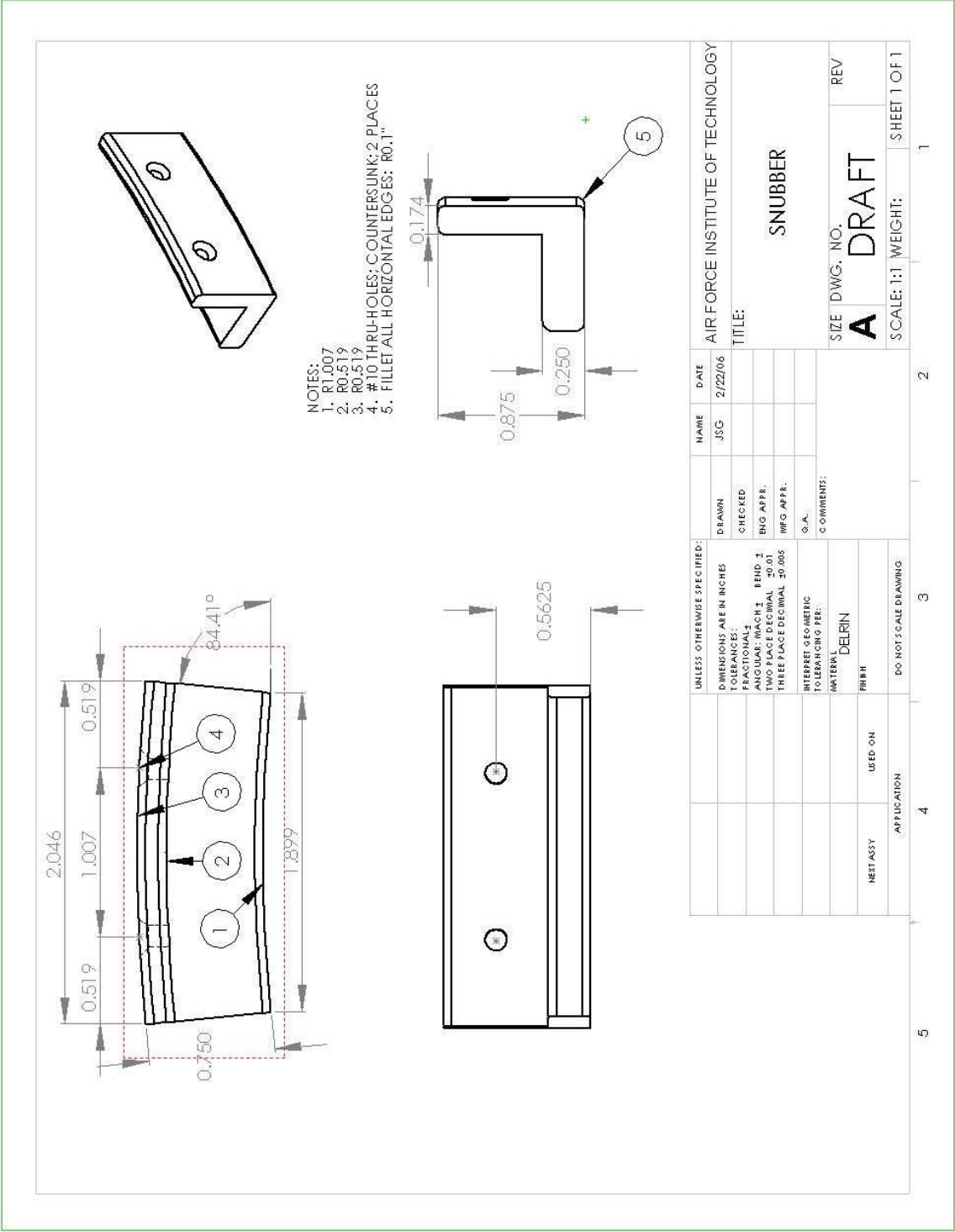
D-21



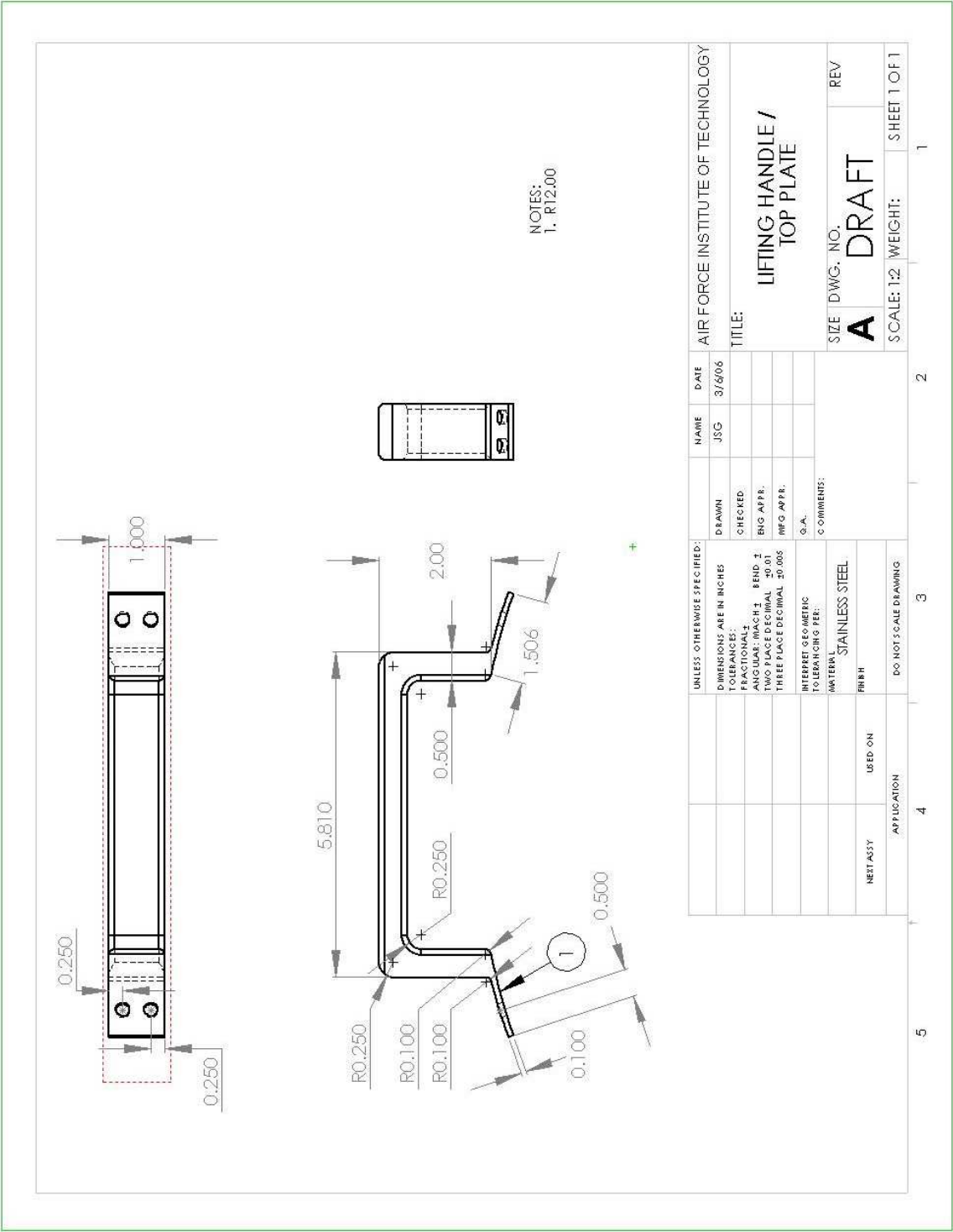
D.9 Inflation Mounting Plate



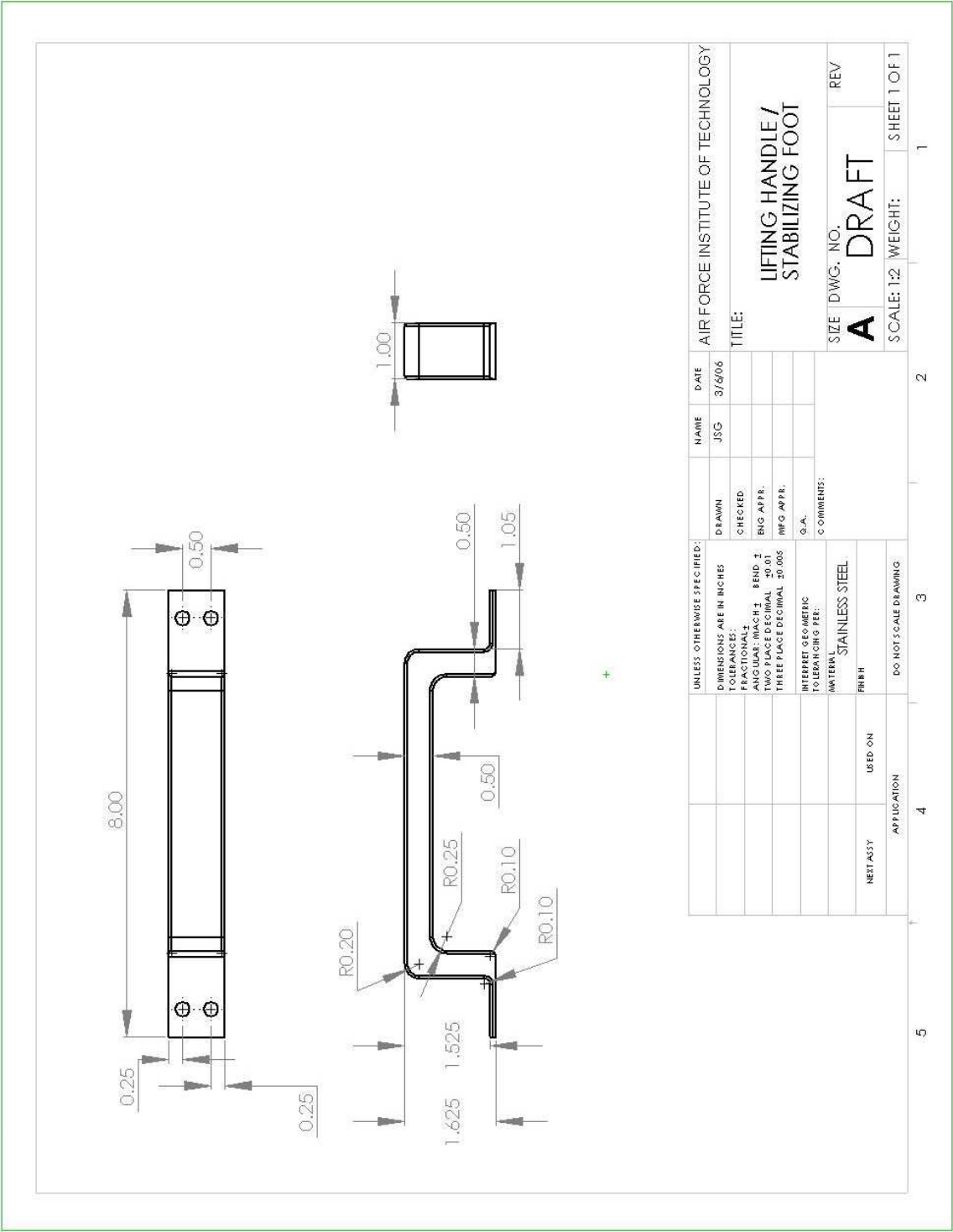
D.10 Snubber



D.11 Top Lifting Handle



D.12 Bottom Lifting Plate



Appendix E. Electrical Architecture

This appendix provides the layout of the computer harness, the external harness, and a digital copy of Moody's filter board.

E.1 Computer Harness Wiring Pinouts

In this section, the following abbreviations are used:

A#	Connector, Accel & Thermocouple (# = 1,2, or 3)
ADC	Analog/Digital Converter Board (also, Digital/Analog Converter)
CB	Camera Board
DAC	Data Acquisition Computer
DACC	Data Acquisition Computer Counter Board
F	Filter Board
IC	Imaging Computer
ICC	Imaging Computer Counter Board
J3	J3 Side of Relay Board
J4	J4 Side of Relay Board
P	Connector, Tank Pressure Transducer
PDP	Connector, Power Distribution Plate
PWR1	DAC Power Supply Board
PWR2	IC Power Supply Board
PXDCR	Pressure Transducer
S	Connector, Solenoid
T#	Connector, Tube # (# = 1,2, or 3)
TC	Thermocouple Board

Table E.1: DAC Power Supply (PWR1) Board Pinout

Board Pin #	Board Pin Description	Reserved For	Connector/ Pin
<i>Power Source</i>			
1	Ground, (-) Terminal of 12V Source	(-) Shuttle Power	PDP/2
2	+9VDC@13.5A to +60VDC@2A Input	(+) Shuttle Power & Solenoid Diode 1&2	PDP/1; J4/12,24
3	(+) Terminal of 12V Source	-	-
<i>Auxiliary Outputs</i>			
4	Ground	-	-
5	+5VDC	Tube 1&2 Oven Relays & Pin Pullers	J4/4,8,16,20
6	Ground	-	-
7	+12VDC	-	-
8	Spare	-	-
9	Spare	-	-

Table E.2: IC Power Supply (PWR2) Board Pinout

Board Pin #	Board Pin Description	Reserved For	Connector/ Pin
<i>J3: Power Source</i>			
1	Ground, (-) Terminal of 12V Source	(-) Shuttle Power	PDP/2
2	+9VDC@13.5A to +60VDC@2A Input	(+) Shuttle Power & Solenoid Diode 3	PDP/1; J4/36
3	(+) Terminal of 12V Source	-	-
<i>J4: Auxiliary Outputs</i>			
4	Ground	Filter Ground	Filter Ground Plane
5	+5VDC	Tube 3 Oven Relay & Pin Puller; Filter; LED Circuit	J4/28,32,40,44
6	Ground	-	-
7	+12VDC	-	-
8	Spare	-	-
9	Spare	-	-

Table E.3: Analog/Digital Converter (ADC) Board Pinout

Connector/ Pin	Reserved For	Board Pin Description	Board Pin #	Board Pin Description	Reserved For	Connector/ Pin
A1,2,3/3	Accel Ground	Analog Ground	1	2	Analog Ground	-
T1/5	Tb1 PXDCR (data +)	Ch 0+	3	4	Ch 0-	Tb1 PXDCR (data -)
T2/5	Tb2 PXDCR (data +)	Ch 1+	5	6	Ch 1-	Tb2 PXDCR (data -)
T3/5	Tb3 PXDCR (data +)	Ch 2+	7	8	Ch 2-	Tb3 PXDCR (data -)
P/1	Tk1 PXDCR (data +)	Ch 3+	9	10	Ch 3-	Tk1 PXDCR (data -)
P/2	Tk2 PXDCR (data +)	Ch 4+	11	12	Ch 4-	Tk1 PXDCR (data -)
P/3	Tk3 PXDCR (data +)	Ch 5+	13	14	Ch 5-	Tk1 PXDCR (data -)
-	-	Ch 6+	15	16	Ch 6-	-
-	-	Ch 7+	17	18	Ch 7-	-
-	-	Ch 8	19	20	Ch 24	Tb3 Accel Axis 1
-	-	Ch 9	21	22	Ch 25	Tb3 Accel Axis 2
A1/7	Tb1 Accel Axis 1	Ch 10	23	24	Ch 26	Tb3 Accel Axis 3
A1/8	Tb1 Accel Axis 2	Ch 11	25	26	Ch 27	-
A1/9	Tb1 Accel Axis 3	Ch 12	27	28	Ch 28	-
A2/7	Tb2 Accel Axis 1	Ch 13	29	30	Ch 29	-
A2/8	Tb2 Accel Axis 2	Ch 14	31	32	Ch 30	-
A2/9	Tb2 Accel Axis 3	Ch 15	33	34	Ch 31	-
-	-	Vout 3	35	36	Vout 2	-
-	-	Vout 1	37	38	Vout 0	Filter (+) input
-	-	Vref out	39	40	Analog Ground	Filter (-) input
-	-	A/D Convert	41	42	Ctr2 Out/Dout2	-
ICC/46	Comm w/ IC	Dout1	43	44	Ctr0 Out/Dout0	Synch w/ IC
-	-	Ext Clk	45	46	Ext Gate/Din2	-
-	-	Gate0/Din1	47	48	Clk0/Din0	-
A1,2,3/1	Accel Power	+5V	49	50	Digital Ground	-

Table E.4: Thermocouple (TC) Board Pinout

Connector/ Pin	Reserved For	Board Pin Description	Board Pin #	Board Pin Description	Reserved For	Connector/ Pin
TC/2	Shorted w/ Pin 2	T/C 7+	1 2	T/C 7-	Shorted w/ Pin 1	TC/1
	—	T/C 6+	3 4	T/C 6-	—	
A3/14	T3 Low T/C (+)	T/C 5+	5 6	T/C 5-	T3 Low T/C (-)	A3/15
A3/12	T3 High T/C (+)	T/C 4+	7 8	T/C 4-	T3 High T/C (-)	A3/13
A2/14	T2 Low T/C (+)	T/C 3+	9 10	T/C 3-	T2 Low T/C (-)	A2/15
A2/12	T2 High T/C (+)	T/C 2+	11 12	T/C 2-	T2 High T/C (-)	A2/13
A1/14	T1 Low T/C (+)	T/C 1+	13 14	T/C 1-	T1 Low T/C (-)	A1/15
A1/12	T1 High T/C (+)	T/C 0+	15 16	T/C 0-	T1 High T/C (-)	A1/13

Table E.5: Filter (F) Board Pinout

Board Pin #	Board Pin Description	Reserved For	Connector/ Pin
1	+5VDC (Filter Power)	Supplied from J4	J4/45
2	-5VDC (Filter Power)	Supplied from J4	J4/49
3	—	—	—
4	Signal (+) Input	(+) Signal from D/A Converter	AD/38
5	Signal (-) Input	(-) Signal from D/A Converter	AD/40
6	—	—	—
7	Signal (+) Output	Relay to PZT	J3/4,8,12
8	Signal (-) Output	PZT Return on Tube Connectors	T1,2,3/8

Table E.6: Camera Board (CB) Board Pinout

Board Pin #	Board Pin Description	Reserved For	Connector/ Pin
1	Image Area Gate	Pass-through	
2	Storage Area Gate 1	Pass-through	
3	Storage Area Gate 2	Pass-through	
4	Anti-Blooming Gate	Pass-through	
5	Combined Serial Register Gates	Pass-through	
6	Not Used	Pass-through	
7	Not Used	Pass-through	
8	Not Used	Pass-through	
9	Analog Video Signal	Pass-through	
10	Combined Transfer/Transfer MUX Gate	Pass-through	
11	Ground	Pass-through	
12	+11VDC (regulated)	Pass-through	
13	Ground	Pass-through	
14	Not Used	Pass-through	
15	Not Used	Pass-through	

Table E.7: Data Acquisition Computer Counter (DACC) Board Pinout

Connector/ Pin	Reserved For	Board Pin Description	Board Pin #	Board Pin Description	Reserved For	Connector/ Pin
–	–	In 1	1 2	In 2	–	–
–	–	Gate 1	3 4	Gate 2	–	–
–	–	Out 1	5 6	Out 2	–	–
–	–	In 3	7 8	In 4	–	–
–	–	Gate 3	9 10	Gate 4	–	–
–	–	Out 3	11 12	Out 4	–	–
–	–	In 5	13 14	Out 5	–	–
–	–	Gate 5	15 16	Fout	–	–
–	–	In 6	17 18	In 7	–	–
–	–	Gate 6	19 20	Gate 7	–	–
–	–	Out 6	21 22	Out 7	–	–
–	–	In 8	23 24	In 9	–	–
–	–	Gate 8	25 26	Gate 9	–	–
–	–	Out 8	27 28	Out 9	–	–
–	–	In 10	29 30	Out 10	–	–
–	–	Gate 10	31 32	Interrupt In	–	–
ICC/34	Comm w/ ICC	Dout 7	33 34	Din 7	Comm w/ ICC	ICC/33
ICC/36	Comm w/ ICC	Dout 6	35 36	Din 6	–	–
–	–	Dout 5	37 38	Din 5	–	–
–	–	Dout 4	39 40	Din 4	–	–
–	–	Dout 3	41 42	Din 3	–	–
–	–	Dout 2	43 44	Din 2	–	–
–	–	Dout 1	45 46	Din 1	–	–
–	–	Dout 0	47 48	Din 0	–	–
–	–	+5V	49 50	Ground	–	–

Table E.8: Imaging Computer Counter (ICC) Board Pinout

Connector/ Pin	Reserved For	Board Pin Description	Board Pin #	Board Pin Description	Reserved For	Connector/ Pin
–	–	In 1	1 2	In 2	–	–
–	–	Gate 1	3 4	Gate 2	–	–
–	–	Out 1	5 6	Out 2	–	–
–	–	In 3	7 8	In 4	–	–
–	–	Gate 3	9 10	Gate 4	–	–
–	–	Out 3	11 12	Out 4	–	–
–	–	In 5	13 14	Out 5	–	–
–	–	Gate 5	15 16	Fout	–	–
–	–	In 6	17 18	In 7	–	–
–	–	Gate 6	19 20	Gate 7	–	–
–	–	Out 6	21 22	Out 7	–	–
–	–	In 8	23 24	In 9	–	–
–	–	Gate 8	25 26	Gate 9	–	–
–	–	Out 8	27 28	Out 9	–	–
–	–	In 10	29 30	Out 10	–	–
–	–	Gate 10	31 32	Interrupt In	–	–
DACC/34	Comm w/ DACC	Dout 7	33 34	Din 7	Comm w/ DACC	DACC/33
–	–	Dout 6	35 36	Din 6	Comm w/ DACC	DACC/35
–	–	Dout 5	37 38	Din 5	–	–
–	–	Dout 4	39 40	Din 4	–	–
–	–	Dout 3	41 42	Din 3	–	–
–	–	Dout 2	43 44	Din 2	–	–
–	–	Dout 1	45 46	Din 1	Comm w/ ADC	ADC/43
–	–	Dout 0	47 48	Din 0	–	–
–	–	+5V	49 50	Ground	–	–

Table E.9: Relay Board Pinout, J4 Side (J4), Relays 1-12

Connector/ Pin	Reserved For	Board Pin Description	Board Pin #	Board Pin Description	Reserved For	Connector/ Pin
T1,2,3/2	Pin Puller Returns	Ground	1 2	Ground	Oven Relay Control Returns	T1,2,3/4
–	–	NC - Relay 1	3 4	Cmn-Relay 1	+5V from PWR1	PWR1/5
T1/1	(+) T1 Oven Relay Control	NO - Relay 1	5 6	Cmn-Relay 1	–	–
–	–	NC - Relay 2	7 8	Cmn-Relay 2	+5V from PWR1	PWR1/5
T1/3	T1 Pin Puller (white lead)	NO - Relay 2	9 10	Cmn-Relay 2	–	–
–	–	NC - Relay 3	11 12	Cmn-Relay 3	+28V from PWR1	PWR1/2
S/1	T1 Solenoid Diode	NO - Relay 3	13 14	Cmn-Relay 3	–	–
–	–	NC - Relay 4	15 16	Cmn-Relay 4	+5V from PWR1	PWR1/5
T2/1	(+) T2 Oven Relay Control	NO - Relay 4	17 18	Cmn-Relay 4	–	–
–	–	NC - Relay 5	19 20	Cmn-Relay 5	+5V from PWR1	PWR1/5
T2/3	T2 Pin Puller (white lead)	NO - Relay 5	21 22	Cmn-Relay 5	–	–
–	–	NC - Relay 6	23 24	Cmn-Relay 6	+28V from PWR1	PWR1/2
S/3	T2 Solenoid Diode	NO - Relay 6	25 26	Cmn-Relay 6	–	–
–	–	NC - Relay 7	27 28	Cmn-Relay 7	+5V from PWR2	PWR2/5
T3/1	(+) T3 Oven Relay Control	NO - Relay 7	29 30	Cmn-Relay 7	–	–
–	–	NC - Relay 8	31 32	Cmn-Relay 8	+5V from PWR2	PWR2/5
T3/3	T3 Pin Puller (white lead)	NO - Relay 8	33 34	Cmn-Relay 8	–	–
–	–	NC - Relay 9	35 36	Cmn-Relay 9	+28V from PWR2	PWR2/2
S/5	T3 Solenoid Diode	NO - Relay 9	37 38	Cmn-Relay 9	–	–
–	–	NC - Relay 10	39 40	Cmn-Relay 10	+5V from PWR2	PWR2/5
A1/10	(+) LED Circuit	NO - Relay 10	41 42	Cmn-Relay 10	–	–
–	–	NC - Relay 11	43 44	Cmn-Relay 11	+5V from PWR2	PWR2/5
F/1	(+) 5V Power to Filter	NO - Relay 11	45 46	Cmn-Relay 11	–	–
–	–	NC - Relay 12	47 48	Cmn-Relay 12	-5V from PWR2	–
F/2	(-) 5V Power to Filter	NO - Relay 12	49 50	Cmn-Relay 12	–	–

Table E.10: Relay Board Pinout, J3 Side (J3), Relays 13-24

Connector/ Pin	Reserved For	Board Pin Description	Board Pin #	Board Pin Description	Reserved For	Connector/ Pin
–	–	Ground	1 2	Ground	–	–
–	–	NC - Relay 13	3 4	Common-Relay 13	(+) Output From Filter	F/7
T1/7	T1 Transformer Input	NO - Relay 13	5 6	Common-Relay 13	–	–
–	–	NC - Relay 14	7 8	Common-Relay 14	(+) Output From Filter	F/7
T2/7	T2 Transformer Input	NO - Relay 14	9 10	Common-Relay 14	–	–
–	–	NC - Relay 15	11 12	Common-Relay 15	(+) Output From Filter	F/7
T3/7	T3 Transformer Input	NO - Relay 15	13 14	Common-Relay 15	–	–
–	–	NC - Relay 16	15 16	Common-Relay 16	–	–
–	–	NO - Relay 16	17 18	Common-Relay 16	–	–
–	–	NC - Relay 17	19 20	Common-Relay 17	–	–
–	–	NO - Relay 17	21 22	Common-Relay 17	–	–
–	–	NC - Relay 18	23 24	Common-Relay 18	–	–
–	–	NO - Relay 18	25 26	Common-Relay 18	–	–
–	–	NC - Relay 19	27 28	Common-Relay 19	–	–
–	–	NO - Relay 19	29 30	Common-Relay 19	–	–
–	–	NC - Relay 20	31 32	Common-Relay 20	–	–
–	–	NO - Relay 20	33 34	Common-Relay 20	–	–
–	–	NC - Relay 21	35 36	Common-Relay 21	–	–
–	–	NO - Relay 21	37 38	Common-Relay 21	–	–
–	–	NC - Relay 22	39 40	Common-Relay 22	–	–
–	–	NO - Relay 22	41 42	Common-Relay 22	–	–
–	–	NC - Relay 23	43 44	Common-Relay 23	–	–
–	–	NO - Relay 23	45 46	Common-Relay 23	–	–
–	–	NC - Relay 24	47 48	Common-Relay 24	–	–
–	–	NO - Relay 24	49 50	Common-Relay 24	–	–

E.2 Experiment Harness Layout

The following pages contain the schematics of the new harness that will connect the computer to the various components on the experiment.

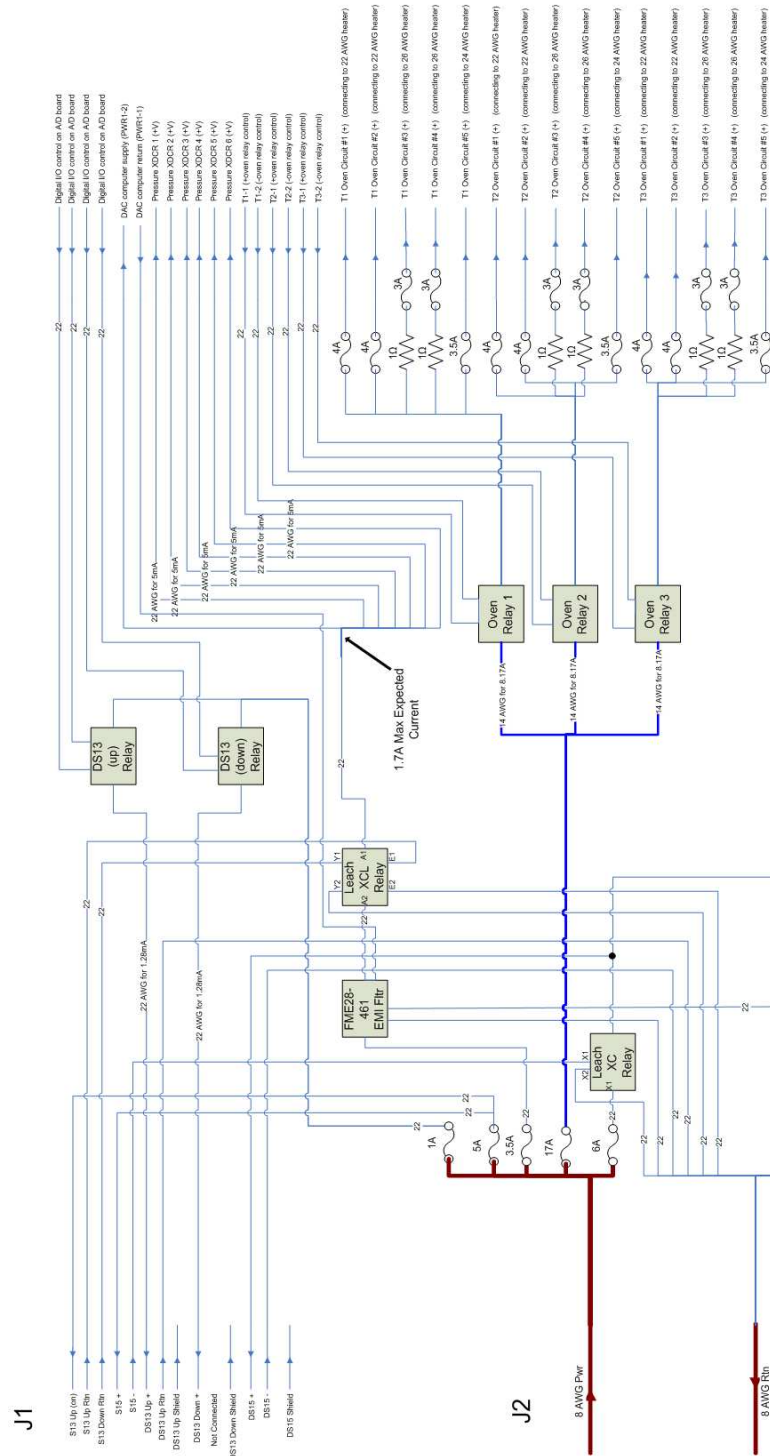


Figure E.1: Experiment Harness Layout (1 of 2)



E.3 Mission Profile

The following is included in the Program Requirements Document (PRD) in Appendix B, but is listed here as well to highlight its importance.

Table E.11: labelapp:MissionProfileMission Profile / Timeline

Computer turns on (CTO) and begins boot up	CTO
DS13(up) gets at least +18V & self-test begins	CTO + 180s
Self-test ends; DS13(up) off; DS13(down) gets at least +18V for 60s	CTO + 380s
DS13(down) off; 5-minute wait period starts (no lights on)	CTO + 440s
Oven #1 heating initialized; DS13(up) gets at least +18V	CTO + 740s
Tube #1 deployment initialized	CTO + 4340s
Tube #1 is fully deployed/begins cooling	CTO + 4360s
Tube #1 is cooled to vent temp & vents	CTO + 4960s
Tube #1 actuation begins	CTO + 4970s
Tube #1 complete; Oven #2 heating begins	CTO + 5000s
Tube #2 deployment initialized	CTO + 4340s
Tube #2 is fully deployed/begins cooling	CTO + 4360s
Tube #2 is cooled to vent temp & vents	CTO + 4960s
Tube #2 actuation begins	CTO + 4970s
Tube #2 complete; Oven #3 heating begins	CTO + 5000s
Tube #3 deployment initialized	CTO + 4340s
Tube #3 is fully deployed/begins cooling	CTO + 4360s
Tube #3 is cooled to vent temp & vents	CTO + 4960s
Tube #3 actuation begins	CTO + 4970s
Tube #3 complete; DS13(up) off; DS13(down) gets at least +18V	CTO + 5000s
<i>Total time:</i>	13520s (225min)

E.4 Filter Design

Lt Moody designed the filter board used on RIGEX. However, the design itself was not documented in his thesis, nor was it kept at AFIT. Therefore, since the possibility exists that a new filter board will need to be built, the existing board has been used to trace out the design shown in Figure E.3.

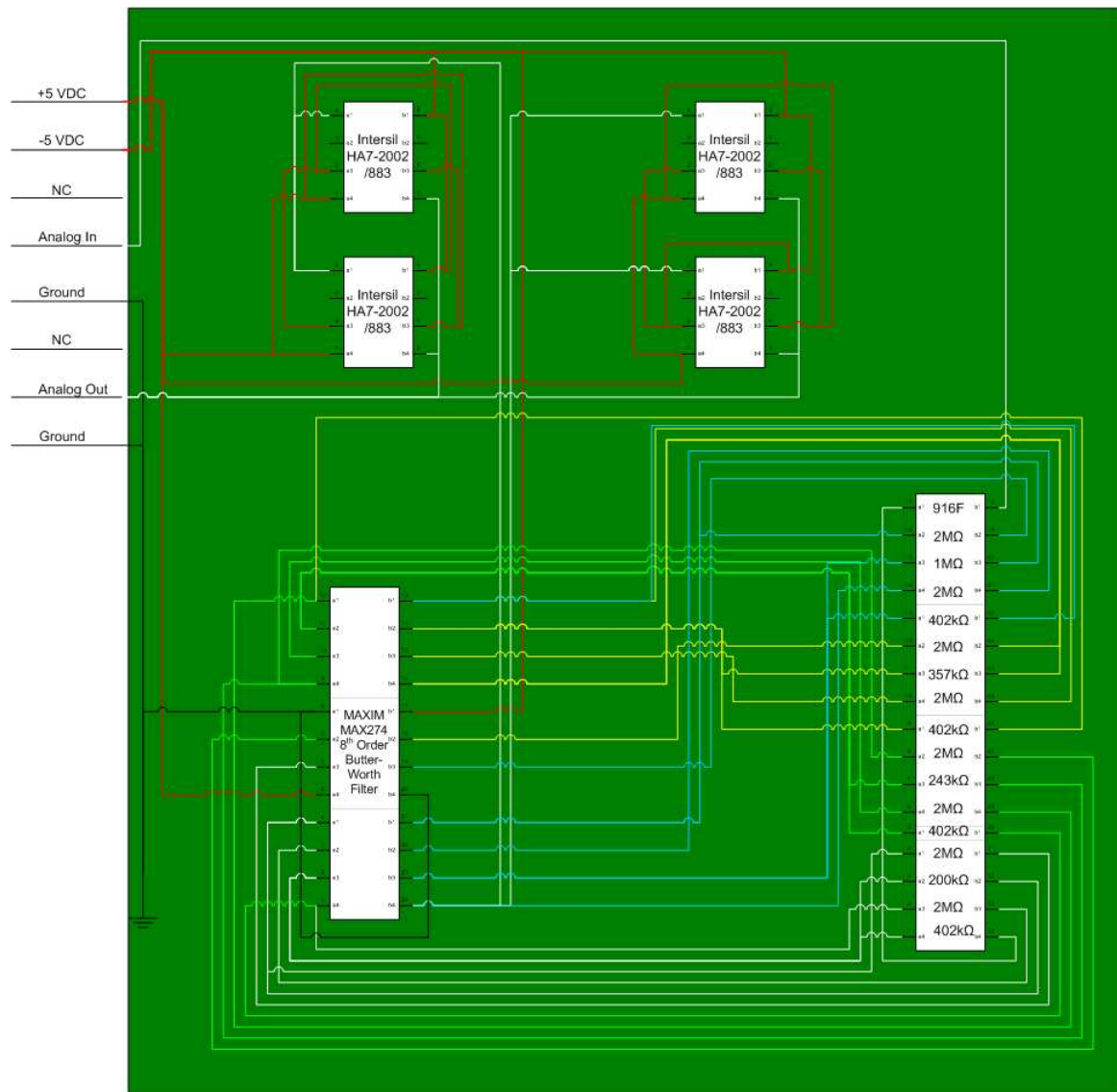


Figure E.3: Schematic of Moody's Filter Board

Appendix F. Experiment Software Code

Included in this appendix are the modified files used to create the FRFs of the tubes. Specifically, Listing F.1 contains the code for generating the tube's excitation signal, while Listing F.2 contains the post-processing code to calculate the FRFs.

Listing F.1: Excitation Signal Generation File; Originally Developed by Moody [24]

```
1 % This file is used to generate excitation signal for DAC. ...
    Originally
% written by Lt David Moody; modified by Capt Jeremy Goodwin
clc; clear; close all
f0 = 5;
f1 = 1000;
6 t = 0:1/5000:1;

% Excitation signals
y1 = 3*cos(2*pi*(5+(1000-5)*t).*t);
y2 = randn(1,5000);
11
data1 = floor((y1/5)*2048 + 2048);
LSB1 = bitand(data1,255);
MSB1 = floor(data1/256);

16 data2 = floor((y2/5)*2048 + 2048);
LSB2 = bitand(data2,255);
MSB2 = floor(data2/256);

fidl = fopen('ex_LSB.dat','w');
21 fidm = fopen('ex_MSB.dat','w');
h = waitbar(0,'Writing data...');
for k = 1:length(y1)
    fprintf(fidl,'%d\n',LSB1(k));
    fprintf(fidm,'%d\n',MSB1(k));
26    waitbar(k/5000,h);
end
fclose(fidl);
fclose(fidm);
close(h);
31
fidl = fopen('ex_LSB_randn.dat','w');
fidm = fopen('ex_MSB_randn.dat','w');
h = waitbar(0,'Writing data...');
for k = 1:length(y2)
36    fprintf(fidl,'%d\n',LSB2(k));
    fprintf(fidm,'%d\n',MSB2(k));
    waitbar(k/5000,h);
end
fclose(fidl);
41 fclose(fidm);
```

```
close(h);

figure
subplot(211)
46 plot(t(1:length(y1)),y1,'b'); axis([0 1 -5 5]);
grid on
title('Tube Chirp Signal')
xlabel('Time (s)')

51 subplot(212); plot(y2);
grid on
xlabel('Time (s)')
```

Listing F.2: FRF Portion of Post-Processing File; Originally Developed by Moody [24]

```

function status = tube_test_interp(filename);
% This file was taken from Lt Moody's overall tube interpretation ...
%   file to
% enhance the quality of the FRF. Its input is the filename of ...
%   the
% accelerometer's time data generated by the PC-104 (.dat file)
5
% Loading data
tube_1_excite = load(filename);

% Converting excitation vibration data to voltage
10 vibx_excite = (tube_1_excite(:,2)+32768*ones(size(tube_1_excite...
    (:,2))))*5/65536;
    viby_excite = (tube_1_excite(:,3)+32768*ones(size(tube_1_excite...
    (:,3))))*5/65536;
    vibz_excite = (tube_1_excite(:,4)+32768*ones(size(tube_1_excite...
    (:,4))))*5/65536;

% Converting excitation waveform data to voltage (assumes 3V ...
%   0-1000MHz
15 % Chirp signal was used to excite the tube
load('PSD_3xChirp.mat');
x_dacout = (Pdac-2048*ones(size(Pdac)))*5/2048;

% Remove the DC bias from the excitation vibration signals
20 vibx_excite = vibx_excite - ones(size(vibx_excite))*mean(...
    vibx_excite);
    viby_excite = viby_excite - ones(size(viby_excite))*mean(...
    viby_excite);
    vibz_excite = vibz_excite - ones(size(vibz_excite))*mean(...
    vibz_excite);

% Using Bilinear transformation to convert DAC smoothing filter ...
%   equations
25 % to z domain equations
[num1d,den1d] = bilinear([3.94784176e7],[1 1.23249113e4 3.9478176...
    e7],5000);
[num2d,den2d] = bilinear([3.94784176e7],[1 1.04485553e4 3.9478176...
    e7],5000);
[num3d,den3d] = bilinear([3.94784176e7],[1 6.98150145e3 3.9478176...
    e7],5000);
[num4d,den4d] = bilinear([3.94784176e7],[1 2.45157729e3 3.9478176...
    e7],5000);
30
% Smoothing digitized excitation waveform with filter
x_dacout = filter(num4d,den4d,filter(num3d,den3d,filter(num2d,...
    den2d,filter(num1d,den1d,x_dacout))));

% Transfer function estimation for each of the three accelerometer...
%   axes

```

```

35 N = 5000; fs = 5000; overlap = []; numave=25; window = hamming(N);

[Tx,F] = tftestimate(x_dacout,vibx_excite>window, overlap, N, fs);
[Ty,F] = tftestimate(x_dacout,viby_excite>window, overlap, N, fs);
[Tz,F] = tftestimate(x_dacout,vibz_excite>window, overlap, N, fs);
40
% PSD estimation for the smoothed DAC signal and vibration signals
[Pdac,Fp] = pwelch(x_dacout>window,overlap,N,fs);
[Pvibx,Fp] = pwelch(vibx_excite>window,overlap,N,fs);
[Pviby,Fp] = pwelch(viby_excite>window,overlap,N,fs);
45 [Pvibz,Fp] = pwelch(vibz_excite>window,overlap,N,fs);

% 4 point average smoothing of transfer functions
h = ones(4,1)/4;
Txh = conv2(Tx,h);
50 Tyh = conv2(Ty,h);
Tzh = conv2(Tz,h);

% Data Plotting
plot_axes=[0 1000 -150 50];
55
figure(4); set(gcf,'Name','Tube Vibration Time Data');
clf
subplot(311)
plot((0:length(vibx_excite)-1)/5000,vibx_excite);
60 grid on;
ylabel('X Axis Vibration Signal');
title('Excitation Vibration Signals')
subplot(312)
plot((0:length(viby_excite)-1)/5000,viby_excite);
65 grid on;
ylabel('Y Axis Vibration Signal');
subplot(313)
plot((0:length(vibz_excite)-1)/5000,vibz_excite);
grid on;
70 ylabel('Z Axis Vibration Signal');
xlabel('Time (sec)');

figure(5); set(gcf,'Name','Data PSDs');
clf
75 subplot(221)
plot(Fp,20*log10(abs(Pdac)));
xlabel('Frequency (Hz)');
ylabel('Magnitude (dB)');
title('PSD of Excitation Waveform');
80 grid on;
subplot(222)
plot(Fp,20*log10(abs(Pvibx)));
grid on;
xlabel('Frequency (Hz)');
85 ylabel('Magnitude (dB)');
title('PSD of Accelerometer X Output');

```

```

subplot(223)
plot(Fp,20*log10(abs(Pviby)));
grid on;
90 xlabel('Frequency (Hz)');
ylabel('Magnitude (dB)');
title('PSD of Accelerometer Y Output');
subplot(224)
plot(Fp,20*log10(abs(Pvibz)));
95 grid on;
xlabel('Frequency (Hz)');
ylabel('Magnitude (dB)');
title('PSD of Accelerometer Z Output');

100 figure(6); set(gcf,'Name','Tube Transfer Functions');
clf
subplot(131)
plot(Fp,20*log10(abs(Tx)))
grid on;
105 title('Transfer Functions of X axis')
ylabel('Magnitude Transfer Function')
xlabel('Frequency (Hz)');
axis(plot_axes)
axis square
110 subplot(132)
plot(Fp,20*log10(abs(Ty)))
grid on;
title('Transfer Functions of Y axis')
ylabel('Magnitude Transfer Function')
115 xlabel('Frequency (Hz)');
axis(plot_axes)
axis square
subplot(133)
plot(Fp,20*log10(abs(Tz)))
120 grid on;
title('Transfer Functions of Z axis')
ylabel('Magnitude Transfer Function')
xlabel('Frequency (Hz)');
axis(plot_axes)
125 axis square

figure(7); set(gcf,'Name','Smoothed Tube Transfer Functions');
clf
130 subplot(131)
plot(Fp,20*log10(abs(Txf(4:length(Txf)))))
grid on;
title('Smoothed TF of X axis')
ylabel('Magnitude Transfer Function')
135 xlabel('Frequency (Hz)');
axis(plot_axes)
axis square
subplot(132)

```

```

    plot(Fp,20*log10(abs(Tyf(4:length(Tyf)))))
140 grid on;
    title('Smoothed TF of Y axis')
    ylabel('Magnitude Transfer Function')
    xlabel('Frequency (Hz)');
    axis(plot_axes)
145 axis square
    subplot(133)
    plot(Fp,20*log10(abs(Tzf(4:length(Tzf)))))
    grid on;
    title('Smoothed TF of Z axis')
150 ylabel('Magnitude Transfer Function')
    xlabel('Frequency (Hz)');
    axis(plot_axes)
    axis square

```

Bibliography

1. *IEEE Standard for the Application and Management of the Systems Engineering Process*. Institute of Electrical and Electronics Engineers(IEEE), 1998.
2. *Space Shuttle Criteria for Preloaded Bolts, Revision A*, July 1998.
3. Analog Devices, Norwood MA. *Thermocouple Conditioner and Setpoint Controller*, 1998.
4. Cobb, Richard G. *Lecture Notes, MECH 719, Vibration Damping and Control*. Air Force Institute of Technology (AFIT), Wright-Patterson AFB OH, Fall Quarter 2005.
5. Cobb, Richard G., Captain, USAF. *Structural Damage Identification From Limited Measurement Data*. Ph.D. thesis, Air Force Institute of Technology (AFIT), Wright-Patterson AFB OH, March 1996.
6. Department of Defense. *Military Handbook 5H*, December 1998.
7. Diamond Systems Corporation, Palo Alto CA. *Pearl-MM 16 Relay Digital Output PC/104 Module User Manual V1.0*, 1997.
8. Diamond Systems Corporation, Palo Alto CA. *Jupiter-MM DC/DC Power Supply PC/104 Module User Manual V1.1*, 1999.
9. Diamond Systems Corporation, Palo Alto CA. *Diamond-MM-32-AT 16-Bit Analog I/O PC/104 Module with Autocalibration User Manual V2.5*, 2001.
10. Diamond Systems Corporation, Palo Alto CA. *Quartz-MM PC/104 Format Counter/Timer & Digital I/O Module User Manual V1.5*, 2001.
11. DiSebastian, John D., Captain, USAF. *RIGEX: Preliminary Design of a Rigidizable Inflatable Get-Away-Special Experiment*. Master's thesis, Air Force Institute of Technology (AFIT), Wright-Patterson AFB OH, March 2001.
12. E.I. du Pont de Nemours and Company. "Delrin®". [http://heritage.dupont.com/floater/fl delrin/floater.shtml](http://heritage.dupont.com/floater/fl%20delrin/floater.shtml), 2003.
13. Electrim Corporation, Princeton NJ. *EDC-1000U Computer Camera Technical Manual*, August 1997.
14. Futron Corporation. *Space Transportation Costs: Trends in Price Per Pound to Orbit 1990-2000*. Technical report, Bethesda MD, September 2002.
15. Gaston, Darilyn M. *Technical Manual 102179, Selection of Wires and Circuit Protective Devices for STS Orbiter Vehicle Payload Electrical Circuits*. National Aeronautics and Space Administration (NASA), June 1991.
16. Hall, Arthur D. "Three-dimensional Morphology of Systems Engineering". *IEEE Transactions on Systems Science and Cybernetics*, SSC-5(No.2), April 1969.

17. Helms, Sarah K., 2nd Lieutenant, USAF. *Development and Testing of an Inflatable, Rigidizable Space Structure Experiment*. Master's thesis, Air Force Institute of Technology (AFIT), Wright-Patterson AFB OH, March 2006.
18. Hillcliff Tools Ltd. "HeliCoil Wire Thread Inserts". www.hillcliff-tools.com/helicoil.html.
19. Holstein III, Raymond G., Captain, USAF. *Structural Design and Analysis of a Rigidizable Space Shuttle Experiment*. Master's thesis, Air Force Institute of Technology (AFIT), Wright-Patterson AFB OH, March 2004.
20. L'Garde Incorporated. "Spartan 207 Mission". www.lgarde.com/gsfsc/207.html, 2006.
21. Lindemuth, Steven N., Captain, USAF. *Characterization and Ground Test of an Inflatable Rigidizable Space Experiment*. Master's thesis, Air Force Institute of Technology (AFIT), Wright-Patterson AFB OH, March 2004.
22. McMaster-Carr. "Socket Cap Screws". www.mcmaster.com.
23. Moeller, Chad R., Captain, USAF. *Design and Ground-Testing of an Inflatable-Rigidizable Structure Experiment in Preparation for Space Flight*. Master's thesis, Air Force Institute of Technology (AFIT), Wright-Patterson AFB OH, June 2005.
24. Moody, David C., 1st. Lieutenant, USAF. *Microprocessor-Based Systems Control for the Rigidized Inflatable Get-Away Special Experiment*. Master's thesis, Air Force Institute of Technology (AFIT), Wright-Patterson AFB OH, March 2004.
25. National Aeronautics and Space Administration (NASA). *Interpretations of NSTS/ISS Payload Safety Requirements, Revision B*, September 1997.
26. National Aeronautics and Space Administration (NASA). *SSP 52005 Revision C*, December 2002.
27. Philley, Thomas Lee, 1st Lieutenant, USAF. *Development, Fabrication, and Ground Test of an Inflatable Structure Space-Flight Experiment*. Master's thesis, Air Force Institute of Technology (AFIT), Wright-Patterson AFB OH, March 2003.
28. Schaffer, Theresa M. "RIGEX Phase 0/1 Safety Review", December 2005.
29. Single, Thomas G., Captain, USAF. *Experimental Vibration Analysis of Inflatable Beams for an AFIT Space Shuttle Experiment*. Master's thesis, Air Force Institute of Technology (AFIT), Wright-Patterson AFB OH, March 2002.
30. Taber Industries, North Tonawanda NY. *Pressure Transducer Series 2, Model 2211/2911*.
31. Tri-M Systems Engineering, Coquitlam BC. *MZ104+ Manual Version 2.03*, 2001.
32. Wertz, James R. and Wiley J. Larson. *Space Mission Analysis and Design*. Microcosm Press, third edition, 2000.

Vita

Captain Jeremy Goodwin graduated from Springfield Central High School in Springfield, Massachusetts in 1995. He then moved to Daytona Beach, Florida, to attend Embry-Riddle Aeronautical University, where he graduated with a Bachelor of Science in Aerospace Engineering. Upon graduation, he was assigned to the Test and Evaluation Directorate of the Space and Missile Systems Center (now known as SMC Detachment 12) at Kirtland Air Force Base in Albuquerque, New Mexico. Over a 5-year tour, he worked as a satellite test engineer, program manager, executive officer to the Commander, and operations officer. He was then awarded a sponsorship to the Air Force Institute of Technology from the National Reconnaissance Office, where he will be assigned upon graduation.

REPORT DOCUMENTATION PAGE			Form Approved OMB No. 0704-0188		
<p>The public reporting burden for this collection of information is estimated to average 1 hour per response, including the time for reviewing instructions, searching existing data sources, gathering and maintaining the data needed, and completing and reviewing the collection of information. Send comments regarding this burden estimate or any other aspect of this collection of information, including suggestions for reducing this burden to Department of Defense, Washington Headquarters Services, Directorate for Information Operations and Reports (0704-0188), 1215 Jefferson Davis Highway, Suite 1204, Arlington, VA 22202-4302. Respondents should be aware that notwithstanding any other provision of law, no person shall be subject to any penalty for failing to comply with a collection of information if it does not display a currently valid OMB control number. PLEASE DO NOT RETURN YOUR FORM TO THE ABOVE ADDRESS.</p>					
1. REPORT DATE (DD-MM-YYYY) 23-03-2006		2. REPORT TYPE Master's Thesis		3. DATES COVERED (From — To) Mar 2005 — Mar 2006	
4. TITLE AND SUBTITLE Detailed Design of the Rigidizable Inflatable Get-Away-Special Experiment			5a. CONTRACT NUMBER		
			5b. GRANT NUMBER		
			5c. PROGRAM ELEMENT NUMBER		
6. AUTHOR(S) Jeremy S. Goodwin, Capt, USAF			5d. PROJECT NUMBER		
			5e. TASK NUMBER		
			5f. WORK UNIT NUMBER		
7. PERFORMING ORGANIZATION NAME(S) AND ADDRESS(ES) Air Force Institute of Technology Graduate School of Engineering and Management (AFIT/EN) 2950 Hobson Way WPAFB OH 45433-7765			8. PERFORMING ORGANIZATION REPORT NUMBER AFIT/GA/ENY/06-M05		
9. SPONSORING / MONITORING AGENCY NAME(S) AND ADDRESS(ES) N/A			10. SPONSOR/MONITOR'S ACRONYM(S)		
			11. SPONSOR/MONITOR'S REPORT NUMBER(S)		
12. DISTRIBUTION / AVAILABILITY STATEMENT APPROVED FOR PUBLIC RELEASE; DISTRIBUTION UNLIMITED					
13. SUPPLEMENTARY NOTES					
14. ABSTRACT The Rigidizable Inflatable Get-Away-Special Experiment is a Space Shuttle experiment that will study the effects of the zero-gravity space environment on the deployment and modal analysis of three inflatable and rigidizable tubes using a sub-Tg rigidization technique. In 2004, RIGEX was transitioned from the Space Shuttle's Get-Away-Special (GAS) canister to its Canister for All Payload Ejections (CAPE), requiring several modifications to the design. The results of these modifications, along with further refinements made to previous efforts, combine to form the detailed design of the experiment. In addition to the design modifications, analyses were conducted to determine the containment capabilities of a shroud for the experiment, as well as to identify and implement potential improvements to the modal testing methods.					
15. SUBJECT TERMS Inflatable Structures, Space Systems, Space Shuttle, Rigidizable Structures, Sub-Tg Structures, Ground Testing, Vibrations Testing, Get-Away-Special, Canister for All Payload Ejections, Space Structures					
16. SECURITY CLASSIFICATION OF:			17. LIMITATION OF ABSTRACT UU	18. NUMBER OF PAGES 190	19a. NAME OF RESPONSIBLE PERSON Dr. Richard G. Cobb
a. REPORT U	b. ABSTRACT U	c. THIS PAGE U			19b. TELEPHONE NUMBER (Include Area Code) (937) 255-3636, ext 4559; e-mail: Richard.cobb@afit.edu